

Spatial and Temporal Distribution of Industrial and Agricultural Contaminants in the Raritan River

*To Complement Historical Baselines
of Sediment Contamination and
Provide Information from Areas With
No Official Records of Sediment
Samples*

Abstract: The main objective of this proposal to start filling in data gaps in river and marsh sediment contamination in the Lower Raritan River. Main tasks of this study are: 1, Measure trace metal and organic contaminant levels in surficial sediments along 20 km of the lower Raritan River; 2, Visualize the spatial distribution of trace metal and organic pollutants in surficial sediments using spatial interpolation techniques; 3, Extract cores from three marsh sites (1) proximal, (2) central and (3) distal to traditional industrial and agricultural sites; 4, Reconstruct pre-industrial environmental reference conditions.

RUTGERS THE STATE UNIVERSITY OF NEW JERSEY – DEPARTMENT OF EARTH AND
ENVIRONMENTAL SCIENCES – MEADOWLANDS ENVIRONMENTAL RESEARCH
INSTITUTE

2018



Spatial and Temporal Distribution of Industrial and Agricultural Contaminants in the Raritan River

To Complement Historical Baselines of Sediment
Contamination and Provide Information from Areas
With No Official Records of Sediment Samples

MERI-Rutgers

6/5/2018

Abstract: The main objective of this proposal is to start filling in data gaps in river and marsh sediment contamination in the Lower Raritan River. Main tasks of this study are: 1, Measure trace metal and organic contaminant levels in surficial sediments along 20 km of the Lower Raritan River; 2, Visualize the spatial distribution of trace metal and organic pollutants in surficial sediments using spatial interpolation techniques; 3, Extract cores from three marsh sites (1) proximal, (2) central and (3) distal to traditional industrial and agricultural sites; 4, Reconstruct pre-industrial environmental reference conditions.

**SPATIAL AND TEMPORAL DISTRIBUTION OF INDUSTRIAL AND AGRICULTURAL
CONTAMINANTS IN THE RARITAN RIVER**

*TO COMPLEMENT HISTORICAL BASELINES OF SEDIMENT CONTAMINATION AND
PROVIDE INFORMATION FROM AREAS WITH NO OFFICIAL RECORDS OF SEDIMENT
SAMPLES*

RUTGERS THE STATE UNIVERSITY OF NEW JERSEY – DEPARTMENT OF EARTH AND
ENVIRONMENTAL SCIENCES – MEADOWLANDS ENVIRONMENTAL RESEARCH
INSTITUTE

Authors

Francisco Artigas, Benjamin Horton, Ildiko C. Pechmann, Margaret Christie

06/05/2018

Lyndhurst, NJ

Table of Contents

Table of Figures	3
Introduction.....	7
1. Component I – River Sediment Quality	9
1.1 Introduction	9
Surficial sediment sampling/surface water quality measurements	9
Chemical analysis.....	9
Data visualization and reporting	10
1.2 Methods.....	11
1.2.1 The study sites	11
1.2.2 Surficial sediment sampling and surface water quality measurements	12
Water Quality Sampling	12
Sediment Sampling.....	12
1.2.3 Chemical analysis	13
PCB and OCP Sample Preparation:.....	13
Metal Sample Preparation	14
1.2.4 Data visualization.....	14
1.3 Results	16
1.3.1 Water Quality in the Raritan River	16
1.3.2 Metal contamination in the Raritan River sediment.....	21
1.3.3 Organics in the Raritan River sediment	23
1.3.3 Spatial interpolation and Geo-Accumulation Index	25
Trace metal and organic pollutant distribution in the river sediment	25
Contamination compared to the natural metal accumulation in the river sediment	42
Comparing current and historical sediment contamination records in the Lower Raritan River sediment.....	56
1.4 Conclusions	60
2. Component II – Historical Land Use Report in the Lower Raritan Basin	62
2.2 Methods.....	64
2.2.1 Coring and Sample Selection	64
2.2.2 Geochemistry	65
2.2.3 Pollen Analysis	67
2.2.4 Constructing of an Age-Depth Model.....	68
2.3 Results	70
2.3.1 Age-Depth Models.....	70

2.3.2 Pollution History	77
2.4 Conclusions	82
3. Discussion	85
4. References	87
5. Acknowledgements	90

Table of Figures

Figure 1: Map of the study area and the sampling plan	11
Equation 1. Geoaccumulation Index.....	15
Figure 2. Geoaccumulation Index Classes	15
Figure 3. Study area map showing the labelled, final sampling locations	16
Figure 4. Salinity in the water column as well as from the bay to New Brunswick.....	17
Figure 5. Turbidity in the water column as well as from the bay to New Brunswick.....	18
Figure 6. Dissolved Oxygen in the water column as well as from the bay to New Brunswick.....	18
Figure 7. pH in the water column as well as from the bay to New Brunswick.	19
Figure 8. Oxygen Reduction Potential in the water column as well as from the bay through New Brunswick.	19
Table 1. Summary table of onsite water quality measurements at the Lower Raritan River	20
Table 2. Summary statistics of metal concentration in the Raritan River sediment, along with the available ERM and ERL criteria.	22
Table 3. Metal concentration in the Raritan River sediment – marking the exceedance of ERM (red) and ERL (yellow) criteria	22
Table 4. Total PCB and total OCP concentration ($\mu\text{g}/\text{kg}$) at each sampling location.....	23
Figure 9. PCB and OCP concentrations in the Raritan River sediment.....	24
Figure 10. Spatial interpolation showing the distribution of Arsenic in the Lower Raritan River surficial sediment.....	26
Figure 11. Spatial interpolation showing the distribution of Beryllium in the Lower Raritan River surficial sediment.....	27
Figure 12. Spatial interpolation showing the distribution of Cadmium in the Lower Raritan River surficial sediment.....	28
Figure 13. Spatial interpolation showing the distribution of Chromium in the Lower Raritan River surficial sediment.....	29
Figure 14. Spatial interpolation showing the distribution of Copper in the Lower Raritan River surficial sediment.....	30
Figure 15. Spatial interpolation showing the distribution of Mercury in the Lower Raritan River surficial sediment.....	31
Figure 16. Spatial interpolation showing the distribution of Nickel in the Lower Raritan River surficial sediment.....	32

Figure 17. Spatial interpolation showing the distribution of Lead in the Lower Raritan River surficial sediment.....	33
Figure 18. Spatial interpolation showing the distribution of Antimony in the Lower Raritan River surficial sediment.....	34
Figure 19. Spatial interpolation showing the distribution of Selenium in the Lower Raritan River surficial sediment.....	35
Figure 20. Spatial interpolation showing the distribution of Silver in the Lower Raritan River surficial sediment.....	36
Figure 21. Spatial interpolation showing the distribution of Thallium in the Lower Raritan River surficial sediment.....	37
Figure 22. Spatial interpolation showing the distribution of Zinc in the Lower Raritan River surficial sediment.....	38
Figure 23. Spatial interpolation showing the distribution of the cumulative metal index values in the Lower Raritan River surficial sediment.....	39
Figure 24. Spatial interpolation showing the distribution of total OCPs in the Lower Raritan River surficial sediment.....	40
Figure 25. Spatial interpolation showing the distribution of total PCBs in the Lower Raritan River surficial sediment.....	41
Figure 26. Spatial interpolation of the geoaccumulation index showing concentration of Antimony in the Lower Raritan River surficial sediment compared to natural background levels.....	43
Figure 27. Spatial interpolation of the geoaccumulation index showing concentration of Arsenic in the Lower Raritan River surficial sediment compared to natural background levels.....	44
Figure 28. Spatial interpolation of the geoaccumulation index showing concentration of Beryllium in the Lower Raritan River surficial sediment compared to natural background levels.....	45
Figure 29. Spatial interpolation of the geoaccumulation index showing concentration of Cadmium in the Lower Raritan River surficial sediment compared to natural background levels.....	46
Figure 30. Spatial interpolation of the geoaccumulation index showing concentration of Chromium in the Lower Raritan River surficial sediment compared to natural background levels.....	47
Figure 31. Spatial interpolation of the geoaccumulation index showing concentration of Copper in the Lower Raritan River surficial sediment compared to natural background levels.....	48
Figure 32. Spatial interpolation of the geoaccumulation index showing concentration of Lead in the Lower Raritan River surficial sediment compared to natural background levels.....	49

Figure 33. Spatial interpolation of the geoaccumulation index showing concentration of Mercury in the Lower Raritan River surficial sediment compared to natural background levels 50

Figure 34. Spatial interpolation of the geoaccumulation index showing concentration of Nickel in the Lower Raritan River surficial sediment compared to natural background levels..... 51

Figure 35. Spatial interpolation of the geoaccumulation index showing concentration of Selenium in the Lower Raritan River surficial sediment compared to natural background levels 52

Figure 36. Spatial interpolation of the geoaccumulation index showing concentration of Silver in the Lower Raritan River surficial sediment compared to natural background levels..... 53

Figure 37. Spatial interpolation of the geoaccumulation index showing concentration of Thallium in the Lower Raritan River surficial sediment compared to natural background levels 54

Figure 38. Spatial interpolation of the geoaccumulation index showing concentration of Zinc in the Lower Raritan River surficial sediment compared to natural background levels..... 55

Figure 39. Map of the study area showing the original sampling locations from EPA’s STORET database and MERI’s current sampling locations 57

Figure 40. Summary of current (2017) and historical (2000-06) sediment metals concentration compared at five distinct sampling locations (P1-P5) from the bay up to New Brunswick 58

Figure 41. Summary of current (2017) and historical (2000-06) sediment PCB congener and OCP concentration compared at five distinct sampling locations (P1-P5) from the bay up to New Brunswick 59

Figure 42: Location of the coring sites..... 64

Figure 43. Brookside Metals, colors in figure represents pre-land clearance (green), post-land clearance, but pre-industrial (yellow), and post-industrial (red) land uses..... 72

Figure 44. Bridge Site Metals, colors in figure represents pre-land clearance (green), post-land clearance, but pre-industrial (yellow), and post-industrial (red) land uses..... 73

Figure 45. Cheesequake Site Metals, colors in figure represents pre-land clearance (green), post-land clearance, but pre-industrial (yellow), and post-industrial (red) land uses..... 74

Figure 48. Brookside Site Age-Depth Model showing the various marker types that were used to determine the pre- and post-settlement as well as the post-industrial contamination levels..... 75

Figure 49. Bridge Site Age-Depth Model showing the various marker types that were used to determine the pre- and post-settlement as well as the post-industrial contamination levels..... 76

Figure 50. Bridge Site Age-Depth Model showing the various marker types that were used to determine the pre- and post-settlement as well as the post-industrial contamination levels..... 76

Table 5 Summary of the metal and organics concentration values from the core samples 77

Figure 51. Brookside Organics, colors in figure represents pre-land clearance (green), post-land clearance, but pre-industrial (yellow), and post-industrial (red) land uses..... 78

Figure 52. Results of Diatom Analysis at the Brookside Site, showing distribution of Low and High Nutrient Diatoms over time..... 78

Figure 53. Bridge Site, colors in figure represents pre-land clearance (green), post-land clearance, but pre-industrial (yellow), and post-industrial (red) land uses. 79

Figure 54. Results of Diatom Analysis at the Bridge Site, showing distribution of Low and High Nutrient Diatoms over time..... 79

Figure 55. Cheesquake Site, colors in figure represents pre-land clearance (green), post-land clearance, but pre-industrial (yellow), and post-industrial (red) land uses..... 80

Figure 56. Results of Diatom Analysis at the Cheesquake Site, showing distribution of Low and High Nutrient Diatoms over time..... 80

Introduction

The challenge for agencies and wetland managers is to sustain the quality and integrity of wetlands by eliminating threats from natural and human causes. The role of monitoring is to detect meaningful levels of change that exceed acceptable historical or natural limits. The proposed study looks at sediment chemistry and contamination in the Lower Raritan River in an effort to promote understanding of levels and extent of heavy metal and organic compound pollution in the river sediment. This study complements historical sediment data collected by various state agencies and NGOs and provides new and updated information critical to the future enhancement and management of this highly impacted urban coastal area.

The objective of this study was to design and implement a sediment sampling system that would be spatially representative of the main stem of the Lower Raritan and cover the previously measured heavy metal and organic compound hotspots. The Raritan River basin is well known for the historical industrial and related commercial uses that left a legacy contamination along its banks that impacts the quality of the ecosystems both in the river, and the surrounding wetlands in the bay. The collaborative restoration effort of the watershed started when under the umbrella of the 1984 renewed Clean Water Act the Hudson-Raritan Estuary had become a national watershed and in 1988 the estuary was accepted into the National Estuary Program (HRECRP, 2014). Ever since, numerous efforts have been dedicated to gage the levels and extent of the legacy contamination in the estuary as the health of the river is central to the quality of life in the region (Rutgers, 2009). 22 municipalities share the main stem of the Raritan River, however 5 counties encompassing 103 municipalities live on the watershed.

Between 2012 and 2015 the U.S. Environmental Protection Agency through a cooperative agreement funded the Rutgers Raritan River project to compile all existing data from superfund sites, brown fields, known contaminated sites and point and non-point sources of pollution into a comprehensive database of the Raritan River watershed. These datasets are meant to assist federal, state and local stakeholders in making decisions related to environmental cleanup but have only a limited number of samples from the main channel of the Lower Raritan that were collected between 2000 and 2006. The Data Compilation and Integration Report (2015)¹ concluded that for a successful restoration of the Raritan River “A more comprehensive

¹ http://cues.rutgers.edu/sustainable-raritan-river/pdfs/EPARutgersRaritanDataReport%20_09292015.pdf

monitoring program needs to be completed on the Lower Raritan to collect water and sediment samples and analyze these samples for priority pollutants and contaminants.” The proposed study is designed to start filling in these data gaps following a sampling and analysis strategy that meets NJDEP and EPA quality assurance criteria.

The study has two components. *Component I – river sediment quality* –measured metal and organic contaminants associated with surficial sediment in the Lower Raritan River. The study is designed to complement historical baselines of sediment contamination measured between 2000 and 2006 (STORET 2016)² and to provide new and updated information from areas where there are no official records of sediment samples in state or federal environmental datasets. The main tasks of this component included: 1, Measure trace metal and organic contaminant levels in surficial sediments along 20 km of the Lower Raritan River using a transversal transect sampling design. 2, Measure water quality parameters at two depths (surface and channel bottom) utilizing the same surficial sediment sampling design. 3, Visualize the spatial distribution of trace metal and organic pollutants in surficial sediments using spatial interpolation techniques. In *Component II – salt marsh sediment assessment* – sediment cores from salt marsh environment were analyzed to assess the environmental impacts of pollutants across space and time. The main tasks of this component included: 1, Extract cores from three marsh sites (1) proximal, (2) central and (3) distal to traditional industrial and agricultural sites, while capturing the elevation gradient within the marsh surface by sampling (a) high- (b) mid- and (c) low-marsh environments at each site. 2, Reconstruct pre-industrial environmental reference conditions and natural variability prior to significant anthropogenic disturbance and identify the distribution and longevity of industrial and agricultural pollution retained within the salt-marsh environments by radiocarbon dating and geochemical analysis of the core sample; 3, observe any ecological shifts that occurred due to the disposal and deposition of pollutants in the Raritan River by assessing diatom and pollen abundance in the core sample.

² <https://www.epa.gov/waterdata/storage-and-retrieval-and-water-quality-exchange>

1. Component I – River Sediment Quality

1.1 Introduction

The objective was to design and implement a sediment sampling campaign that would be spatially representative of the main stem of the Lower Raritan river and also re-sample the previously identified heavy metal and organic contaminant hotspots from 2000-2006.

Component I. is divided into three main tasks: 1.- surficial sediment sampling and surface water quality measurements, 2.- chemical analysis and 3.- data visualization and reporting.

Surficial sediment sampling/surface water quality measurements

The main stem of the Lower Raritan River between New Brunswick and the Raritan bay was sampled according to the design presented in Figure 1. The design includes the seven locations already in the STORET dataset (sampled between 2000 and 2006) and adds 33 new samples along transects covering areas with data gaps. This approach is designed to capture a shore to shore general pattern of contaminant distribution with sufficient resolution to understand the overall pattern and possibly guide future collections around problem areas at even greater resolutions. Surficial sediments were collected using a ponar grab sampler from a boat equipped with a capstan winch and survey grade GPS to record coordinates for each sampling location. In an attempt to eliminate the influence from the bay sampling took place during the ebb cycle of the tide. Each sediment sample was a composite of three ponar grabs. Collected samples were registered in a chain of custody form and transported to the lab in a cooler in pre-labeled Ziploc bags. Along with the sediment sampling, surface water quality parameters (salinity, conductivity, dissolved oxygen (DO), oxygen reduction potential (ORP), pH, turbidity, and temperature) were measured at each sediment sampling location on the surface and close to the channel bottom (when depth permitted) using a calibrated YSI 6920 V2-2 multi-parameter water quality sonde. Water quality measurements were recorded in a field note book and later entered in Microsoft Excel for further analysis.

Chemical analysis

Metal contaminants were analyzed at MERI's Environmental Chemistry lab using ICP-MS. Determinations were made for the following priority pollutants: Antimony, Arsenic, Beryllium, Cadmium, Chromium, Copper, Lead, Mercury, Nickel, Selenium, Silver, Thallium and Zinc.

Total organic matter was determined by weight loss-on-ignition (LOI) method following Wang (2012). Particle size distribution was determined from 100 gram samples from each of the sampling stations. The major persistent organic pollutants (POPs) including 109 PCB congeners and 18 OCPs were analyzed on an Agilent 6890 gas chromatograph equipped with electron capture detector (ECD). Certified reference marine sediment (MESS-1) for soils was run every tenth sample, and a method blank were run every sixth sample during the gas chromatographic analysis.

Data visualization and reporting

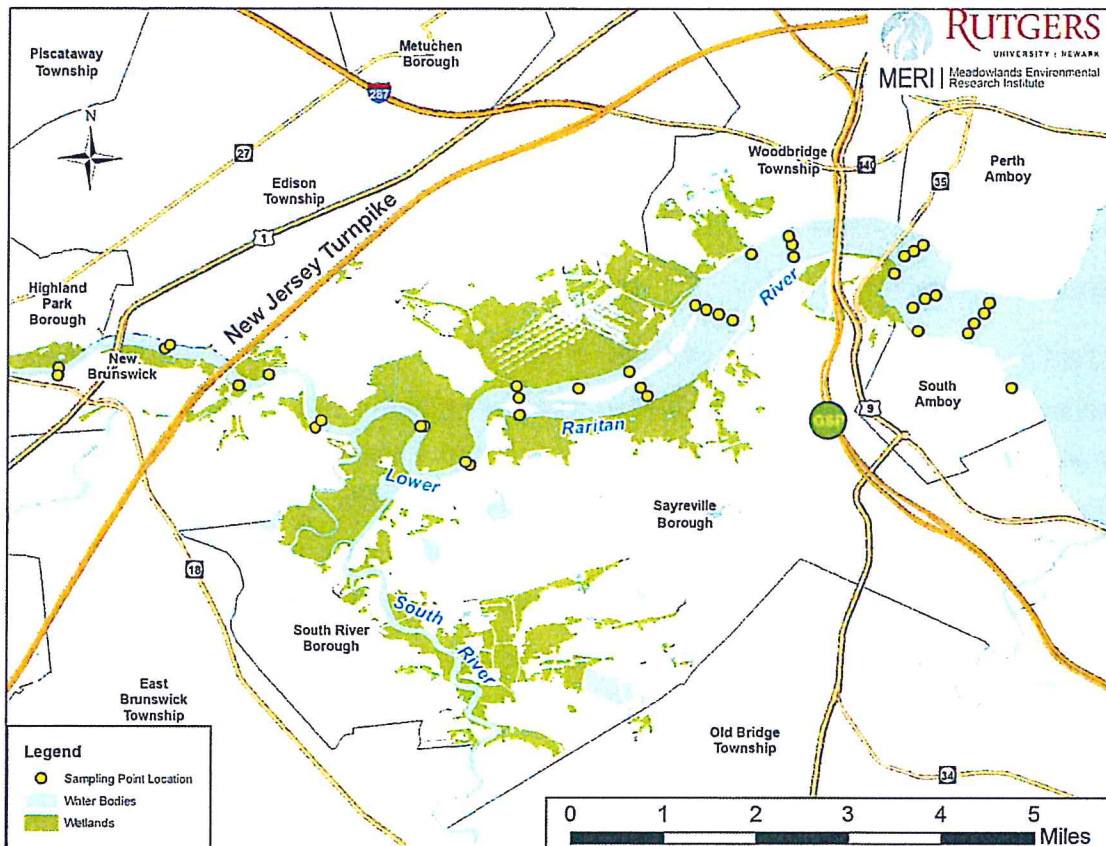
The concentration values that resulted from the sediment chemical analysis were used to visualize the distribution of contaminants of the main channel utilizing spatial interpolation techniques. A spatial analyst toolset from ArcGIS software was run to interpolate concentrations from measured locations at each of the 40 sampling points and fill in concentrations (with known variance) for the entire main channel of the river. We chose to utilize the Inverse Distance Weighted (IDW) raster interpolation technique as it references the observed concentration sampling point values to predict values for cells that are in close proximity. This IDW process assumes each sample point has a local influence that weakens with increasing distance. The raster interpolation helps to visualize concentration gradients or hotspots of priority pollutants and persistent organic pollutants in the channel. The geochemical index (Igeo) for each metal was calculated by comparing the measured concentration to natural background levels according to the local geology. The geochemical index value symbolizes the degree of contaminant enrichment beyond the natural background value. Finally, IDW interpolation of the cumulative trace metal pollutants at the 40 sampling points were mapped for visualization. This process took the sum of all the priority pollutants at each sampling location and created a ranking system to render which of these sampling locations are most impaired with respect to heavy metals

1.2 Methods

1.2.1 The study sites

Surface sediment samples were taken at 40 sampling locations (Figure 1) and analyzed for major contaminants of concern. State of the art interpolation techniques were then used to extend the point data over the entire study area and provide estimation of levels and distribution of contaminants in the sediment.

Figure 1: Map of the study area and the sampling plan



1.2.2 Surficial sediment sampling and surface water quality measurements

Sampling was completed in two separate missions. On April 10th, 2017 the Rutgers' Research Vessel boat (RV Rutgers) was used to sample the majority of the points at rising tide. A second outing on April 26th was necessary to reach the shallow sampling points.

Water Quality Sampling

A YSI 6600 EDS multi-parameter water quality sonde was used at each sampling location to obtain the following data: Turbidity, Temperature, Conductivity, Salinity, pH, DO, and ORP. The sensor is certified by NJDEP for all listed parameters and was calibrated before the outing according to NJDEP guidelines. At each site location, the sensor was submerged into the water one foot deep for surface measurements and approximately 1 foot above the river bottom for deep measurements. The monitor was attached to an YSI 650 MDS reader and the instantaneous results on the screen were recorded in a field notebook.

Sediment Sampling

For the first round of sampling we used the RV Rutgers that is equipped with a capstan winch (a revolving cylinder with a vertical axis) used for winding a rope or cable, powered by an onboard 5kw generator and operated by foot pedal on a swing arm thus allowing for the quick retrieval of the ponar (clamshell) grab sampler after each surficial sediment grab. Each sample collected is a composite of three ponar sediment grabs. The planned sampling points based on the sampling design were loaded into the RV Rutgers Garmin 1040xs radar/plotter/sounder, making accurate navigation to each point possible. The RV Rutgers also used the Rio Grande Acoustic Doppler Current Profiler to record the path that the boat took.

The second sampling mission was accomplished using a Go-Devil boat equipped with a mud motor that allowed access to the shallow water areas. Samples were again taken with a ponar grab sampler.

At each sampling location, three sediment samples were collected in labeled sample bags and combined into one composite sample to ensure that the sediment sample is representative of that site. Samples were then brought back to the lab and stored in a refrigerator set at 4 °C. Samples were analyzed for: percent moisture, percent organic matter, metals, polychlorinated biphenyls (PCBs), and organochlorine pesticides (OCPs).

The GPS location of each sample site was recorded within a one to two meter vicinity of the actual collection location. The locations were determined using a Trimble GeoXH 6000 Series handheld GPS. Sampling locations were post-processed using GPS Pathfinder Office version 5.40 in order to achieve decimeter horizontal accuracy. Sampling locations were later associated with the results from the chemical analysis and this spatial information was used to generate thematic maps showing contamination distribution in the river sediment.

1.2.3 Chemical analysis

PCB and OCP Sample Preparation:

An accelerated solvent extractor (ASE 100, Dionex, USA) was used to extract PCBs and OCPs from the sediment samples by using a mixture of hexane and acetone in a 1:1 ratio. After extraction, gel permeation chromatography (GPC, Autoprep 2000, O I Analytical, USA) was used to clean the samples before GC-ECD. The extracts were concentrated to 1mL by rotary evaporation at a temperature 30°C. The extracted samples were fractionated by florisil column (10mm i.d. x 300 mm length) filled with 10 g of florisil (60-100 mesh; J.T Baker, NJ, activated at 550 °C for 4 hours), and then partially deactivated by the addition of deionized H₂O (2.5% by wt.). The sample was loaded into the head of the florisil column and covered with a layer of sodium sulfate to a depth of 10mm. The concentrated extracts were transferred to the florisil column and subsequently eluted with 35 mL of hexane for PCB analysis. A second fraction for OCP analysis was eluted with 50 mL of dichloromethane and hexane in a 1:1 ratio and collected in a separate vial. Each fraction was solvent exchanged into hexane while concentrated to 5 mL via rotary evaporation. Each sample was finally reduced to 1 mL using a gentle stream of dry nitrogen evaporator (N-EVAP 111, OA-SYS). All samples for 109 PCB congeners and 18 OCPs were analyzed on a gas chromatograph equipped with 63 Ni electron capture detectors (GC-ECD, Hewlett Packard 6890, Santa Clara, CA) with DB-5 (60m x 250 µm in inner diameter x 0.25 µm film thickness, J&W Scientific, CA). The temperature program of GC oven condition was as follows: 100 °C held for 2 minutes; 4 °C/min to 170 °C, 2 °C/min to 280 °C, 1 °C/min to 290 °C; total time, 84.5 minutes. Daily single point calibration was used to generate response factors for each congener relative to internal standards. Congeners were identified based on

relative retention time, and PCB and OCP surrogates were spiked for QC recovery check.

Metal Sample Preparation

Metal concentrations were analyzed for the sediment samples with particle size less than 63 μ m using microwave assisted digestion and Inductively Coupled Plasma Mass Spectrometry (ICP-MS). Dried sediment samples went through the 63 μ m sieve first, and then about 0.2 g of sediment sample was collected and digested with 10 mL of ultrapure nitric acid (HNO₃, 67-70%, w/w, EMD) in a microwave digestion system (MiniWave microwave digestion, SCP science). Standard reference material 1944 (New York/New Jersey Waterway Sediment, NIST) was digested with samples for quality control. After digestion, the samples were diluted to 50 mL with ultrapure DI water and stored in polypropylene centrifuge tubes at 4°C for further analysis. Solutions were analyzed using an ICP-MS (Agilent ICP-MS 7700X), and helium collision mode with kinetic energy discrimination (KED) was used to effectively remove the multiple polyatomic interferences in ICP-MS. Li, Sc, Ge, Y, In, Tb, and Bi were used as internal standards for calibration. The recovery rates of quality control (QC) sample are 90-110%.

1.2.4 Data visualization

Following the chemical analysis of the Raritan samples, concentrations of the sampled sediments were inputted into ArcGIS 10.3 geospatial software to visualize the sediment contaminants in the main channel of the Lower Raritan River. The Spatial Analyst toolset was used to take the sediment concentrations in parts per million (ppm) at our 40 sampling points and extrapolate values in between these sampling transects to create a continuous surface of sediment contaminant information for the Lower Raritan. We chose the Inverse Distance Weighted (IDW) linear raster interpolation tool for this visualization. The IDW spatial analyst tool inputs the observed concentration sampling point values from the shapefile to predict and generate values for cells that are surrounding it. The product of this IDW interpolation is a raster layer with each pixel representing a discrete contaminant concentration value. This is done using a linear algorithm built within the tool that assumes a decrease in target value with increasing distance

from an input point until it gets influenced by a neighboring input point. The raster interpolation helps to visualize concentration gradients or hotspots of trace metal or organic pollutants in the designated area of interest. In addition to visualizing the sediment concentrations, the Geochemical Index (Igeo) of these samples was calculated by finding available background sediment concentration values derived from the local geology. This index value represents the degree of contaminant enrichment of the observed sediment beyond the natural background value from the local geology. The Geoaccumulation Index formula (Forstner&Muller, 1981) is calculated below (Eq. 1):

$$I_{geo} = \log_2 \frac{C_n}{1.5 \cdot B_n}$$

Equation 1. Geoaccumulation Index

The index is the logarithmic ratio of the observed concentration value to the background geologic source concentrations. The background values referenced for these calculations were documented in ‘Characterization of Ambient Levels of Selected Metals and Other Analytes in New Jersey Soils: Year 1, Urban Piedmont Region’ (BEM Systems Inc., 1997). The Igeo values fall into several classes that describe the degree of sediment contamination, below (Figure 2):

Figure 2. Geoaccumulation Index Classes

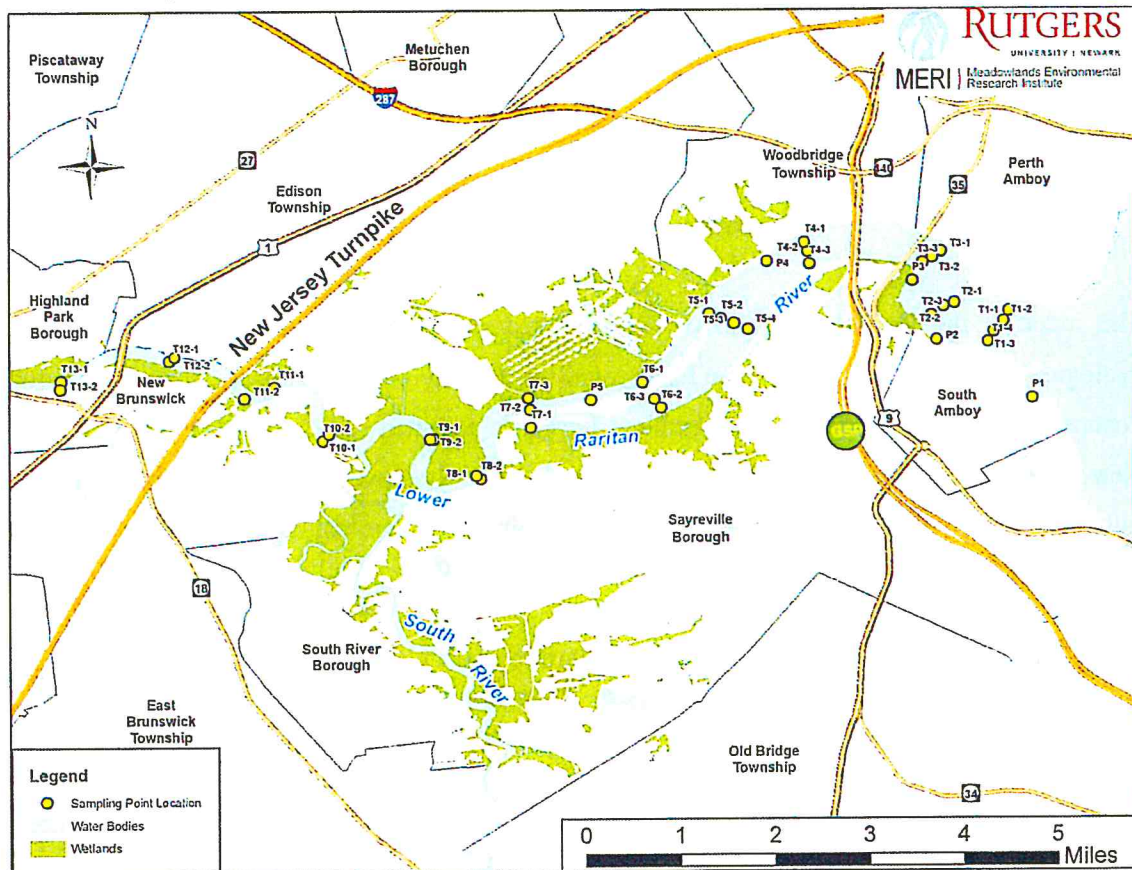
Index of Geoaccumulation, Igeo	Designation of Sediment Quality
> 3	Contaminated
2 - 3	Moderately Contaminated
1 - 2	Mildly Contaminated
< 1	Practically Uncontaminated

The Geoaccumulation Index was also interpolated using the IDW raster interpolation tool in ArcGIS. This generated raster outputs that represent the degree of sediment contamination compared to the natural geologic background values, and represent the amount of anthropogenic influence on sediments in the Lower Raritan.

1.3 Results

Figure 3 shows the locations of the final sampling sites. Several points more upriver had to be moved 10-30 feet compared to the original design as the water became shallower and the bottom more rocky, making it hard to collect enough sediment samples for the chemical analysis.

Figure 3. Study area map showing the labelled, final sampling locations



1.3.1 Water Quality in the Raritan River

The results of the water quality data show as expected that there is a decreasing gradient of Total Dissolved Solids (TDS), salinity (Figure 4) and conductivity from the mouth of the river (P1) to the final sampling point (T13-2). Turbidity exhibits the same trend from P1 through T13-2 (Figure 5). Dissolved oxygen (DO) remained about the same throughout the extent of the study

area and at about 90% saturation (9.4 ppm, Figure 6). pH (Figure 7) follows similar trends with a median of 7.5. The Oxygen Reduction Potential (ORP) measurements show a more oxidative environment as one moves upriver from the bay. ORP measurements were in the vicinity of 200 mV. No negative ORP readings were found. (Figure 8). Table 1 summarizes the water quality data. There were a few sampling locations where the water was too shallow to submerge the sonde's sensors and reliably conduct water quality measurements. Hence water quality data from locations T5-2, T7-1, T11-2, T12-2, T13-1 were not recorded. In case of T11-1, T12-1, T13-2 the water was deep enough to conduct surface measurements however not deep enough to warrant the bottom measurements and thus deep water quality records are missing from these locations. We observed that differences between deep and surface samples are greater near the bay than up river, especially for salinity. All other parameter measurements were similar at depth and on the surface indicating a fully mixed system.

Figure 4. Salinity in the water column as well as from the bay to New Brunswick

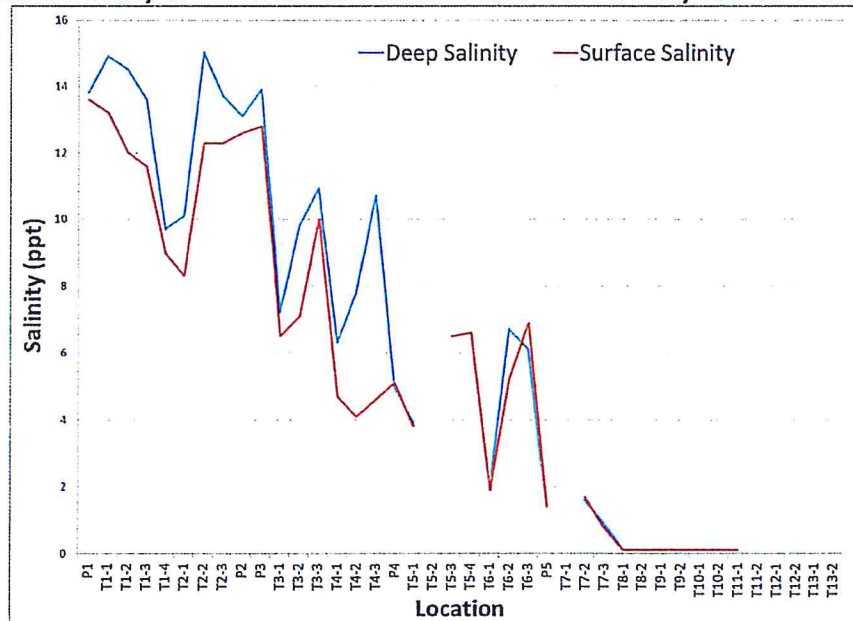


Figure 5. Turbidity in the water column as well as from the bay to New Brunswick.

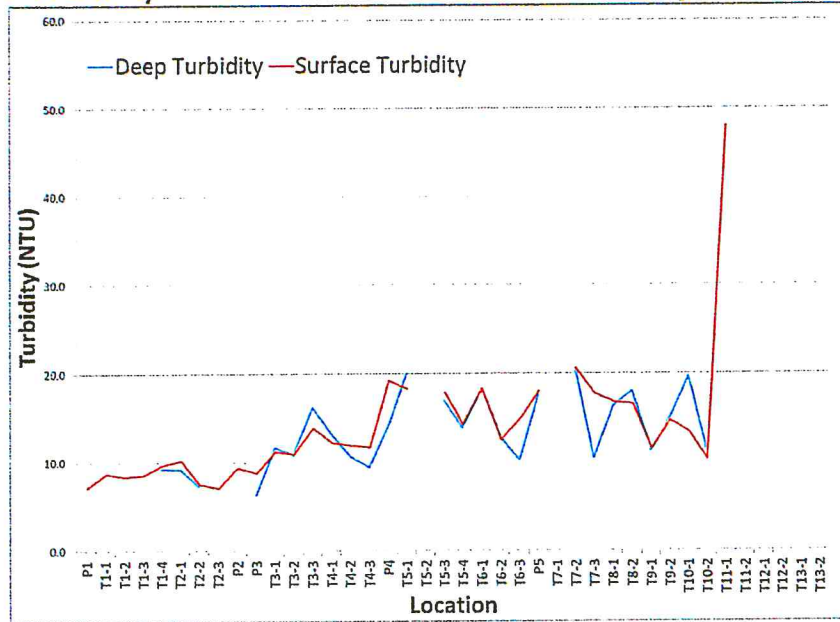


Figure 6. Dissolved Oxygen in the water column as well as from the bay to New Brunswick.

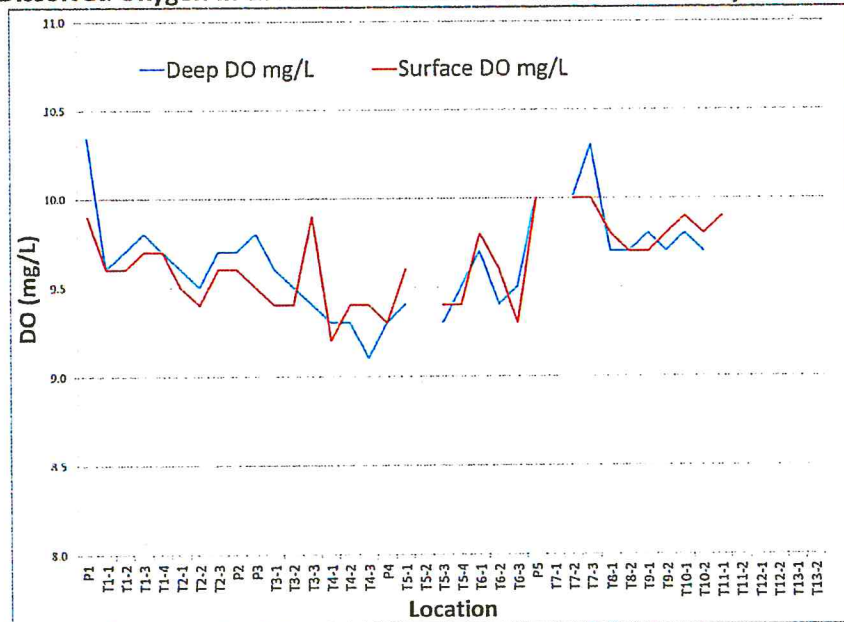


Figure 7. pH in the water column as well as from the bay to New Brunswick.

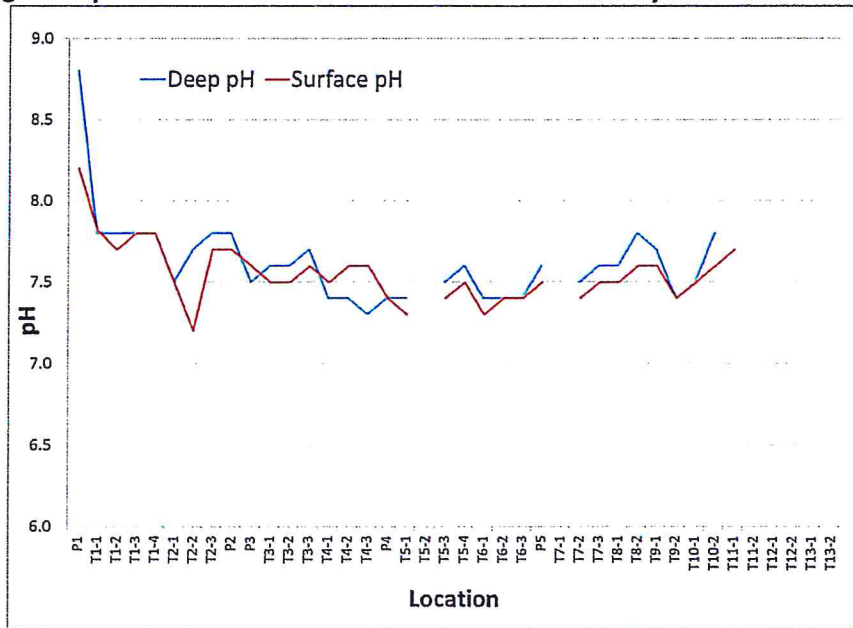


Figure 8. Oxygen Reduction Potential in the water column as well as from the bay through New Brunswick.

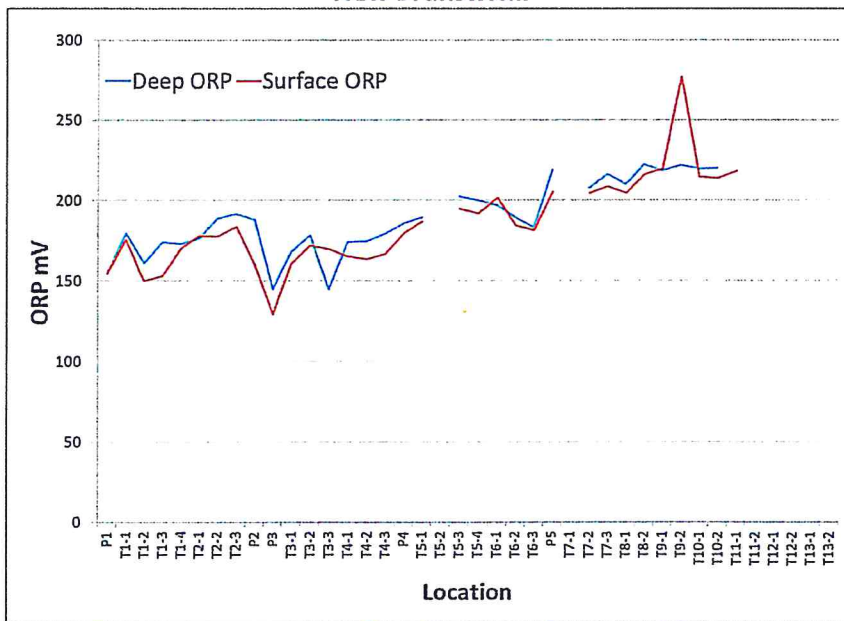


Table 1. Summary table of onsite water quality measurements at the Lower Raritan River

Location	Temp oC	Cond S/m	TDS mg/L	Sal ppt	pH	ORP mV	Turb NTU	DO% DO mg/L	Temp oC	Cond S/m	TDS mg/L	Sal ppt	pH	ORP mV	Turb NTU	DO% DO mg/L		
P1	8.6	22.9	14.9	13.8	8.8	155	7.6	97.2	10.3	22.7	14.7	13.6	8.2	155	7.2	93.2	9.9	
P2	8.7	21.9	14.2	13.1	7.8	188	N/A	91.7	9.7	19.4	12.6	12.6	7.7	160	9.4	90.7	9.6	
P3	8.9	23.0	14.9	13.9	7.5	145	6.3	92.8	9.8	21.4	13.9	12.8	7.6	129	8.8	90.8	9.5	
P4	9.9	10.3	6.7	5.0	7.4	186	14.1	96.1	9.3	9.1	5.9	5.1	7.4	180	19.2	82.7	9.3	
P5	11.5	2.8	1.8	1.4	7.6	219	17.5	93.1	10.0	2.6	1.7	1.4	7.5	206	18.0	93.2	10.0	
T1-1	8.3	24.6	16.0	14.9	7.8	180	N/A	90.7	9.6	28.3	14.4	13.2	7.8	176	8.7	90.1	9.6	
T1-2	8.3	23.9	15.6	14.5	7.8	161	N/A	91.5	9.7	20.1	13.1	12.0	7.7	150	8.4	90.4	9.6	
T1-3	8.5	22.7	14.7	13.6	7.8	174	N/A	92.0	9.8	19.6	12.7	11.6	7.8	153	8.6	90.7	9.7	
T1-4	9.0	18.5	11.3	9.7	7.8	173	9.3	90.9	9.7	9.3	15.4	10.0	9.0	7.8	171	9.7	90.5	9.7
T2-1	9.7	17.2	11.2	10.1	7.5	176	9.2	90.2	9.6	14.3	9.3	8.3	7.5	178	10.2	88.8	9.5	
T2-2	8.4	22.9	14.3	15.0	7.7	189	7.4	89.8	9.5	20.6	13.4	12.3	7.2	178	7.6	90.0	9.4	
T2-3	8.6	22.8	14.7	13.7	7.8	192	N/A	91.5	9.7	20.6	13.4	12.3	7.7	184	7.1	91.5	9.6	
T3-1	10.2	12.6	8.2	7.2	7.6	168	11.7	86.6	9.6	11.5	7.4	6.5	7.5	161	11.2	88.3	9.4	
T3-2	9.5	15.1	9.8	9.8	7.6	178	10.8	88.9	9.5	12.4	8.0	7.1	7.5	172	10.9	88.6	9.4	
T3-3	9.1	18.4	11.9	10.9	7.7	144	16.2	88.3	9.4	9.9	17.0	10.0	7.6	170	13.9	87.6	9.9	
T4-1	9.8	11.5	7.6	6.3	7.4	174	13.1	86.2	9.3	10.6	8.5	4.7	7.5	166	12.2	86.4	9.2	
T4-2	10.0	13.6	8.8	7.8	7.4	174	10.6	86.6	9.3	7.8	5.5	4.7	7.5	166	11.9	88.6	9.4	
T4-3	9.1	18.0	11.7	10.7	7.3	179	9.4	84.7	9.1	10.5	8.3	5.8	4.6	167	11.7	86.9	9.4	
T5-1	10.8	7.1	4.6	3.9	7.4	189	20.0	87.4	9.4	7.0	4.5	3.8	7.3	187	18.3	89.1	9.6	
T5-2	N/R	N/R	N/R	N/R	N/R	N/R	N/R	N/R	N/R	N/R	N/R	N/R	N/R	N/R	N/R	N/R	N/R	
T5-3	10.5	11.4	7.4	6.5	7.5	203	16.9	88.3	9.3	10.5	11.5	6.5	7.4	195	17.9	88.5	9.4	
T5-4	10.3	11.0	7.5	6.6	7.6	200	13.9	89.3	9.5	11.2	11.6	6.6	7.5	202	14.3	88.2	9.4	
T6-1	11.1	9.6	2.3	1.9	7.4	197	18.2	83.2	9.7	3.6	2.3	1.9	7.3	202	18.3	80.3	9.8	
T6-2	10.9	10.0	6.5	6.7	7.4	189	12.8	89.1	9.4	8.9	5.9	5.2	7.4	185	12.5	89.9	9.6	
T6-3	10.4	10.8	6.9	6.1	7.4	183	10.2	87.0	9.5	10.4	6.8	6.9	7.4	182	14.9	87.3	9.3	
T7-1	N/R	N/R	N/R	N/R	N/R	N/R	N/R	N/R	N/R	N/R	N/R	N/R	N/R	N/R	N/R	N/R	N/R	
T7-2	11.6	3.2	2.0	1.6	7.5	208	20.6	93.7	10.0	3.2	2.1	1.7	7.4	205	20.6	93.1	10.0	
T7-3	11.8	1.7	1.1	0.9	7.6	216	10.4	95.6	10.3	1.7	1.1	0.8	7.5	209	17.7	93.0	10.0	
T8-1	12.0	0.3	0.2	0.1	7.6	210	16.3	90.2	9.7	0.3	0.2	0.1	7.5	205	16.8	91.8	9.8	
T8-2	12.0	0.3	0.2	0.1	7.8	222	18.0	91.1	9.7	0.3	0.2	0.1	7.6	216	16.6	90.8	9.7	
T9-1	11.9	0.3	0.2	0.1	7.7	219	11.3	91.1	9.8	0.3	0.2	0.1	7.6	220	11.5	90.8	9.7	
T9-2	12.5	0.3	0.2	0.1	7.4	222	14.9	92.2	9.7	0.3	0.2	0.1	7.4	277	14.7	92.6	9.8	
T10-1	12.1	0.3	0.2	0.1	7.5	220	19.6	92.6	9.8	0.3	0.2	0.1	7.5	215	13.4	93.4	9.9	
T10-2	11.8	0.3	0.2	0.1	7.8	220	11.4	90.0	9.7	0.3	0.2	0.1	7.6	214	10.3	91.1	9.8	
T11-1	N/R	N/R	N/R	N/R	N/R	N/R	N/R	N/R	N/R	N/R	N/R	N/R	N/R	N/R	N/R	N/R	N/R	
T11-2	N/R	N/R	N/R	N/R	N/R	N/R	N/R	N/R	N/R	N/R	N/R	N/R	N/R	N/R	N/R	N/R	N/R	
T12-1	N/R	N/R	N/R	N/R	N/R	N/R	N/R	N/R	N/R	13.9	0.3	0.2	0.1	7.8	217	22.5	97.4	10.0
T12-2	N/R	N/R	N/R	N/R	N/R	N/R	N/R	N/R	N/R	N/R	N/R	N/R	N/R	N/R	N/R	N/R	N/R	N/R
T13-1	N/R	N/R	N/R	N/R	N/R	N/R	N/R	N/R	N/R	N/R	N/R	N/R	N/R	N/R	N/R	N/R	N/R	N/R
T13-2	N/R	N/R	N/R	N/R	N/R	N/R	N/R	N/R	N/R	14.4	0.3	0.1	0.1	7.9	233	41.0	104	10.6

*N/A – the readings were below the sensor's detection limit

**N/R – no water quality readings recorded due to too shallow water

1.3.2 Metal contamination in the Raritan River sediment

Thirteen metals were analyzed, including silver (Ag), arsenic (As), beryllium (Be), cadmium (Cd), chromium (Cr), copper (Cu), mercury (Hg), nickel (Ni), lead (Pb), antimony (Sb), selenium (Se), thallium (Tl), and zinc (Zn). Average, standard deviation, minimum, and maximum concentrations are summarized in the Table 2. Metal concentrations for all the sampling locations are detailed in Table 3.

Metal concentrations were compared to the low effects range (ERL) and medium effects range (ERM) values defined by Long (1979) for marine/estuarine sediment. The medium effects range implies that contamination concentration exceeding the ERM value indicates adverse benthic impacts in more than 50% of cases studied. The (ERL) on the other hand represents a concentration threshold, which when exceeded adverse benthic impacts are likely found in approximately 10% of studies.

Site P1 located in the bay itself showed the lowest concentrations for metals compared to all other sites. All metals with the exception of Cd and Cr exceed the ERL criteria in almost all sites. Mercury on the other hand exceeded the ERM criteria in almost all sites (Table 3). Lead showed higher concentrations near the bay with decreasing concentrations upriver and never exceeded the ERM criteria at any of the sampling locations.

P1, T8-2 and T13-2 locations show the least concern in terms of ecotoxicology. On the other hand T12-2 is the most trouble among the measured locations as it exceeds ERM values for Ag, As and Hg and exceeded the ERL threshold for all the other metals.

Table 2. Summary statistics of metal concentration in the Raritan River sediment, along with the available ERM and ERL criteria.

	Ag, mg/kg	As, mg/kg	Be, mg/kg	Cd, mg/kg	Cr, mg/kg	Cu, mg/kg	Hg, mg/kg	Ni, mg/kg	Pb, mg/kg	Sb, mg/kg	Se, mg/kg	Ti, mg/kg	Zn, mg/kg
Average	1.75	25.5	20.7	1.30	0.71	52.2	156	1.17	27.6	82.2	0.50	1.27	0.24
Std	1.12	20.7	3.67	0.30	0.90	25.0	91.4	0.50	5.53	34.0	0.47	0.94	0.06
Min.	0.12	3.67	0.31	0.08	0.08	3.86	10.3	0.27	5.47	11.0	0.01	0.18	0.04
Max.	6.25	103	70	2.32	6.12	160	543	2.45	39.2	173	2.31	4.57	0.45
ERM	3.70	70	70	9.60	370	270	34	0.71	52	218	47	218	410
ERL	1.00	8.20	8.20	1.20	81	34	34	0.15	21	21	47	21	150

Table 3. Metal concentration in the Raritan River sediment – marking the exceedance of ERM (red) and ERL (yellow) criteria

Location	Ag, mg/kg	As, mg/kg	Be, mg/kg	Cd, mg/kg	Cr, mg/kg	Cu, mg/kg	Hg, mg/kg	Ni, mg/kg	Pb, mg/kg	Sb, mg/kg	Se, mg/kg	Ti, mg/kg	Zn, mg/kg
P1	0.116	3.67	0.078	3.86	3.86	10.3	0.27	5.47	11.0	0.01	0.18	0.04	0.06
P2	1.65	21.1	6.12	53.6	247	247	1.01	29	153	27.6	82.2	0.24	198
P3	2.37	40.5	0.823	74.2	217	217	1.03	35.6	173	34.0	0.47	0.94	54.1
P4	1.99	20.9	0.661	55.2	138	138	1.11	28.8	80.7	27.6	82.2	0.24	198
P5	0.888	24.2	0.457	45.4	110	110	1.01	25.9	56.6	11.0	0.01	0.18	0.04
T1-1	2.32	26.6	1.01	58.1	179	179	1.92	30.1	110	238	238	0.04	44.3
T1-2	2.35	23.2	0.702	64.6	205	205	1.99	30.1	110	241	241	0.04	44.3
T1-3	1.93	18.7	0.496	51.6	136	136	1.38	28.7	95.9	202	202	0.04	44.3
T1-4	1.87	19.7	0.52	51.8	172	172	1.32	29.6	97.5	216	216	0.04	44.3
T2-1	1.87	20.4	0.476	62.6	145	145	1.42	29.1	91.7	223	223	0.04	44.3
T2-2	2	23.7	0.618	20.1	163	163	1.33	30	102	236	236	0.04	44.3
T2-3	1.84	41.8	0.63	73.6	241	241	1.93	31.5	124	240	240	0.04	44.3
T3-1	0.76	16.3	0.57	41.9	83	83	1.13	26.2	60.8	149	149	0.04	44.3
T3-2	1.68	23.6	0.634	62.9	116	116	1.17	29.5	100	226	226	0.04	44.3
T3-3	1.56	28	0.639	56.1	134	134	1.16	27.6	86.5	220	220	0.04	44.3
T4-1	1.07	15.7	0.528	45.6	159	159	0.95	23.8	67.8	183	183	0.04	44.3
T4-2	1.48	21.4	0.463	56.7	143	143	1.03	27.1	86.1	196	196	0.04	44.3
T4-3	1.69	24.6	0.507	80.3	110	110	1.03	27.7	90.5	203	203	0.04	44.3
T5-1	0.888	14.3	0.47	41.5	77.6	77.6	1.13	21.4	51.4	145	145	0.04	44.3
T5-2	1.57	20.5	0.512	57.5	107	107	0.959	28.4	85	201	201	0.04	44.3
T5-3	2.04	17.8	0.6	15.3	94.9	94.9	1.32	24.9	77.4	179	179	0.04	44.3
T5-4	2.66	23.2	0.772	63	113	113	1.23	30.1	96.1	218	218	0.04	44.3
T6-1	1.24	13.1	0.438	41.4	129	129	0.939	25.4	51.7	174	174	0.04	44.3
T6-2	1.93	21.3	0.467	51.9	131	131	1.04	26.8	74.1	174	174	0.04	44.3
T6-3	2.65	34.6	0.712	56.1	149	149	1.14	36.6	105	209	209	0.04	44.3
T7-1	0.85	16.2	0.875	96.9	247	247	2.93	39.2	144	234	234	0.04	44.3
T7-2	1.79	66.3	0.314	64.1	311	311	0.911	28.3	94.2	232	232	0.04	44.3
T7-3	1.51	27.3	0.396	49.6	102	102	0.535	26.2	70.7	142	142	0.04	44.3
T8-1	1.03	26.9	0.486	51.3	191	191	0.644	24.8	55.7	241	241	0.04	44.3
T8-2	0.292	4.7	0.088	11.6	147	147	0.273	15.5	11	48.1	48.1	0.04	44.3
T9-1	0.76	13.1	0.337	11.7	194	194	1.27	28.6	35.1	133	133	0.04	44.3
T9-2	1.29	12.7	0.492	43.6	140	140	1	35.9	57.6	163	163	0.04	44.3
T10-1	2.08	17.4	0.721	50.1	101	101	1.01	29.6	78.4	203	203	0.04	44.3
T10-2	2.43	20.4	0.77	55.8	105	105	1.05	31.1	81.4	220	220	0.04	44.3
T11-1	1.33	13.1	0.622	45.8	78.9	78.9	0.671	28	61	191	191	0.04	44.3
T11-2	1.14	11.8	0.687	43.4	95.3	95.3	0.587	27.8	56.3	180	180	0.04	44.3
T12-1	1.09	11.1	0.587	42.1	196	196	0.593	26.4	54.1	180	180	0.04	44.3
T12-2	1.06	10.3	1.12	160	162	162	1.21	37.5	130	295	295	0.04	44.3
T13-1	1.28	13.7	0.633	51.4	79.6	79.6	0.576	15.7	66.4	171	171	0.04	44.3
T13-2	0.32	6.61	0.437	34.5	49.9	49.9	0.271	26.6	38.1	133	133	0.04	44.3

1.3.3 Organics in the Raritan River sediment

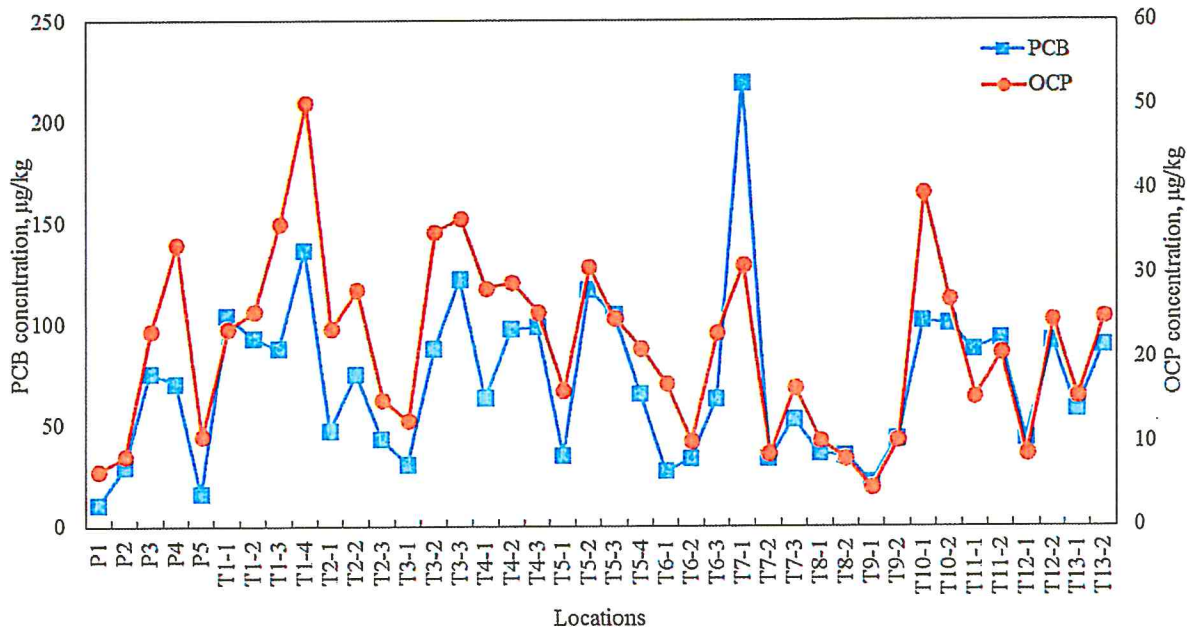
The total PCB concentration of 109 PCB congeners and total OCP concentration of 18 OCPs at each sampling location are listed in the Table 4. The PCB and OCP concentration showed the same pattern over different sampling locations as shown in the Figure 9.

The ERL and ERM for total PCB for marine/estuarine sediment are 23 µg/kg and 180 µg/kg, respectively. Except for P1 in the bay and P5 on the north side of the sand bar, all other sampling locations have PCB concentrations higher than the ERL. Location T7-1 near Crab Island has PCB concentration higher than the ERM criteria.

Table 4. Total PCB and total OCP concentration (µg/kg) at each sampling location.

Location	PCB	OCP	Location	PCB	OCP
	ug/Kg	ug/Kg		ug/Kg	ug/Kg
P1	10.5	6.59	T5-3	105	24.7
P2	29.1	8.33	T5-4	65.3	21.1
P3	75.7	23.2	T6-1	27.2	16.9
P4	70.6	33.5	T6-2	33.4	10.1
P5	16.1	10.7	T6-3	63.1	23.0
T1-1	104	23.4	T7-1	219	30.9
T1-2	93.1	25.5	T7-2	33.3	8.62
T1-3	87.6	35.8	T7-3	53.0	16.5
T1-4	136	50.2	T8-1	35.9	10.2
T2-1	47.2	23.4	T8-2	35.1	8.03
T2-2	75.2	28.0	T9-1	21.7	4.56
T2-3	43.0	15.0	T9-2	43.3	10.2
T3-1	30.4	12.5	T10-1	101	39.6
T3-2	87.7	34.9	T10-2	100.0	26.9
T3-3	122	36.5	T11-1	87.1	15.4
T4-1	63.2	28.2	T11-2	93.0	20.5
T4-2	97.6	28.9	T12-1	43.7	8.65
T4-3	98.5	25.4	T12-2	91.6	24.5
T5-1	35.0	16.1	T13-1	58.0	15.5
T5-2	117	30.7	T13-2	89.6	24.9

Figure 9. PCB and OCP concentrations in the Raritan River sediment.



1.3.3 Spatial interpolation and Geo-Accumulation Index

Trace metal and organic pollutant distribution in the river sediment

Trace metals and organic concentrations of the sampled sediments were inputted into ArcGIS 10.3 geospatial software to visualize the sediment pollution of the main channel of the Lower Raritan River. The Spatial Analyst toolset was used to take the sediment concentrations in parts per million units (ppm) at our 40 sampling points and extrapolate values in between these sampling transects to create a continuous surface of sediment contaminant information for the Lower Raritan. We chose the Inverse Distance Weighted (IDW) linear raster interpolation tool for this visualization. The raster interpolation helps to visualize any concentration gradients or hotspots of trace metal or organic pollutants in the designated area of interest.

The result of the spatial statistical analysis is shown from figure 10 through Figure 22. The most prevalent hotspot was along the TP7 transect (Crab Island), where high concentrations were observed for all metals with the exception of Cd. High concentrations also occurred along the T2 and T3 transect – close to the mouth of the river – where Hg, Pb, Ni, Sb, Se, Tl and Zn were all high compared to the rest of the study area. Cd had a single hot spot in the area of P2. Cr was prevalent in the sediment showing a clear hot spot along T12, close to New Brunswick. T7 (Crab Island) and T12 (north of the turnpike) are the sites where most of the measured metal concentrations exceed the ecological screening criteria.

To assess the collective occurrence of trace metal contamination, a cumulative metal index value was calculated for each sampling location after Gallagher (2008) using rank order transformation (Juang et al, 2001). Figure 23 shows the interpolation results. Here again we see higher concentrations clustering around the T1, T2, and T3 transect between the mouth of the river and the Garden State Parkway bridge. Another well-defined hotspot is along the P7 transect, at Crab Island. Smaller hotspots form along T12 mainly due to the high Cr, As and Zn concentration and around T5 and T6 caused by higher Zn, Tl, Pb, Ni, and Hg levels than in the rest of the study area.

Figure 24 and 25 shows the interpolation results for total PCB and OCP respectively. There appears to be a continuing presence of enriched sediments near the elbow of the river right before opening to the bay, along the T3 transect, as well as the sediments near Crab Island in Sayreville again along the T7 transect.

Figure 10. Spatial interpolation showing the distribution of Arsenic in the Lower Raritan River surficial sediment

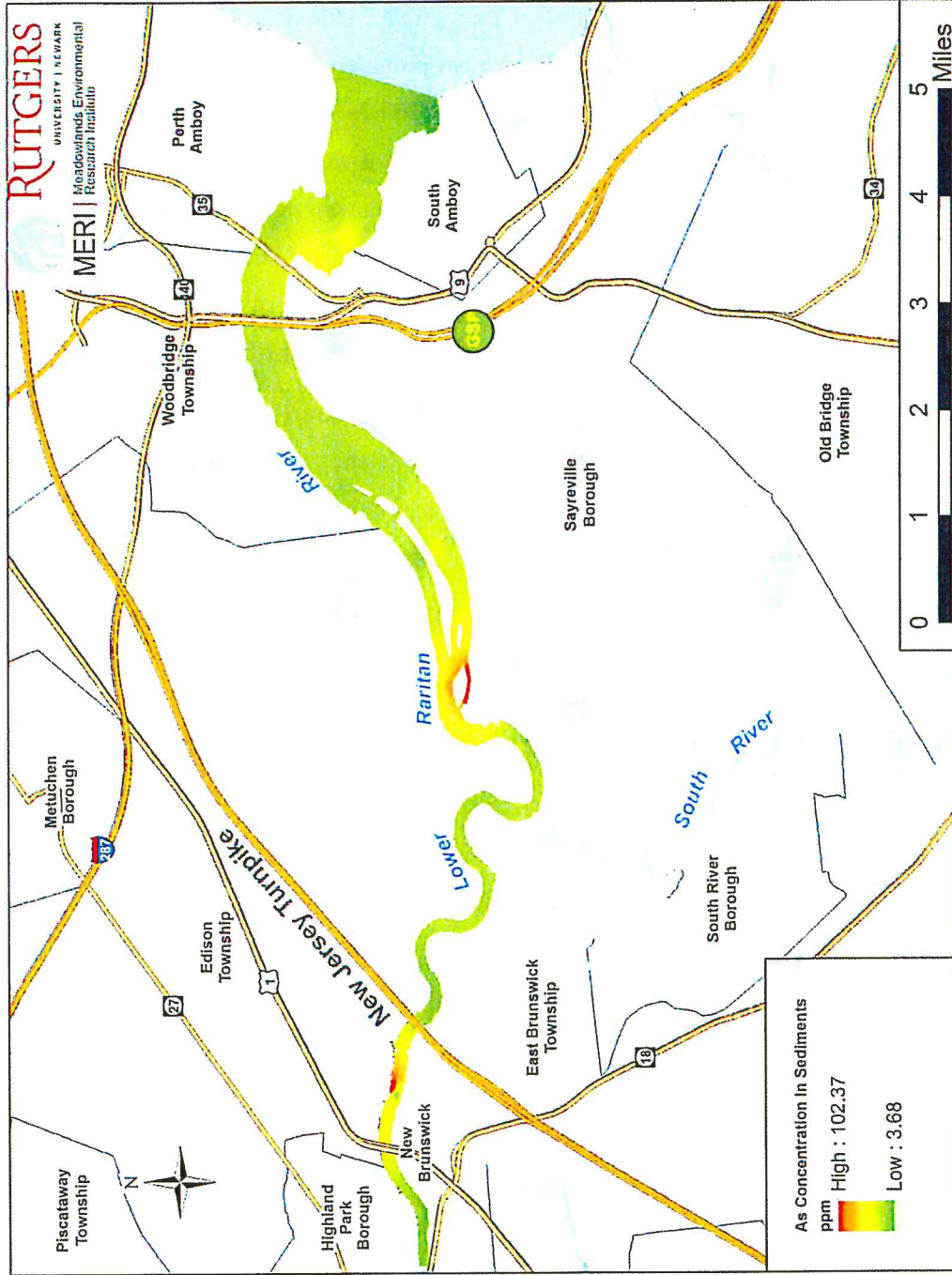


Figure 11. Spatial interpolation showing the distribution of Beryllium in the Lower Raritan River surficial sediment

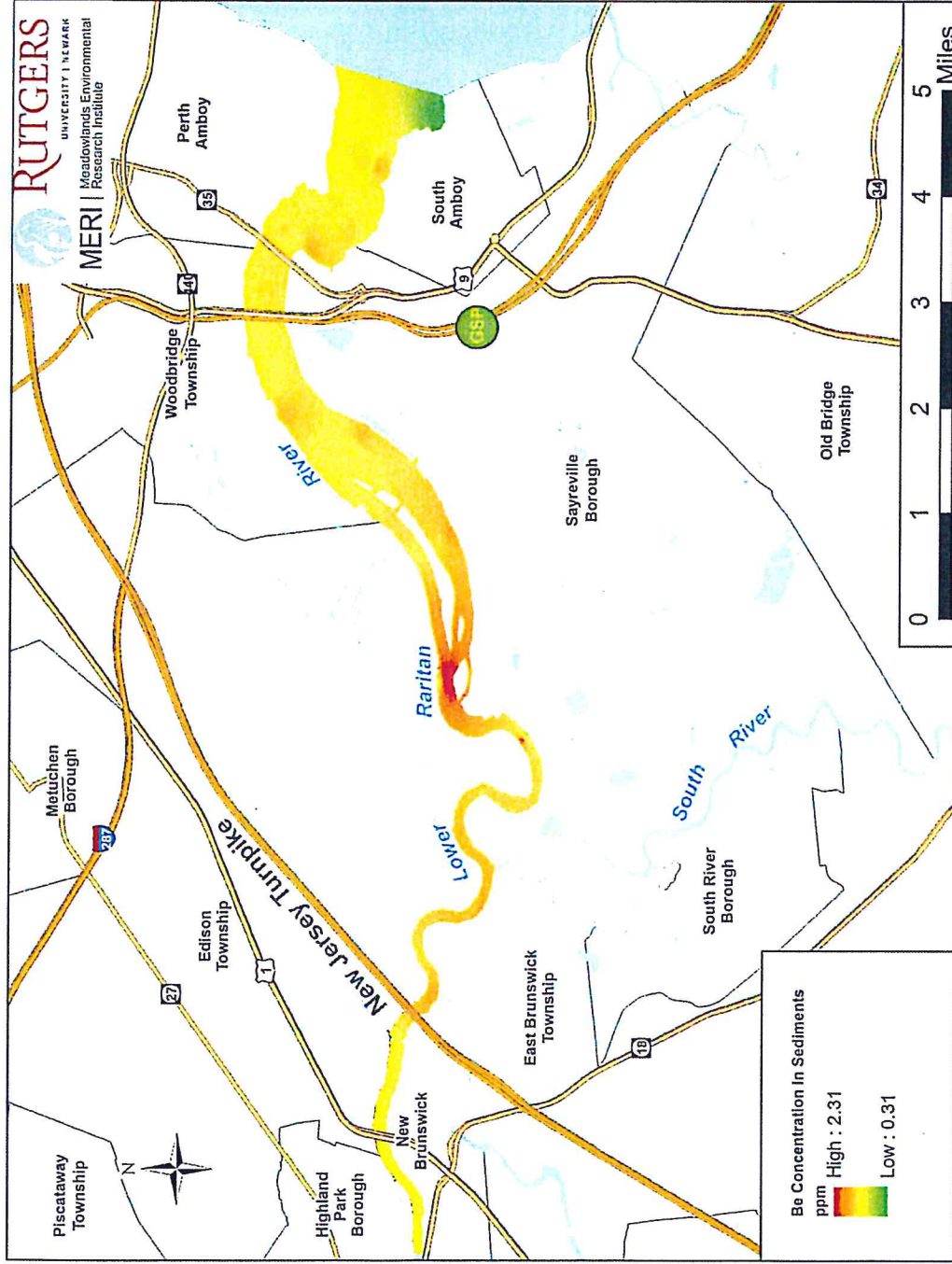


Figure 12. Spatial interpolation showing the distribution of Cadmium in the Lower Raritan River surficial sediment

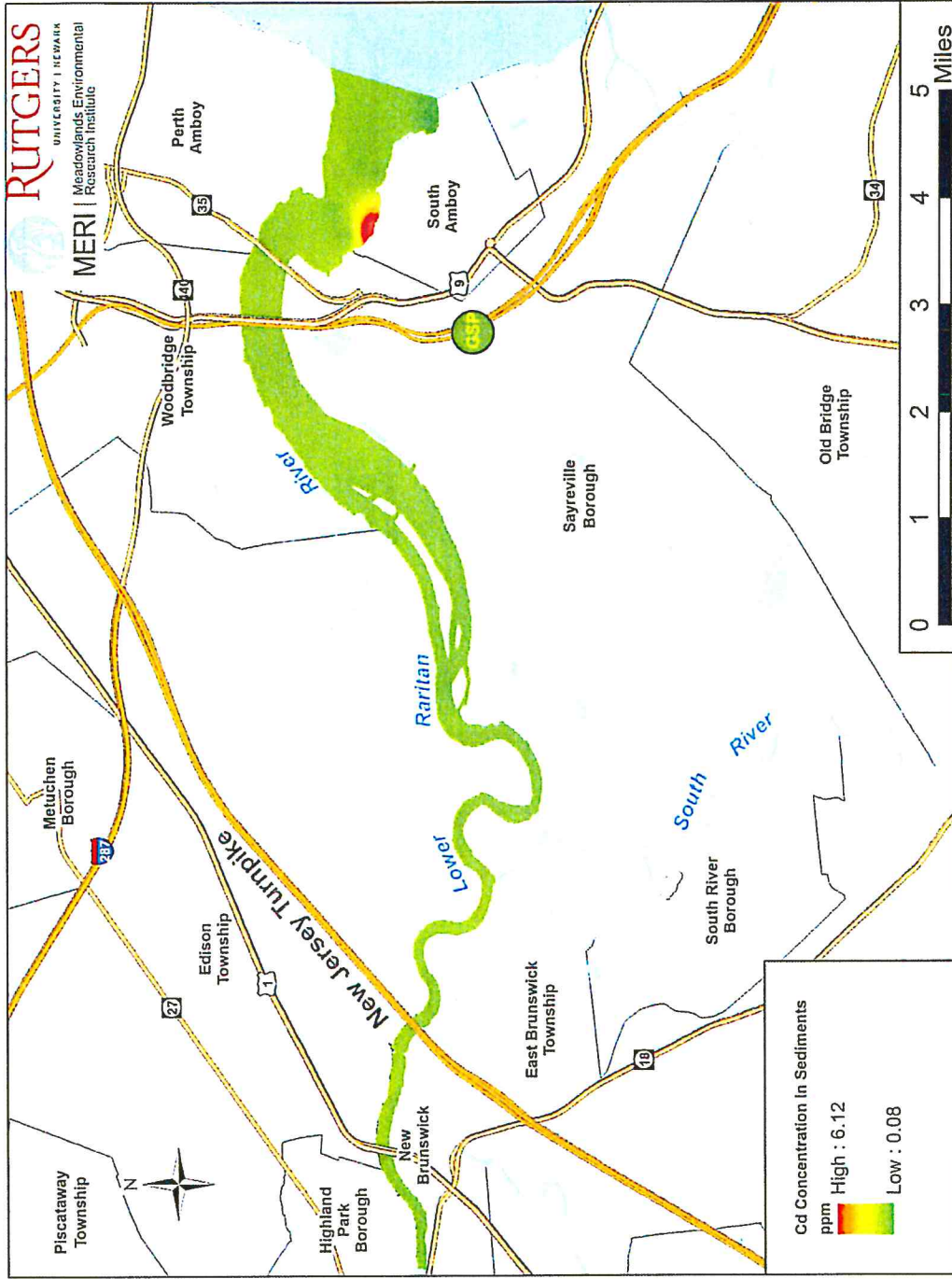


Figure 13. Spatial interpolation showing the distribution of Chromium in the Lower Raritan River surficial sediment

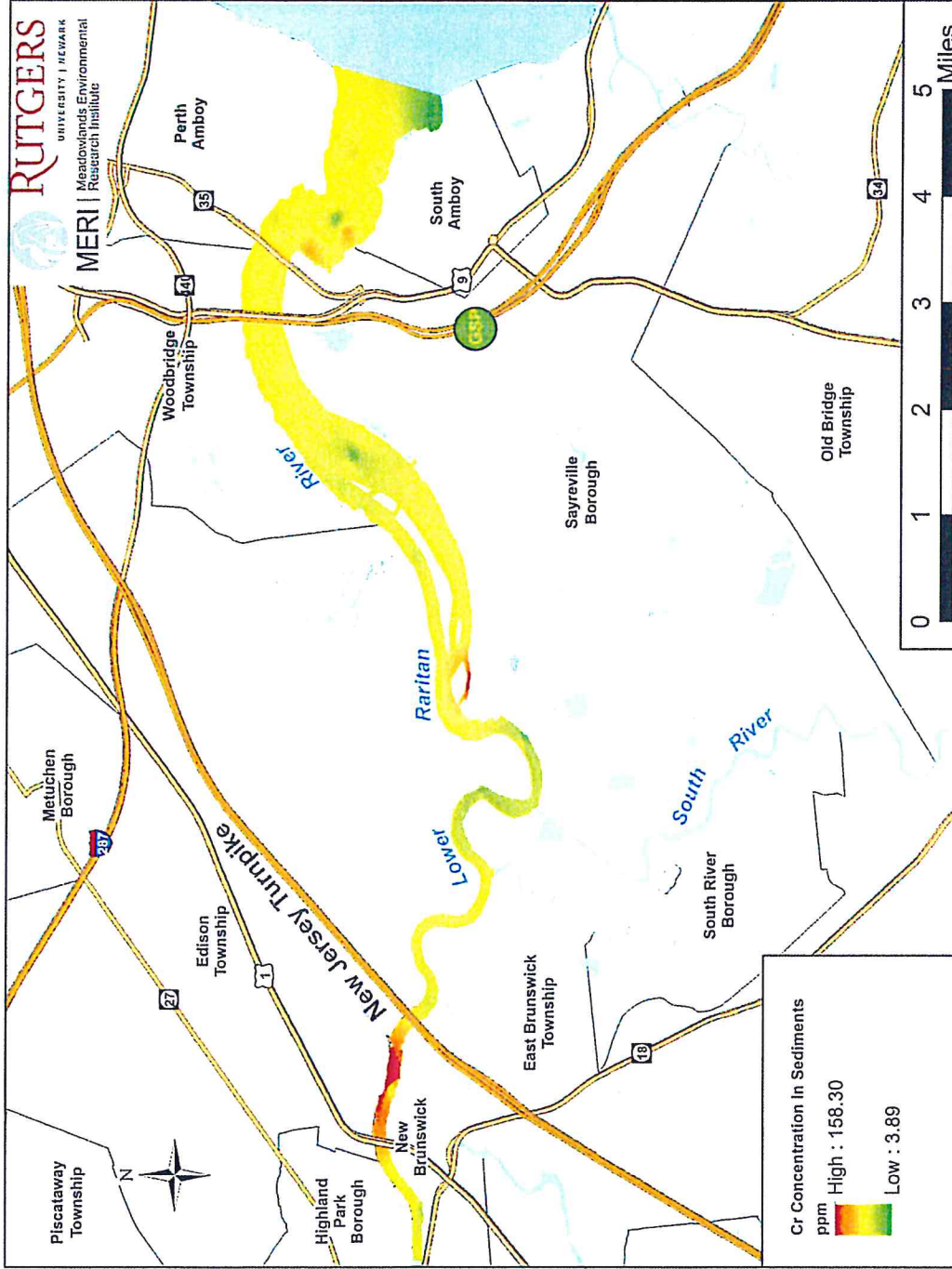


Figure 14. Spatial interpolation showing the distribution of Copper in the Lower Raritan River surficial sediment

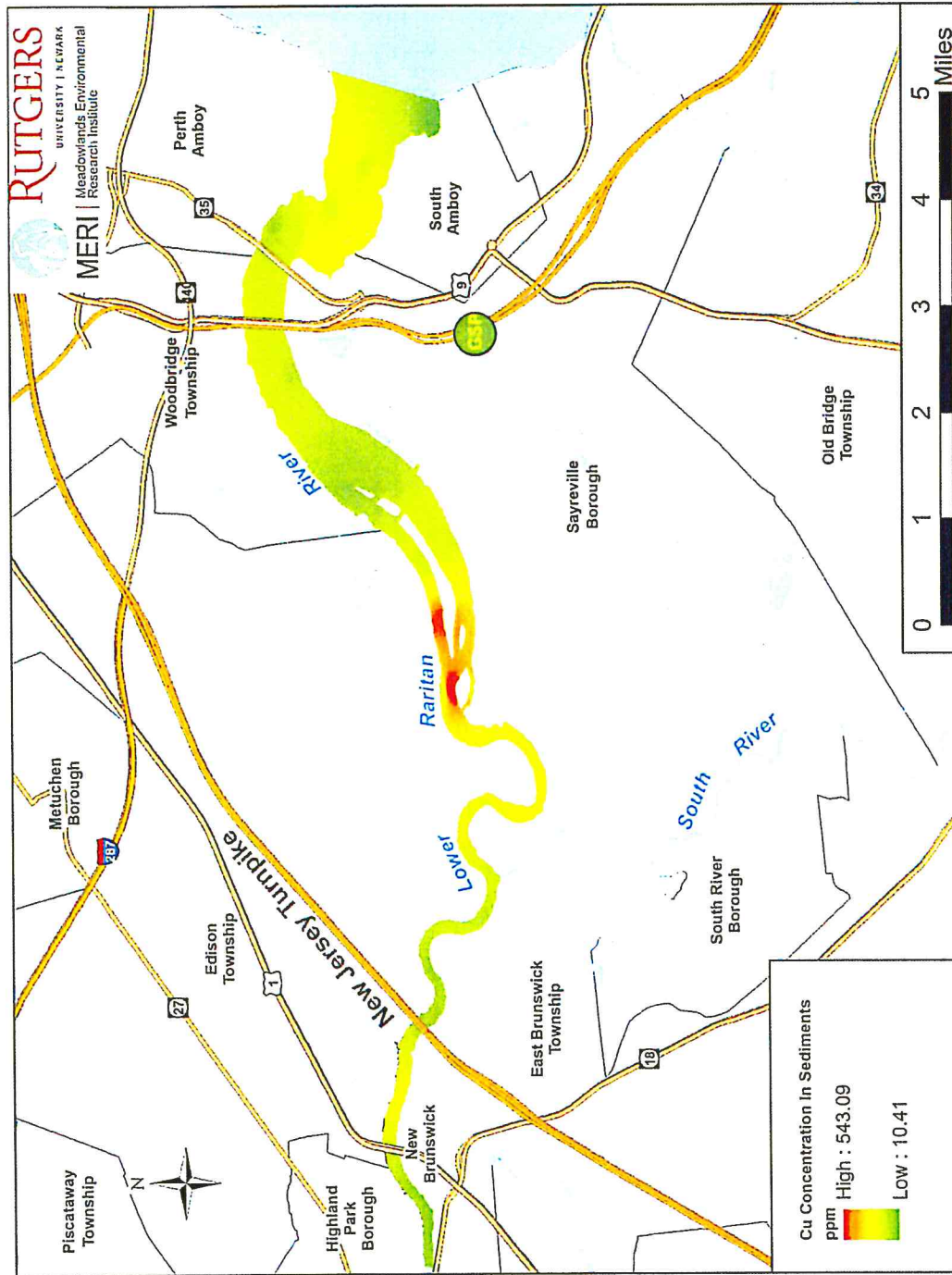


Figure 15. Spatial interpolation showing the distribution of Mercury in the Lower Raritan River surficial sediment

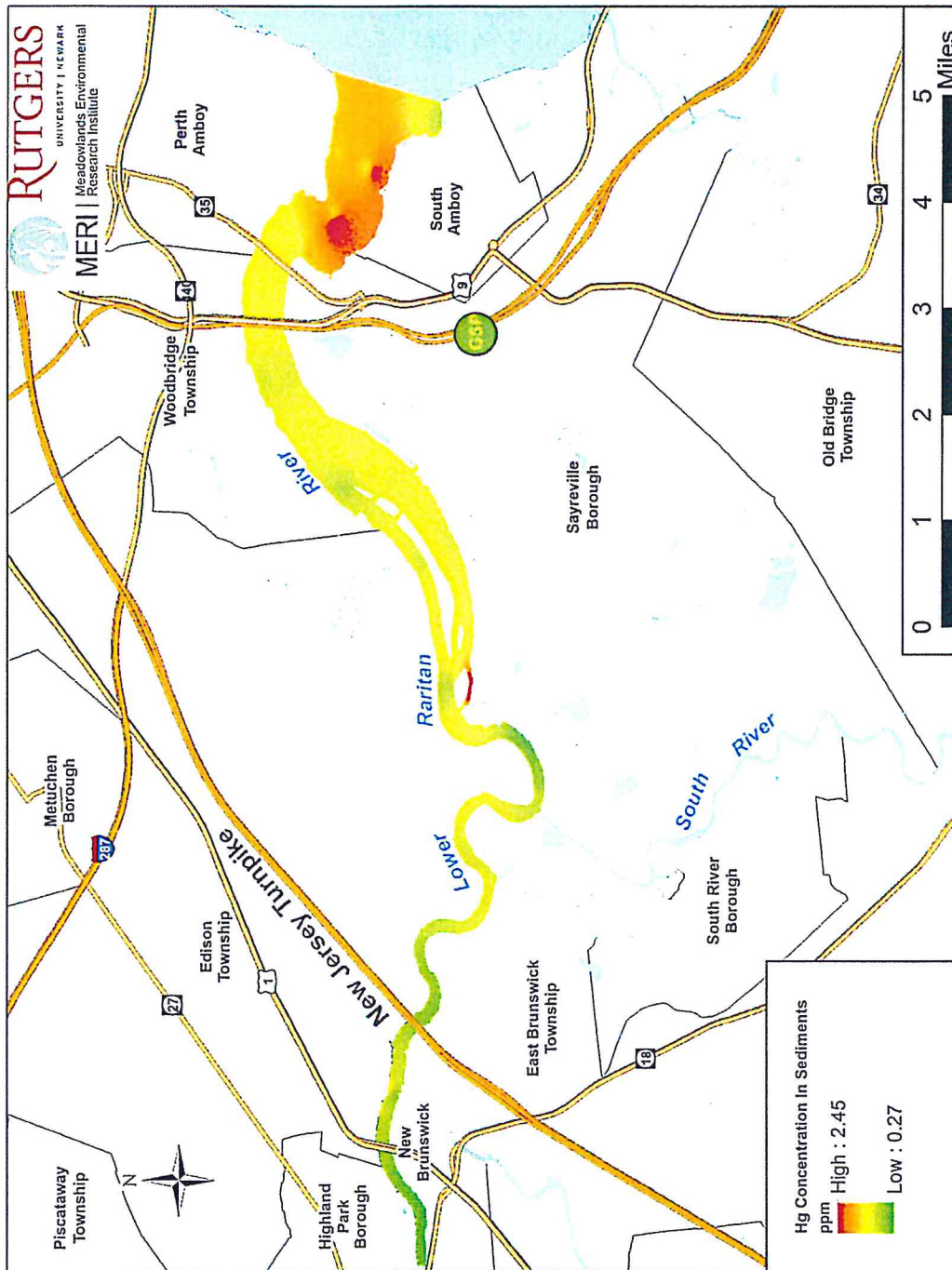


Figure 16. Spatial interpolation showing the distribution of Nickel in the Lower Raritan River surficial sediment

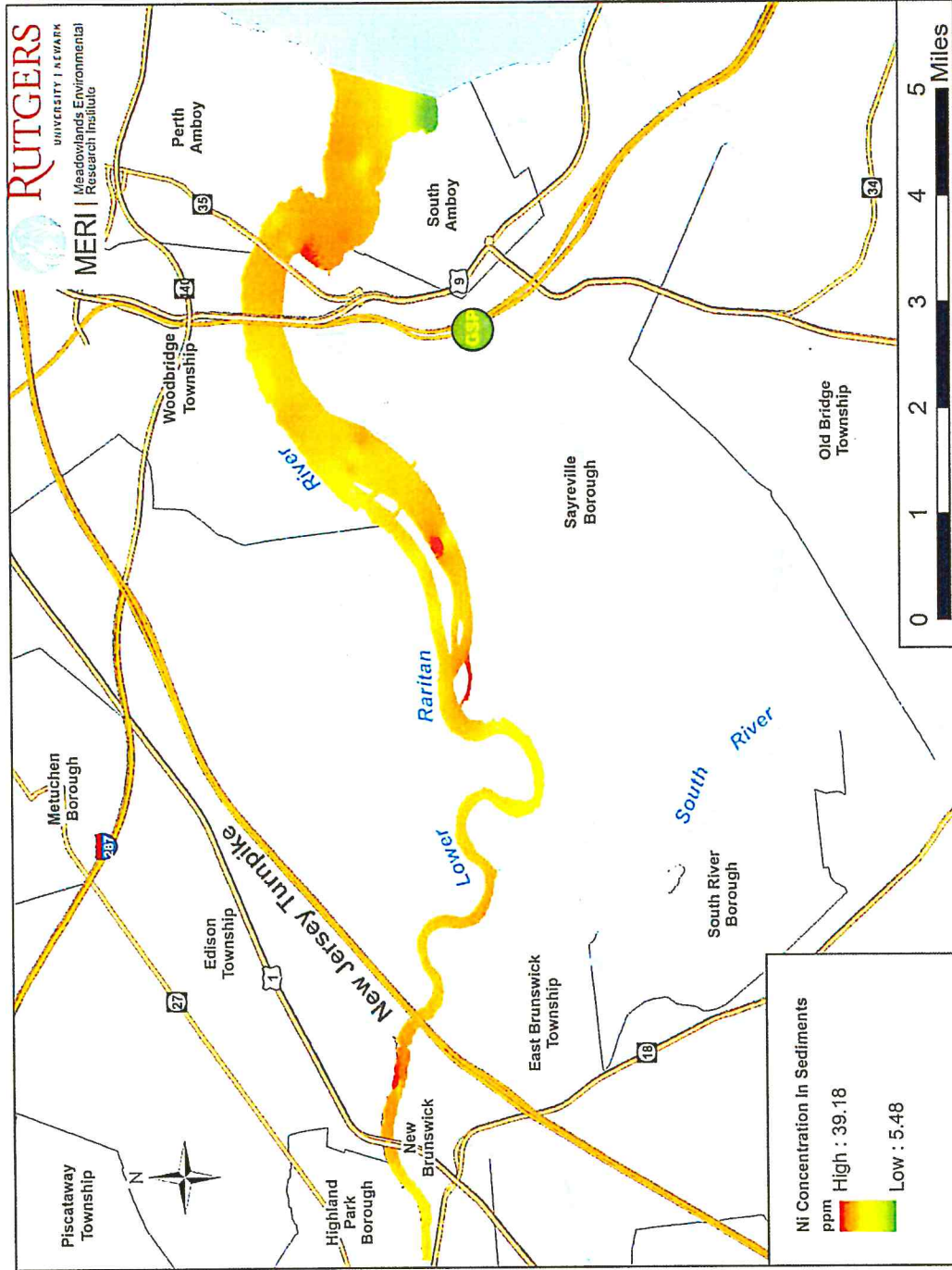


Figure 17. Spatial interpolation showing the distribution of Lead in the Lower Raritan River surficial sediment

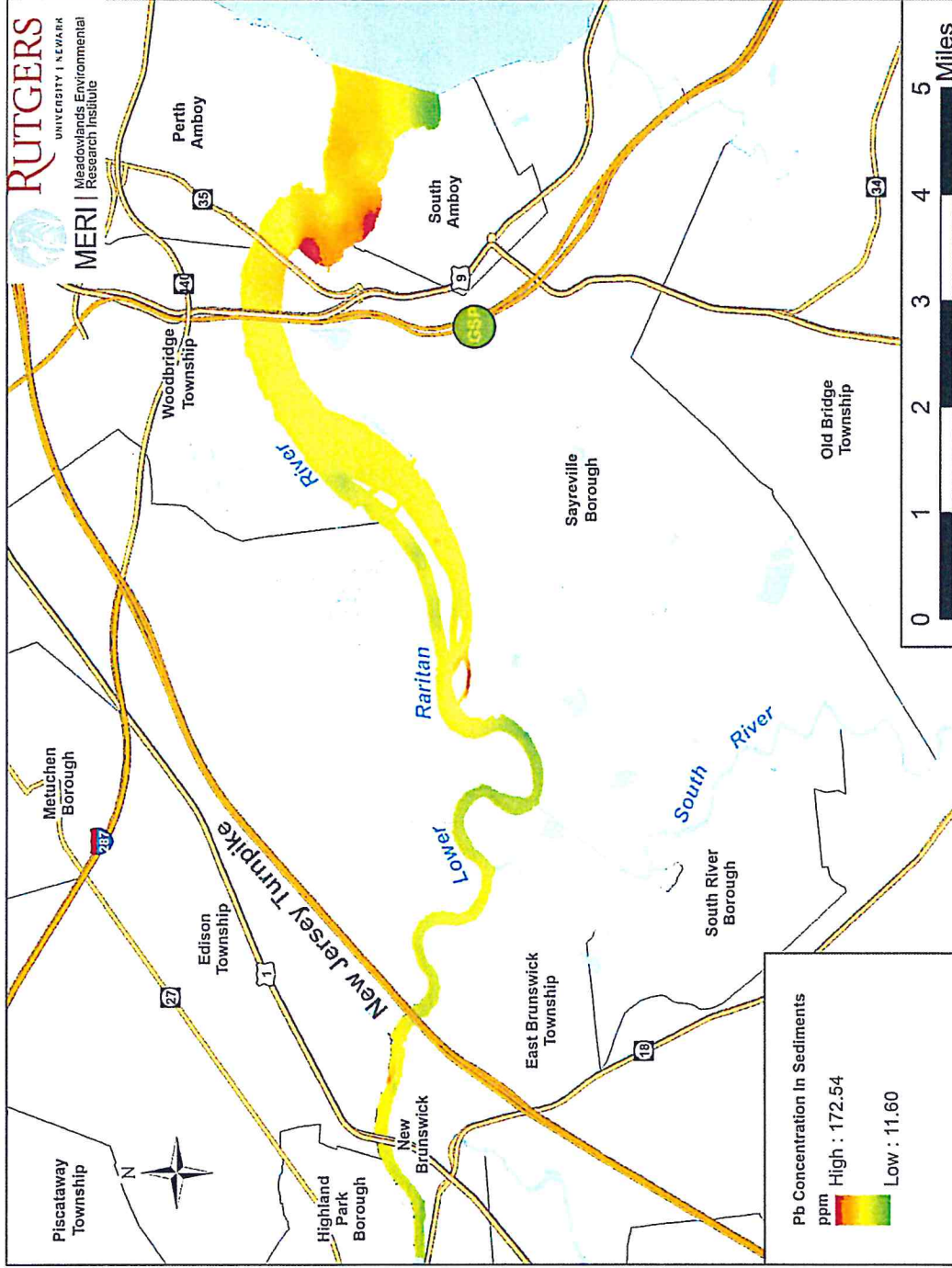


Figure 18. Spatial interpolation showing the distribution of Antimony in the Lower Raritan River surficial sediment

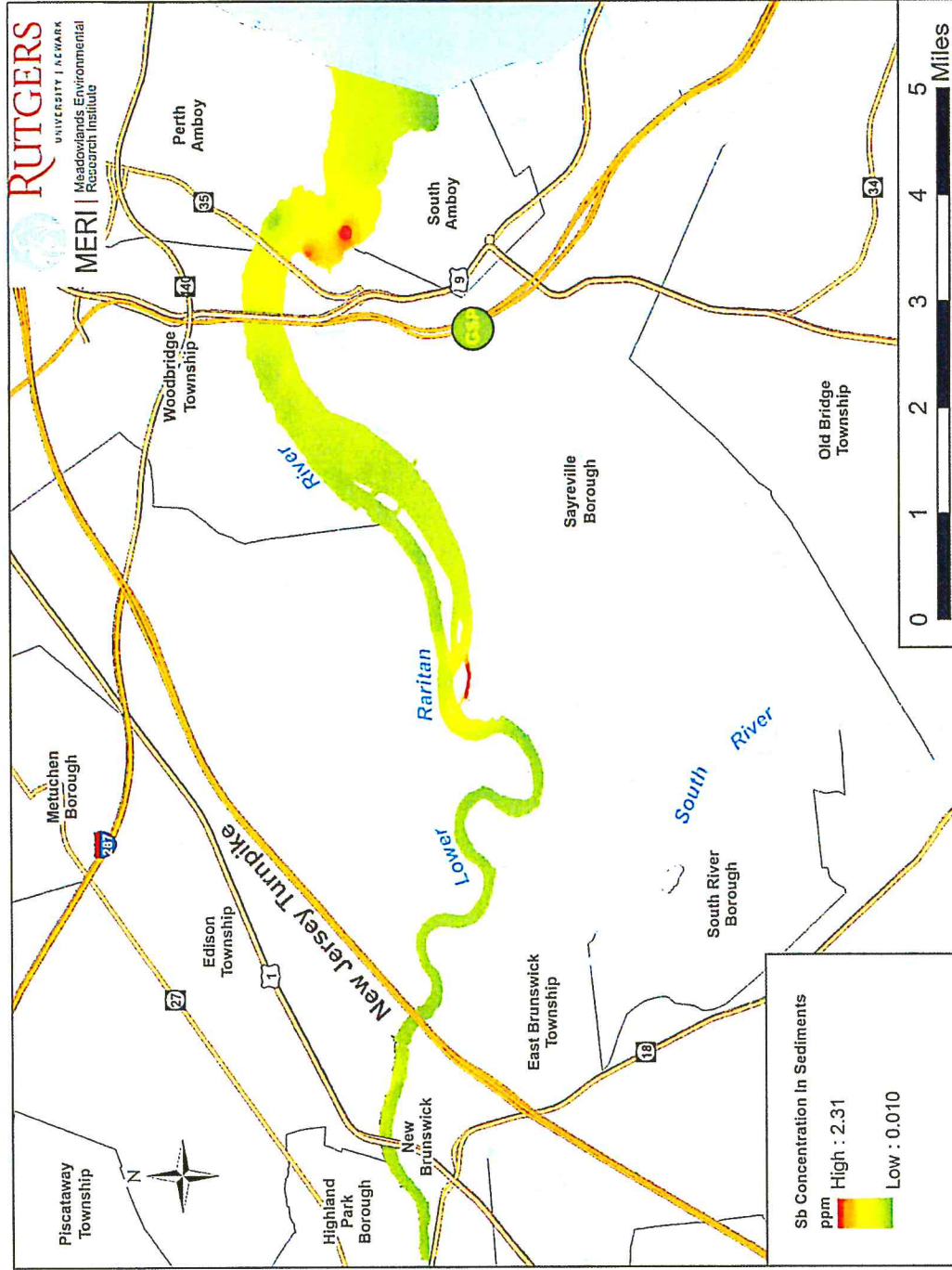


Figure 19. Spatial interpolation showing the distribution of Selenium in the Lower Raritan River surficial sediment

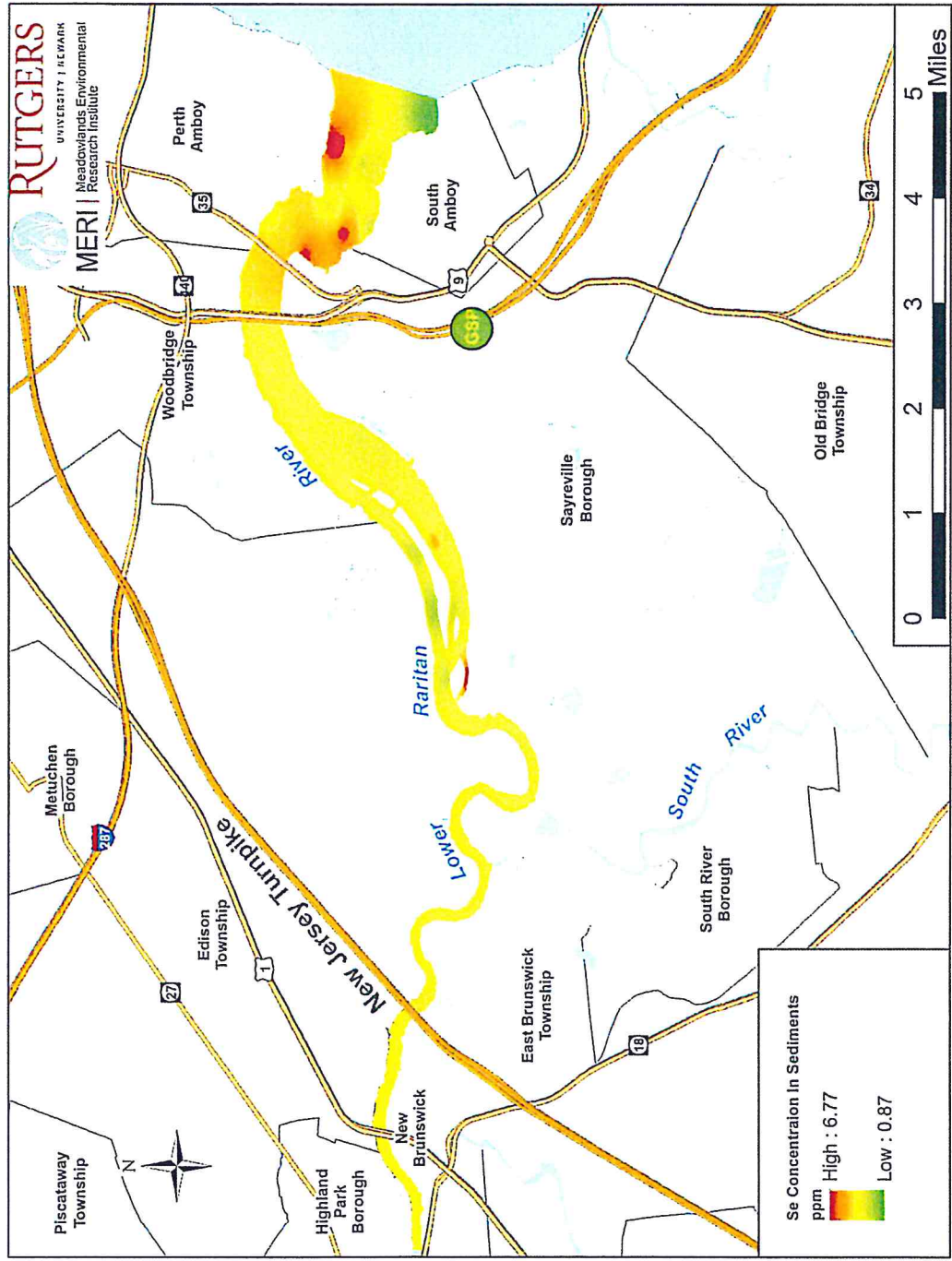


Figure 20. Spatial interpolation showing the distribution of Silver in the Lower Raritan River surficial sediment

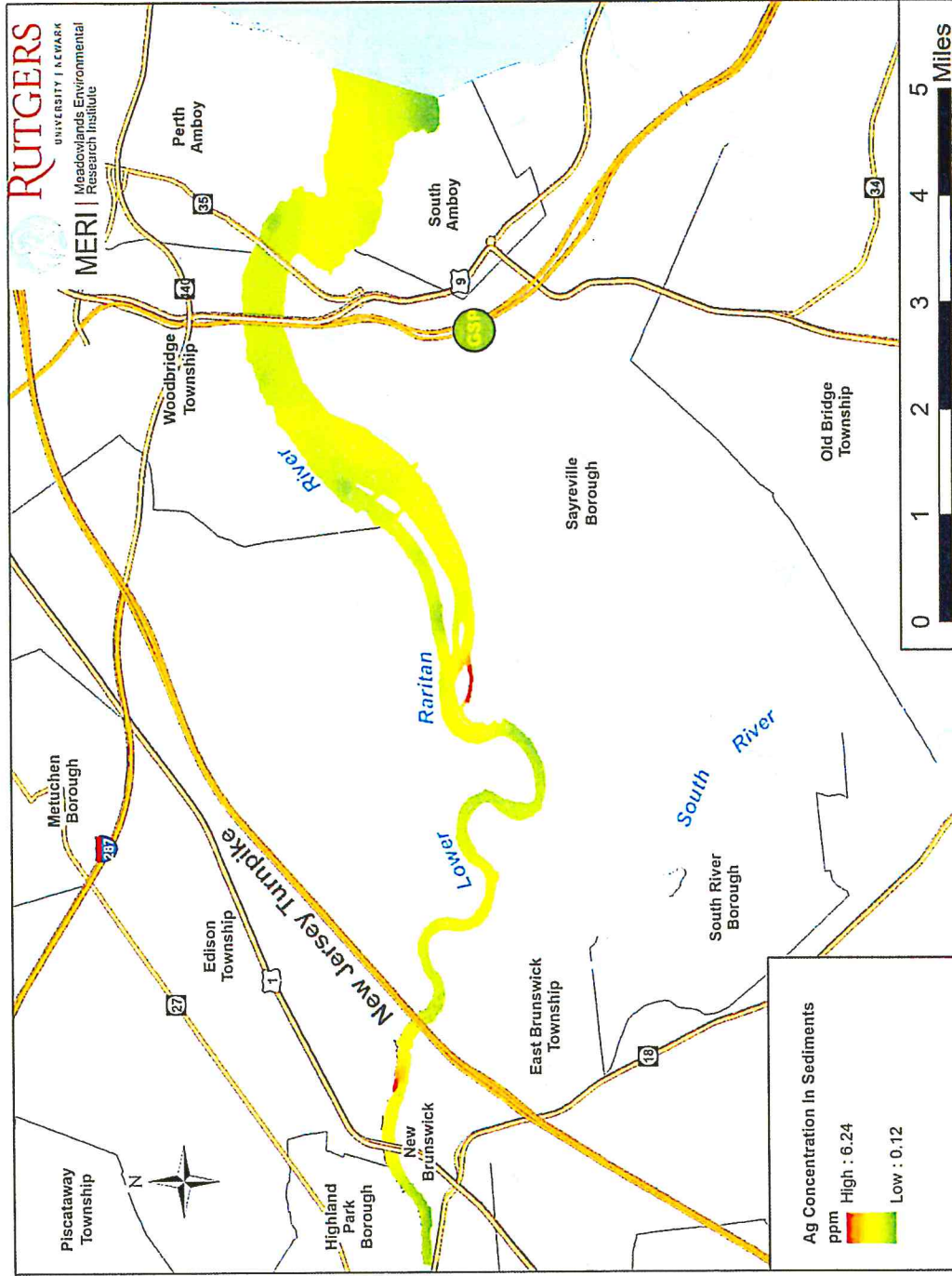


Figure 21. Spatial interpolation showing the distribution of Thallium in the Lower Raritan River surficial sediment

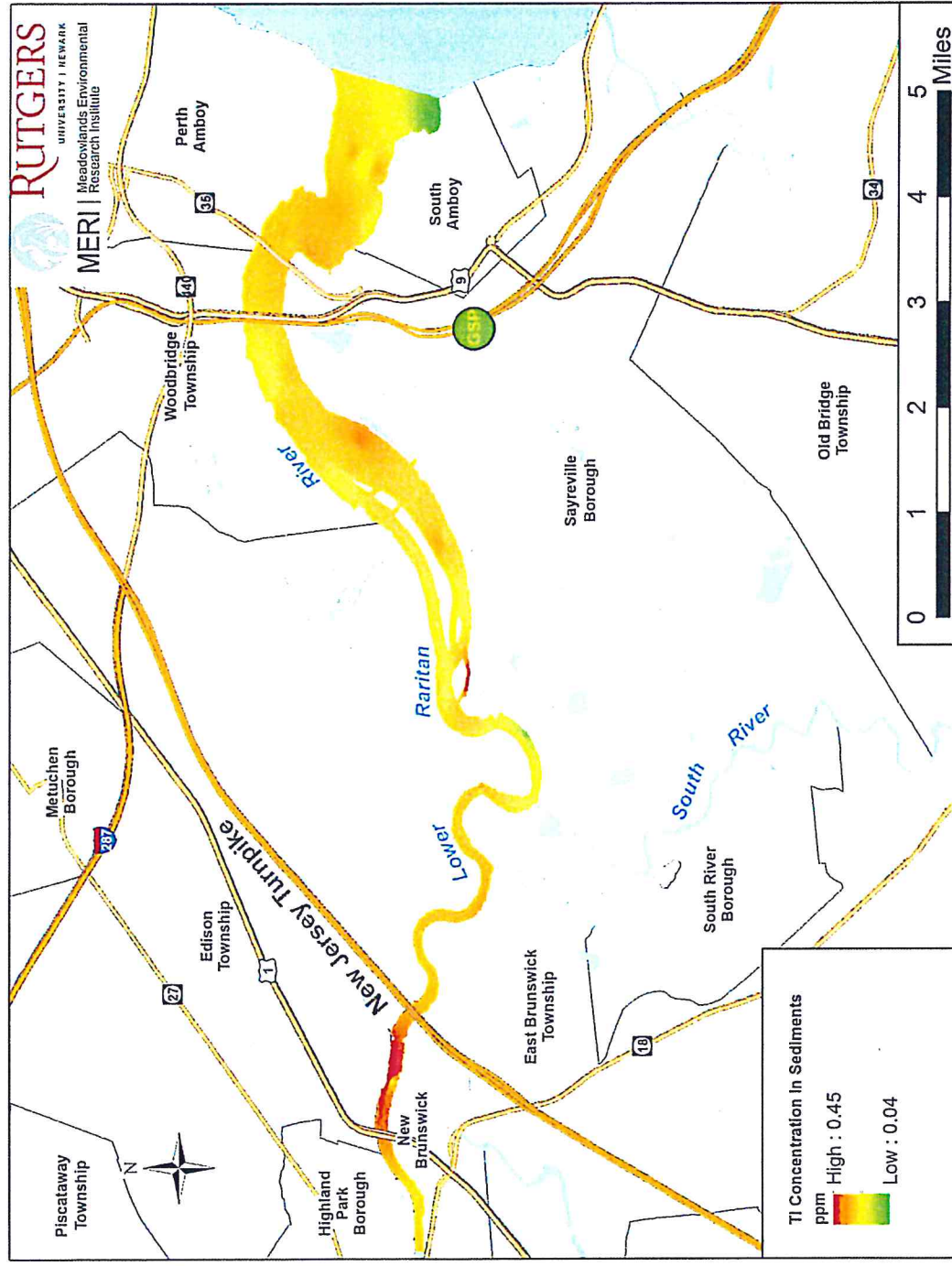


Figure 22. Spatial interpolation showing the distribution of Zinc in the Lower Raritan River surficial sediment

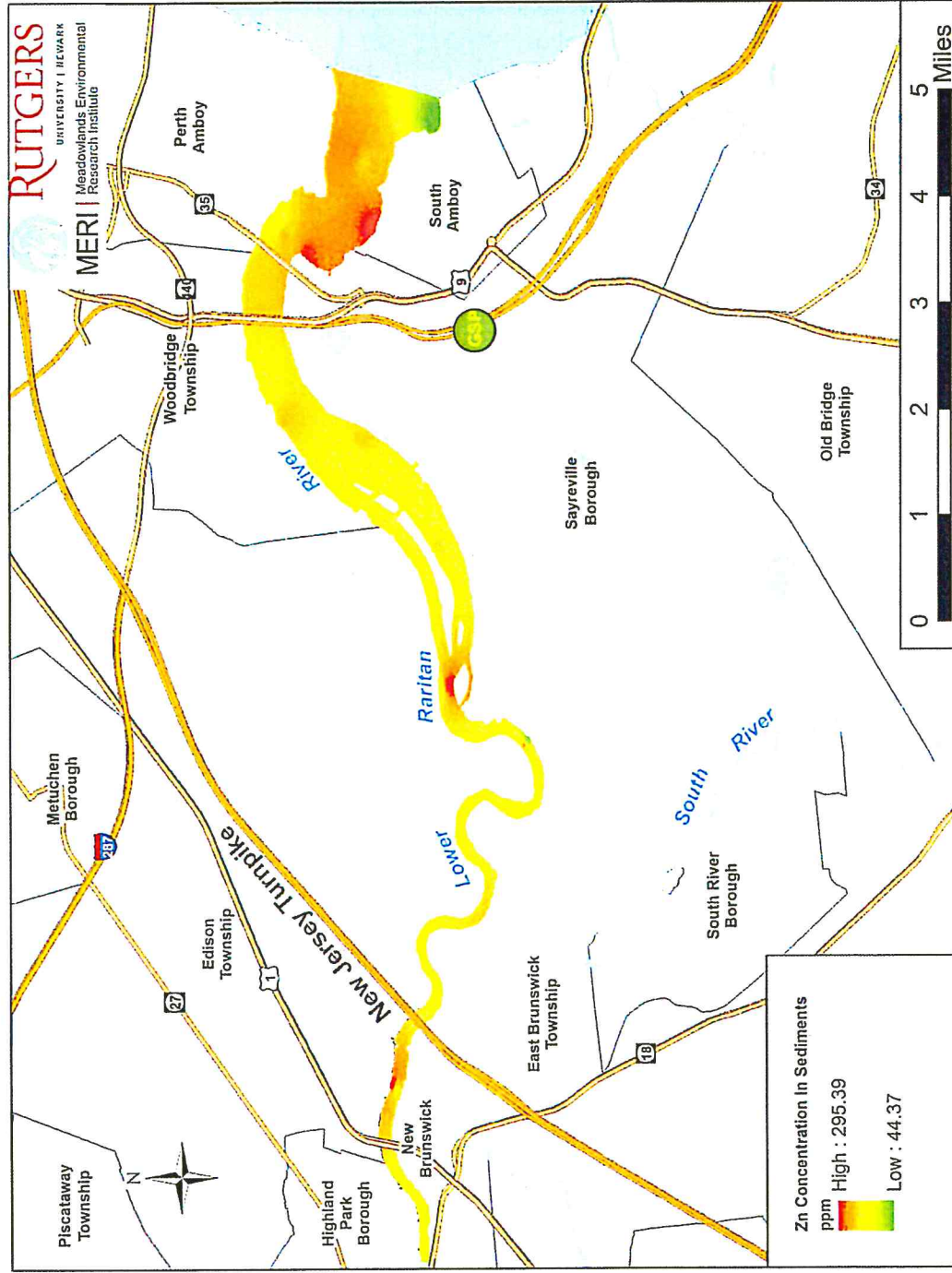


Figure 23. Spatial interpolation showing the distribution of the cumulative metal index values in the Lower Raritan River surficial sediment

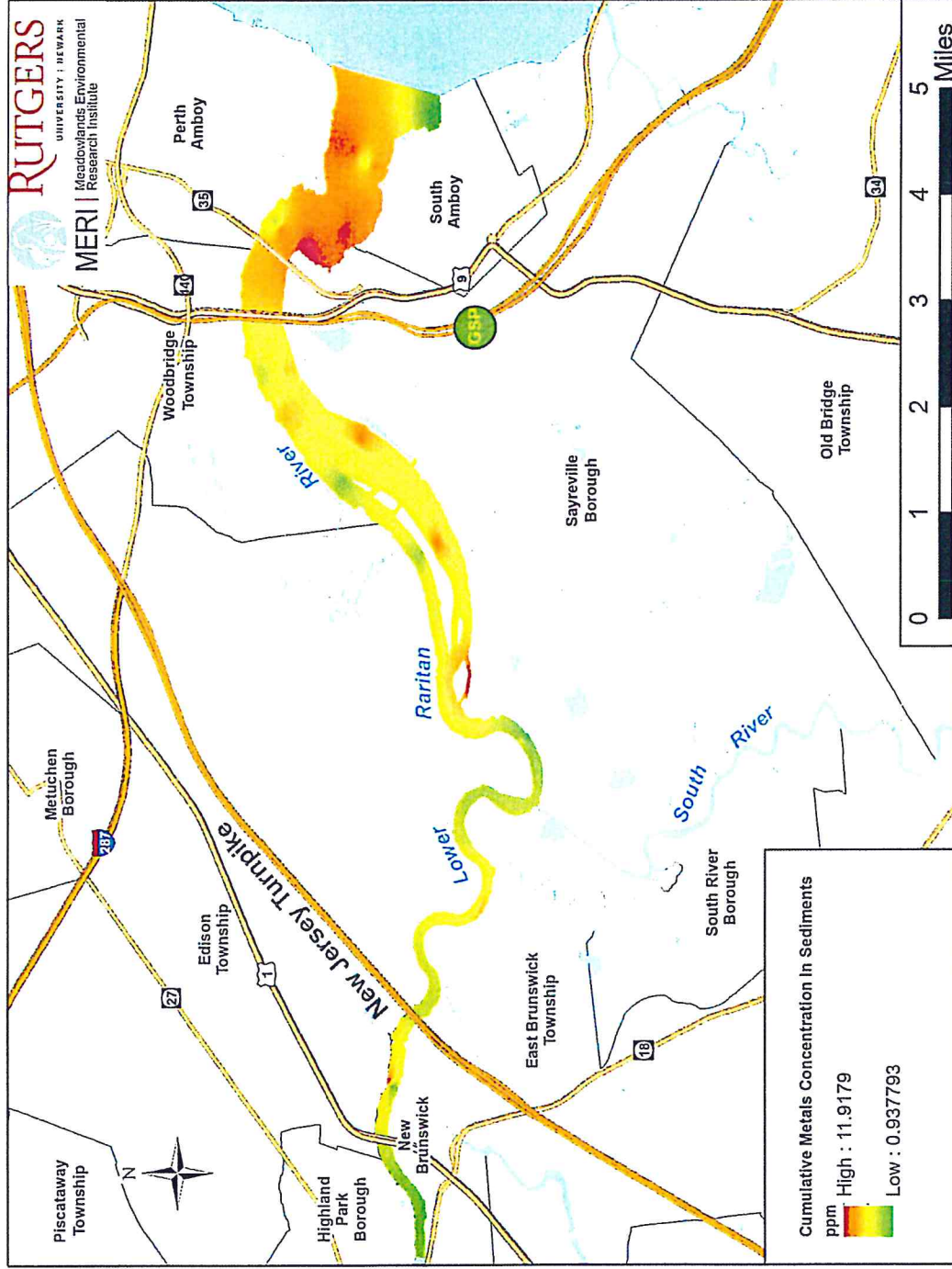


Figure 24. Spatial interpolation showing the distribution of total OCPs in the Lower Raritan River surficial sediment

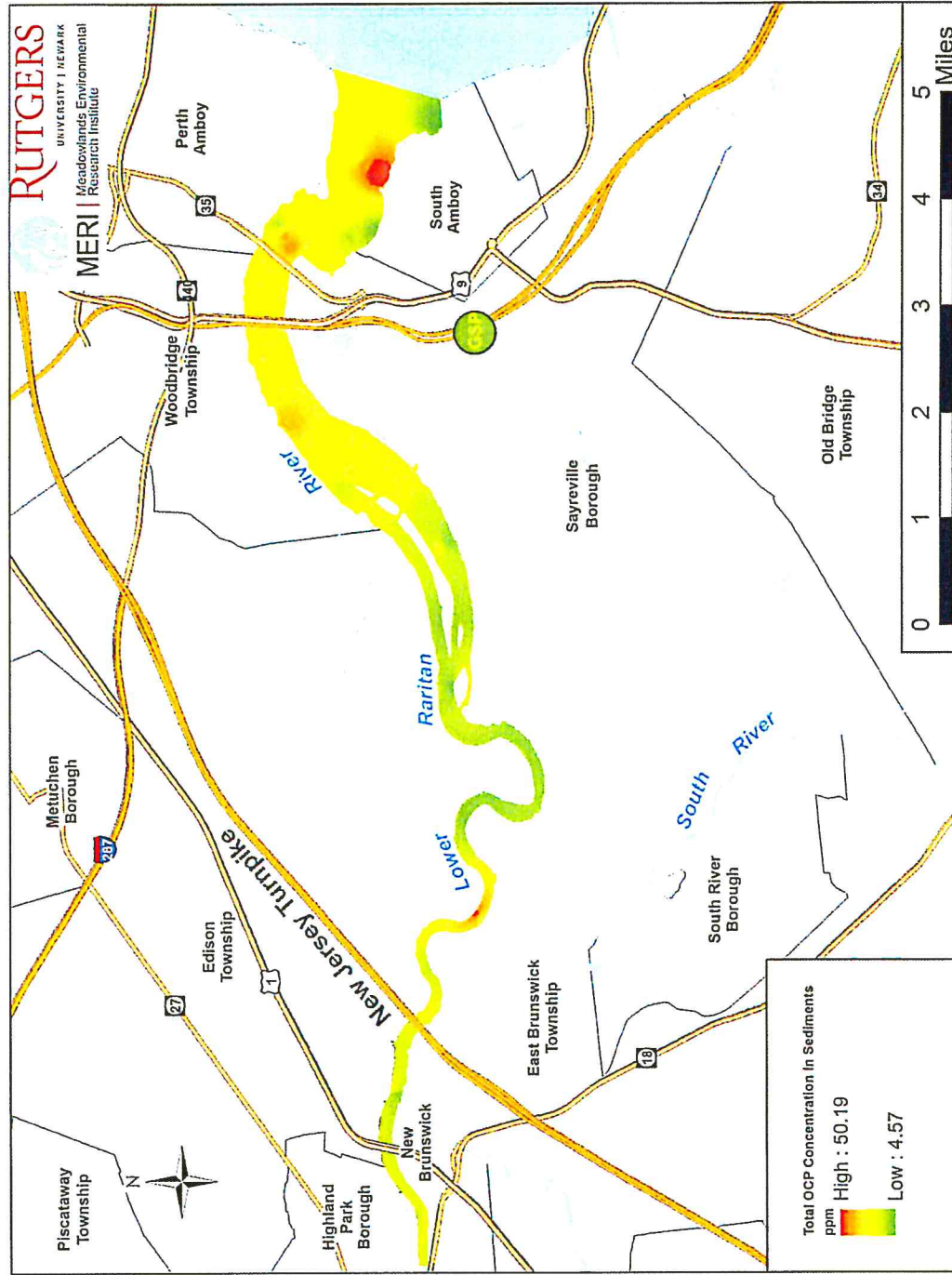
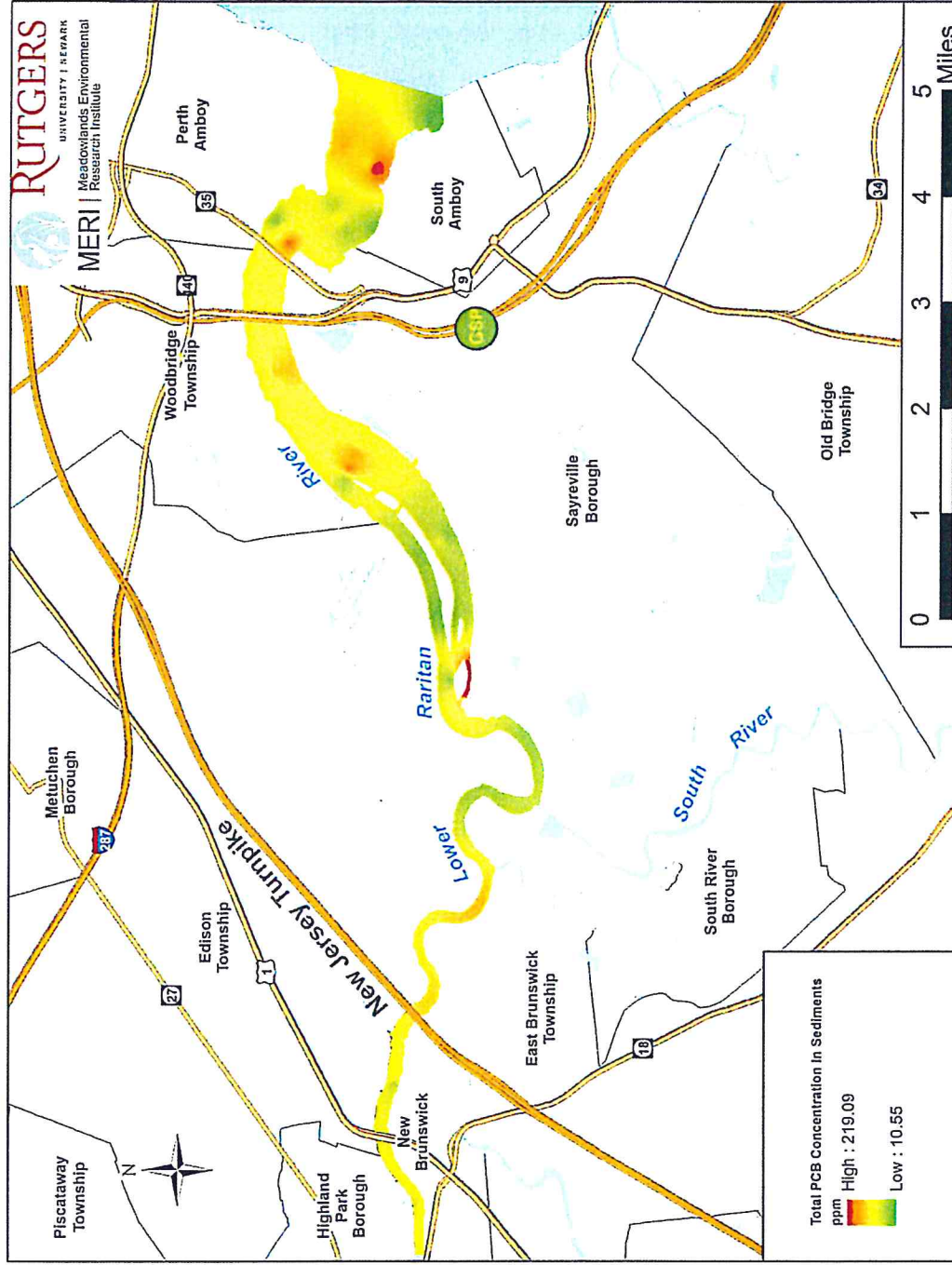


Figure 25. Spatial interpolation showing the distribution of total PCBs in the Lower Raritan River surficial sediment



Contamination compared to the natural metal accumulation in the river sediment

The Geochemical Index (Igeo) of these samples was calculated by finding available background sediment concentration values derived from the local natural geology. This index value represents the degree of anthropogenic contaminant enrichment of the observed sediment beyond the natural background value from the local geology.

The index is the logarithmic ratio of the observed concentration value to the background geologic source concentrations. The background values referenced for these calculations were documented in 'Characterization of Ambient Levels of Selected Metals and Other Analytes in New Jersey Soils: Year 1, Urban Piedmont Region' (BEM Systems Inc., 1997). The Igeo values fall into several classes that describe the degree of sediment contamination, with values less than 1 assigned 'practically uncontaminated', 1-2 being 'mildly contaminated', 2-3 being 'moderately contaminated', and Igeo values larger than 3 assigned as 'contaminated'.

The geospatial analysis of the Lower Raritan sediment data (Figures 26-38) revealed that several trace metals had significant concentrations from anthropogenic sources with Geoaccumulation Indices exceeding 2. These trace elements include: As (Figure 27), Cd (Figure 29), Cu (Figure 31), Hg (Figure 33), Se (Figure 35), and Ag (Figure 36). Interestingly Pb only shows mildly increased contamination along the T3 and T2 transects, barely exceeding the background sediment levels.

Except for Silver, Arsenic, Copper, and Mercury, none of the other metals that exceed either ERL or ERM criteria values (Table 3) show significant enrichment in the sediment when compared to the background values.

Figure 26. Spatial interpolation of the geoaccumulation index showing concentration of Antimony in the Lower Raritan River surficial sediment compared to natural background levels

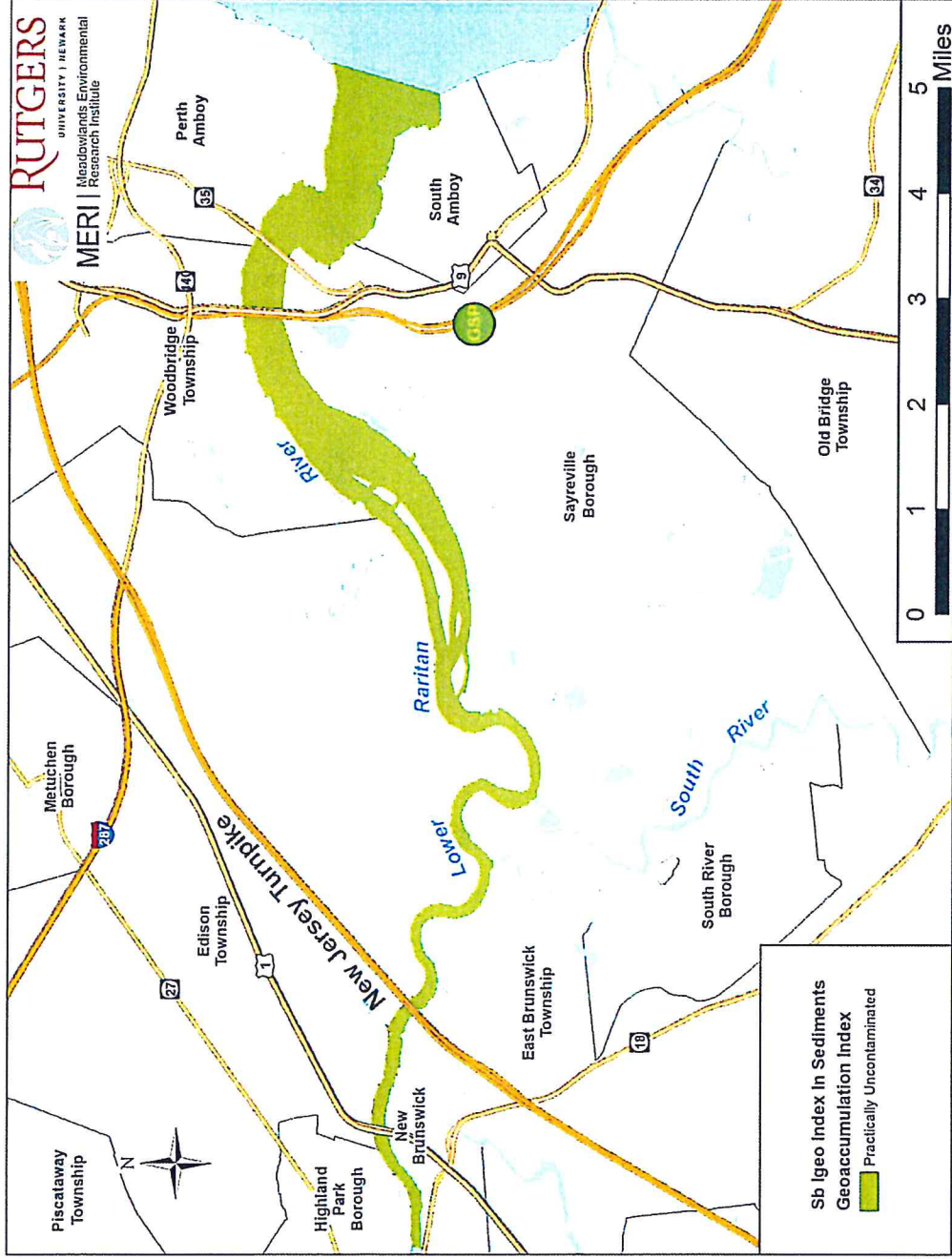


Figure 27. Spatial interpolation of the geoaccumulation index showing concentration of Arsenic in the Lower Raritan River surficial sediment compared to natural background levels

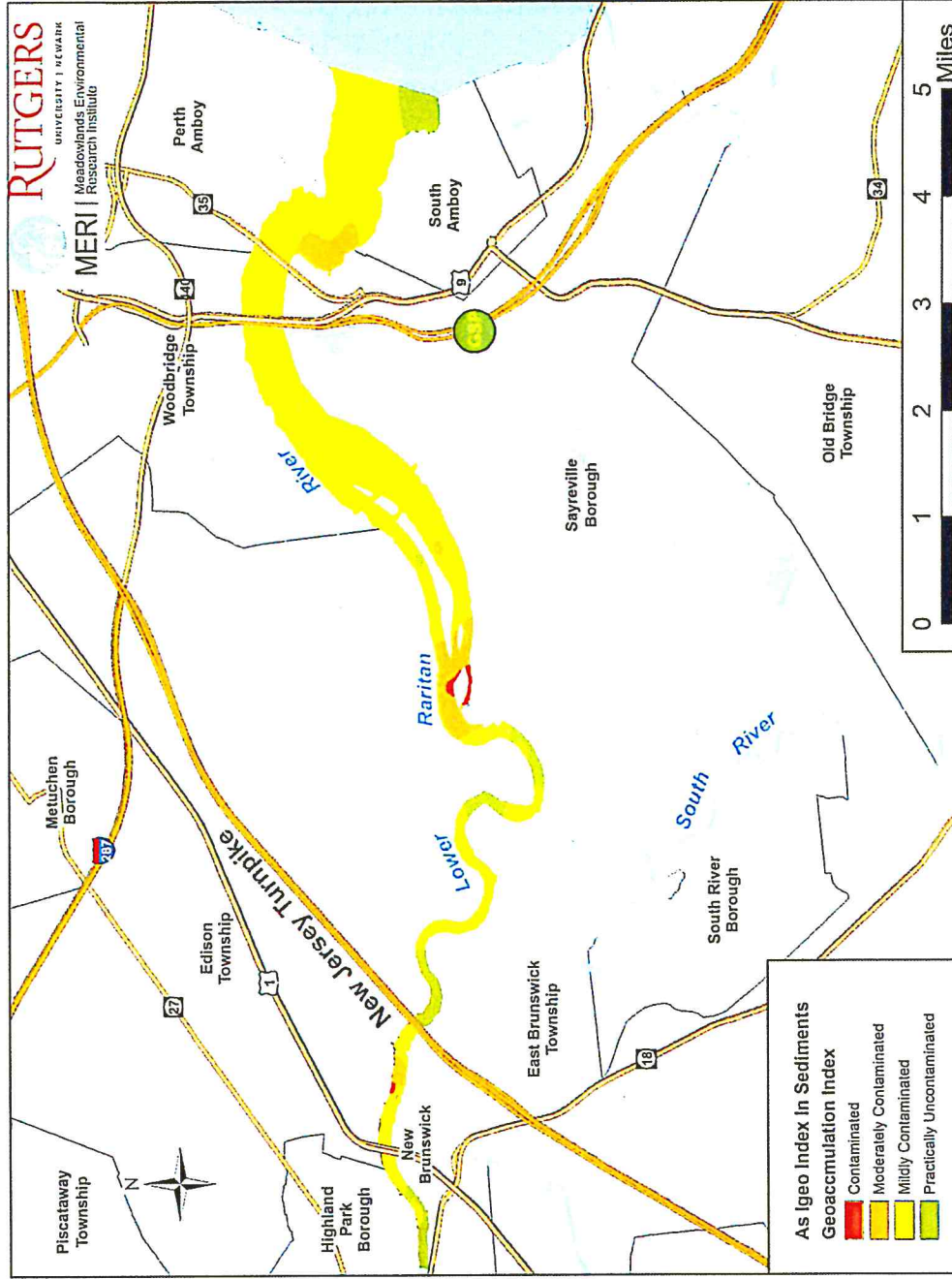


Figure 28. Spatial interpolation of the geoaccumulation index showing concentration of Beryllium in the Lower Raritan River surficial sediment compared to natural background levels

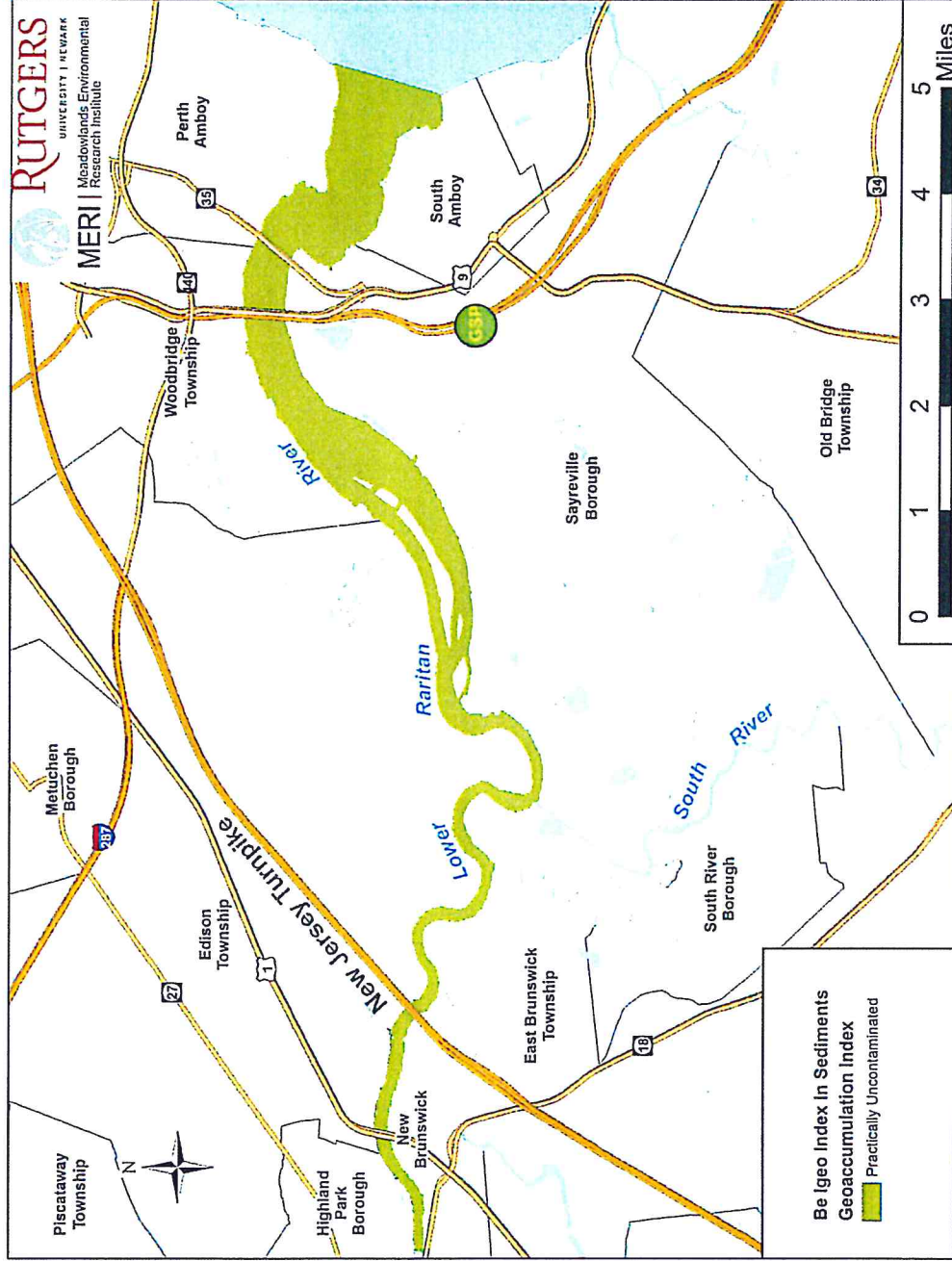


Figure 29. Spatial interpolation of the geoaccumulation index showing concentration of Cadmium in the Lower Raritan River surficial sediment compared to natural background levels

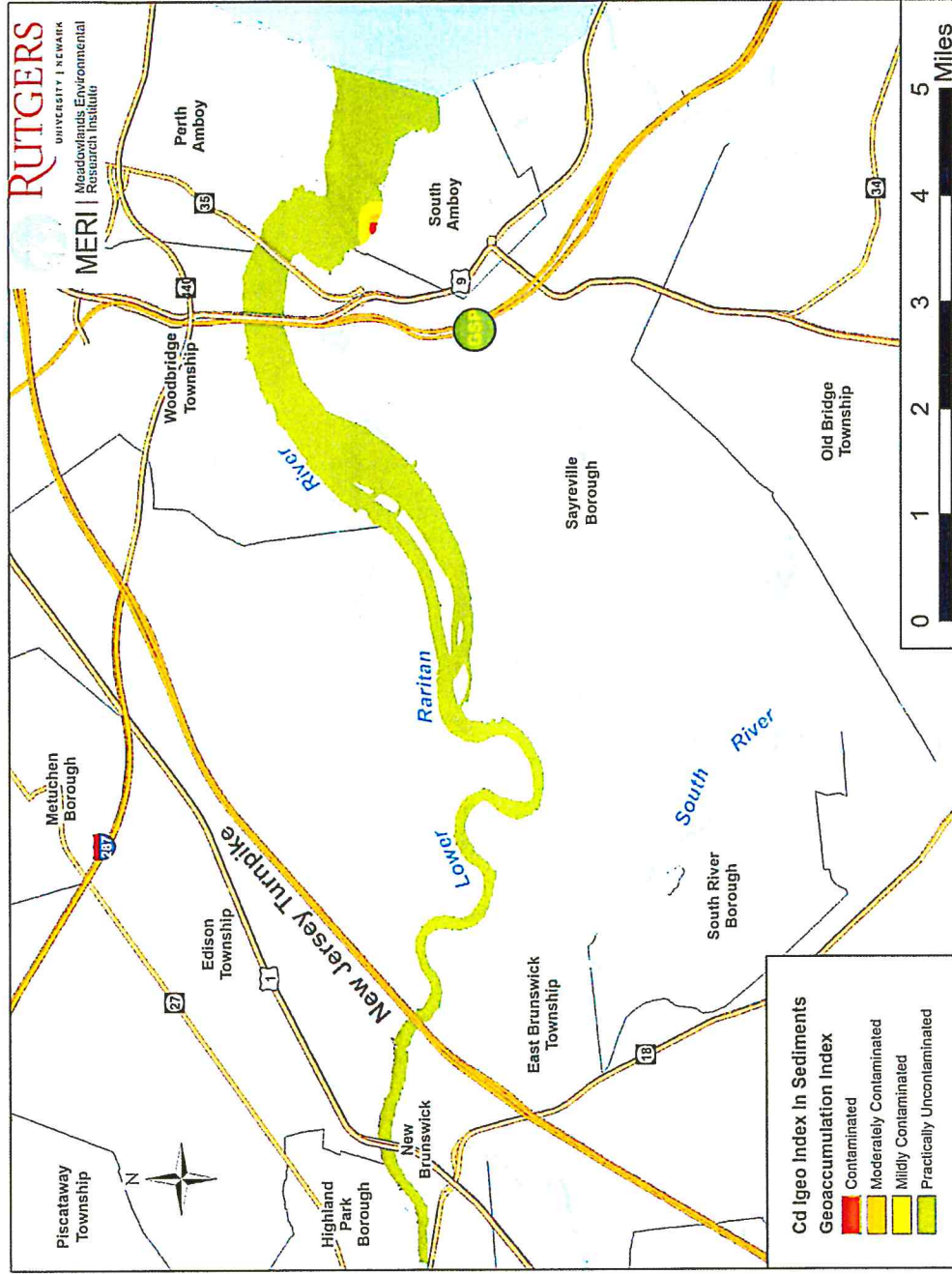


Figure 30. Spatial interpolation of the geoaccumulation index showing concentration of Chromium in the Lower Raritan River surficial sediment compared to natural background levels

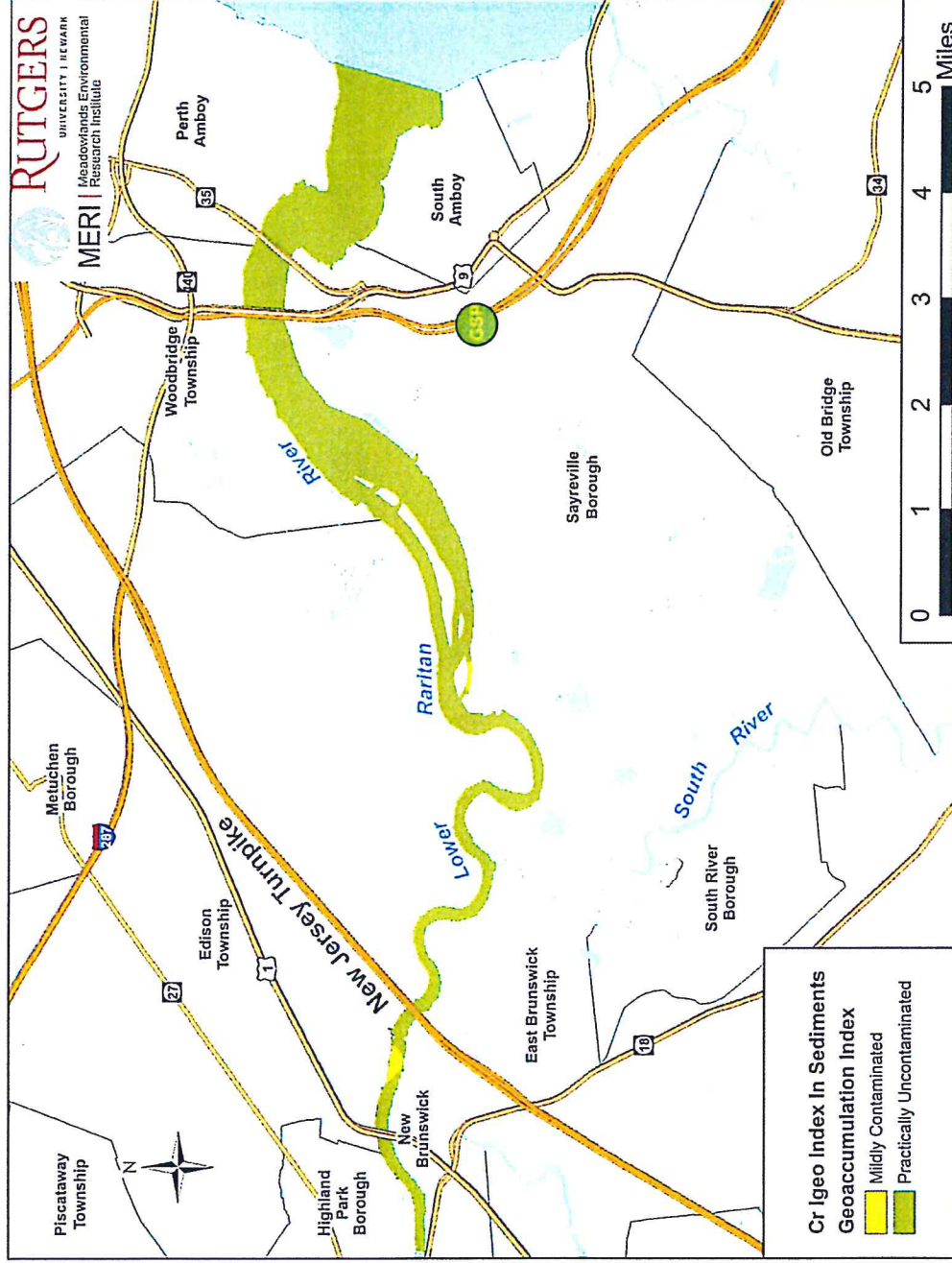


Figure 31. Spatial interpolation of the geoaccumulation index showing concentration of Copper in the Lower Raritan River surficial sediment compared to natural background levels

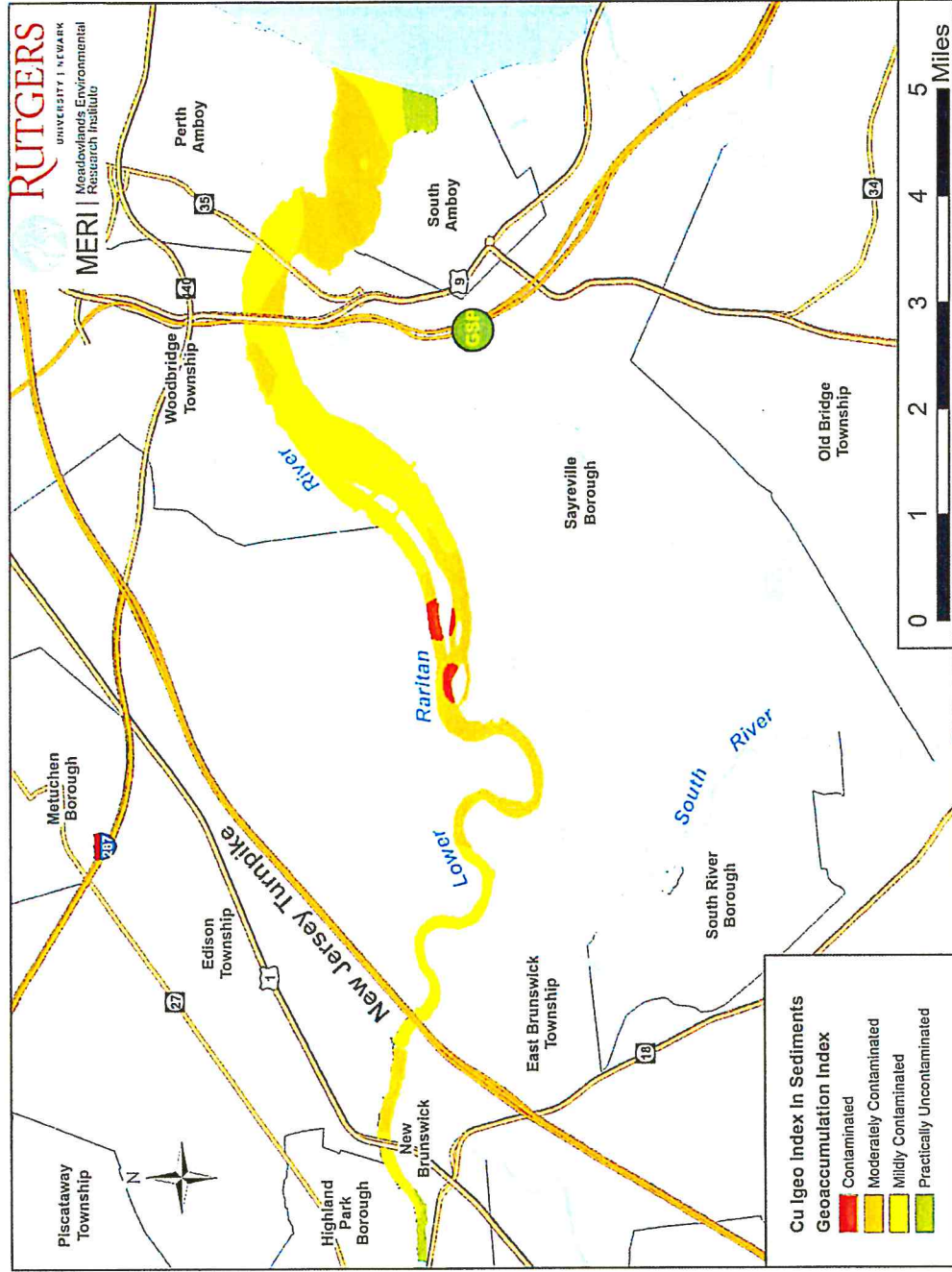


Figure 32. Spatial interpolation of the geoaccumulation index showing concentration of Lead in the Lower Raritan River surficial sediment compared to natural background levels

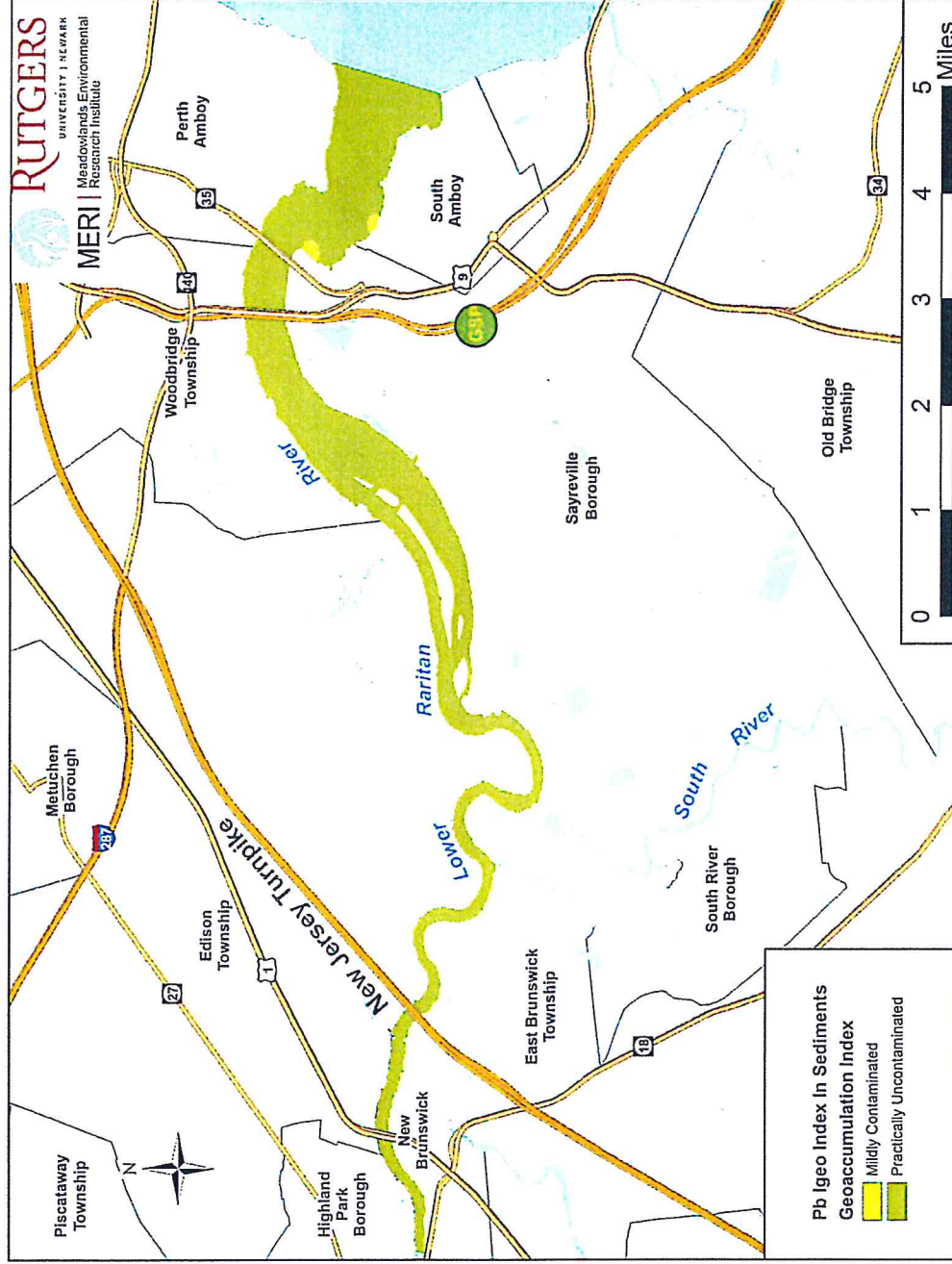


Figure 33. Spatial interpolation of the geoaccumulation index showing concentration of Mercury in the Lower Raritan River surficial sediment compared to natural background levels

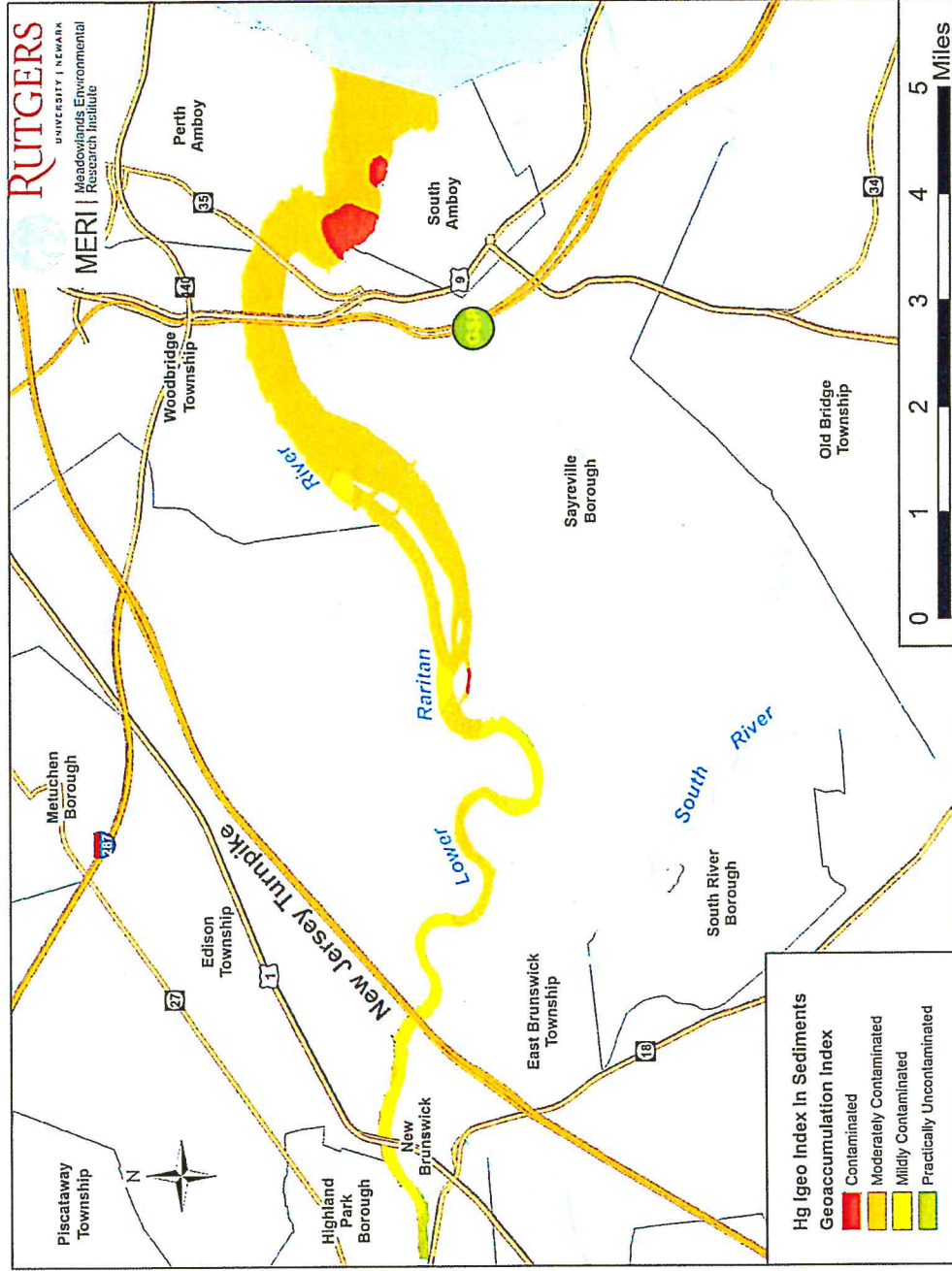


Figure 34. Spatial interpolation of the geoaccumulation index showing concentration of Nickel in the Lower Raritan River surficial sediment compared to natural background levels

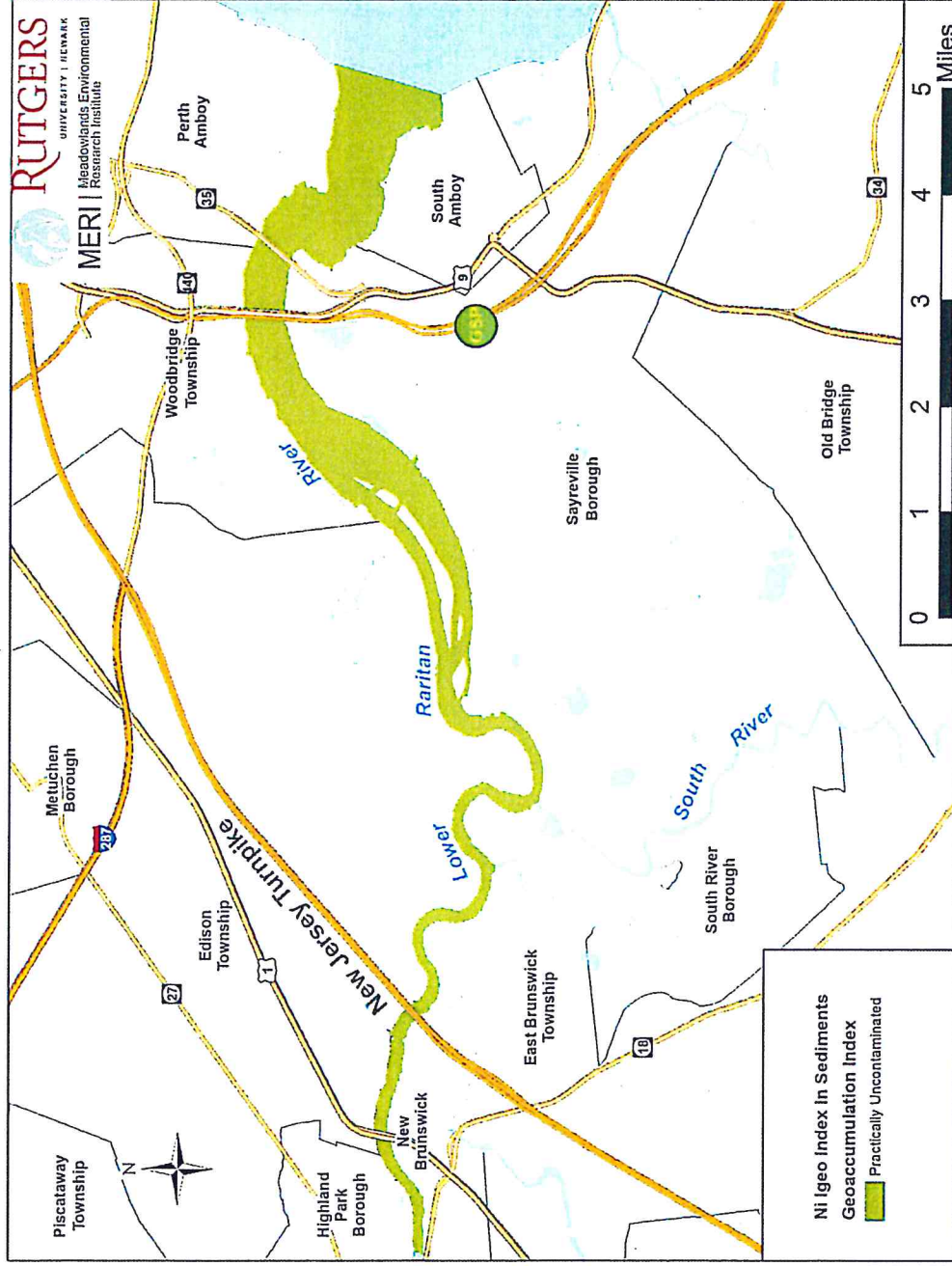


Figure 35. Spatial interpolation of the geoaccumulation index showing concentration of Selenium in the Lower Raritan River surficial sediment compared to natural background levels

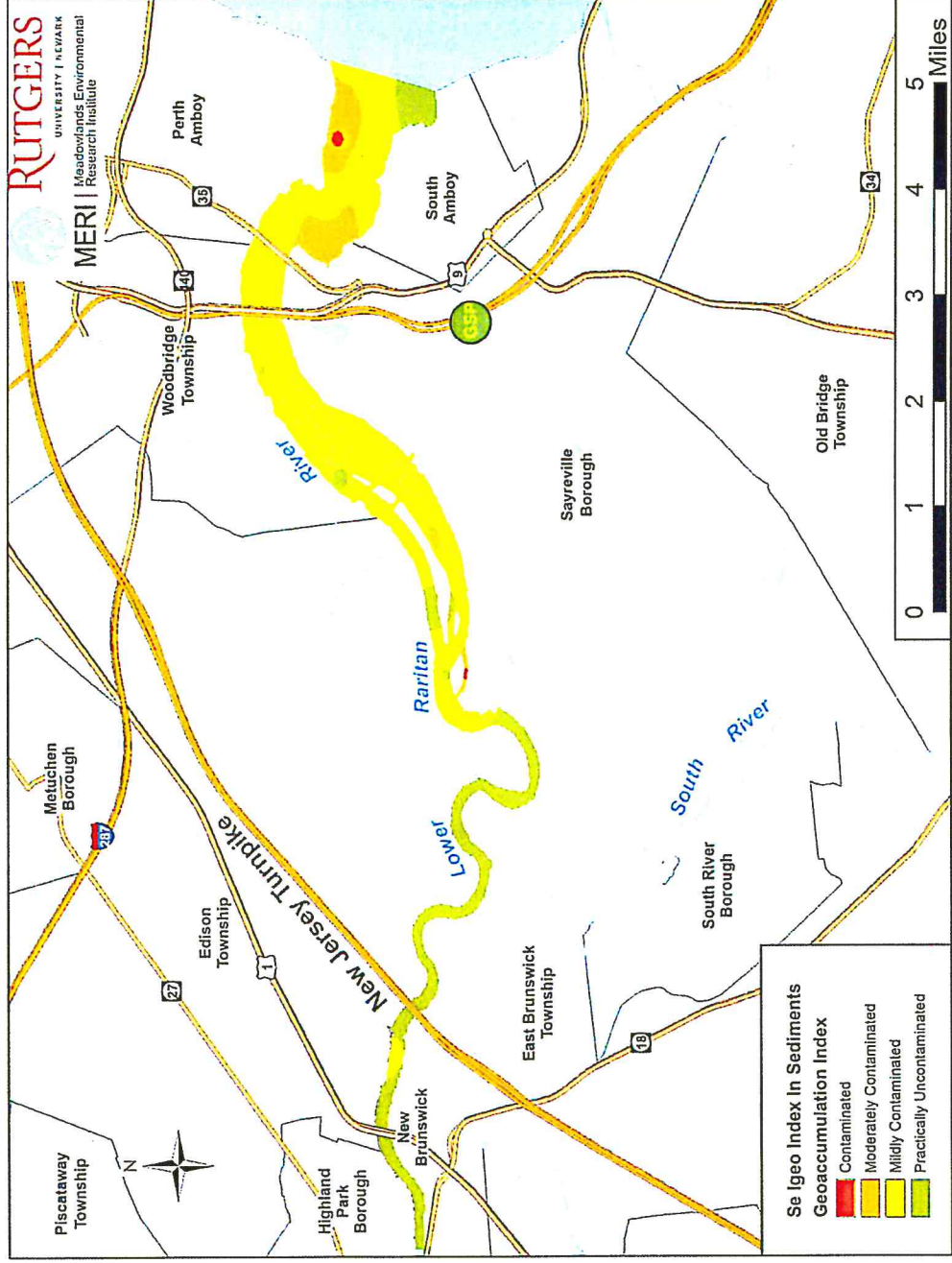


Figure 36. Spatial interpolation of the geoaccumulation index showing concentration of Silver in the Lower Raritan River surficial sediment compared to natural background levels

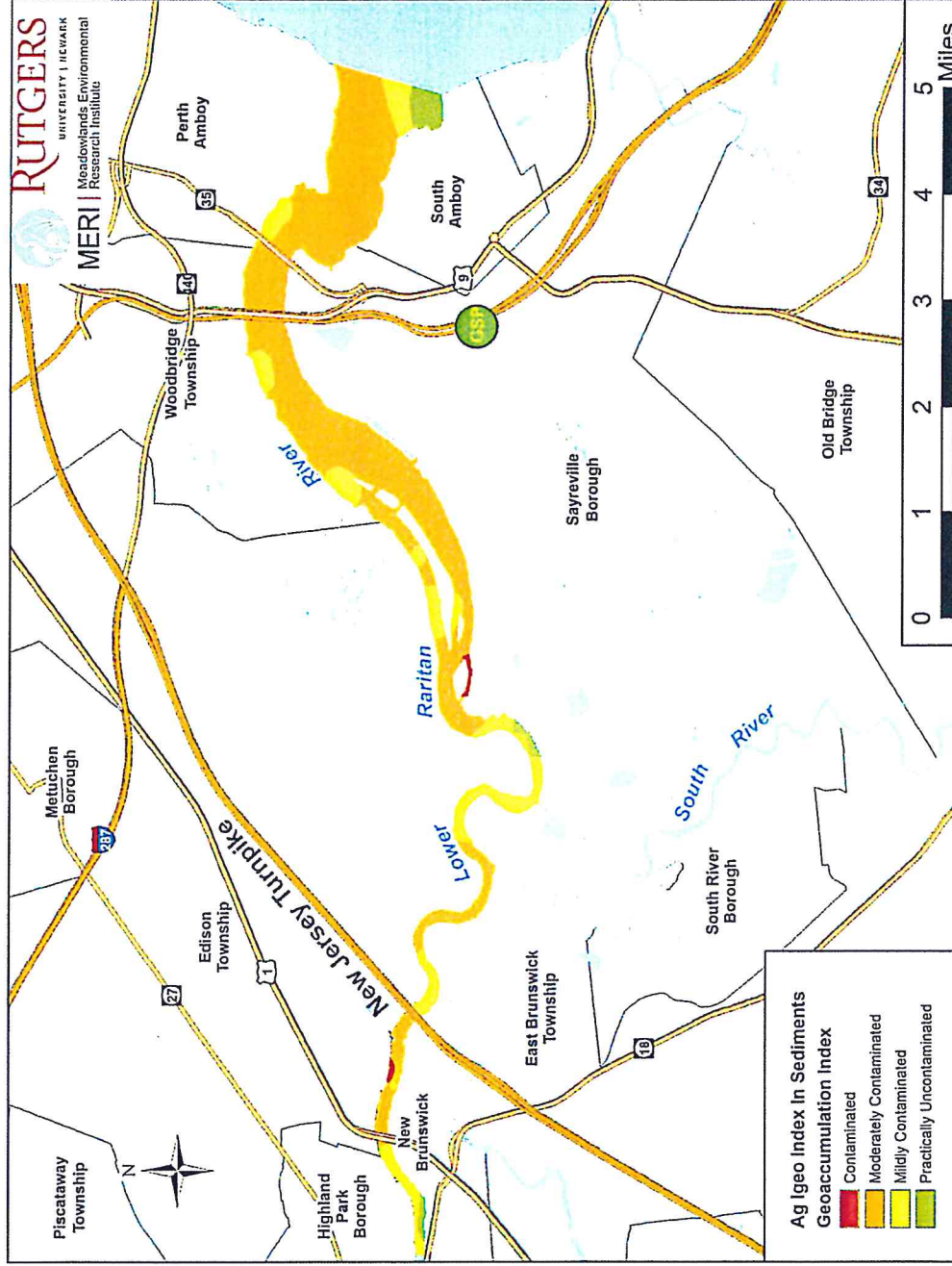


Figure 37. Spatial interpolation of the geoaccumulation index showing concentration of Thallium in the Lower Raritan River surficial sediment compared to natural background levels

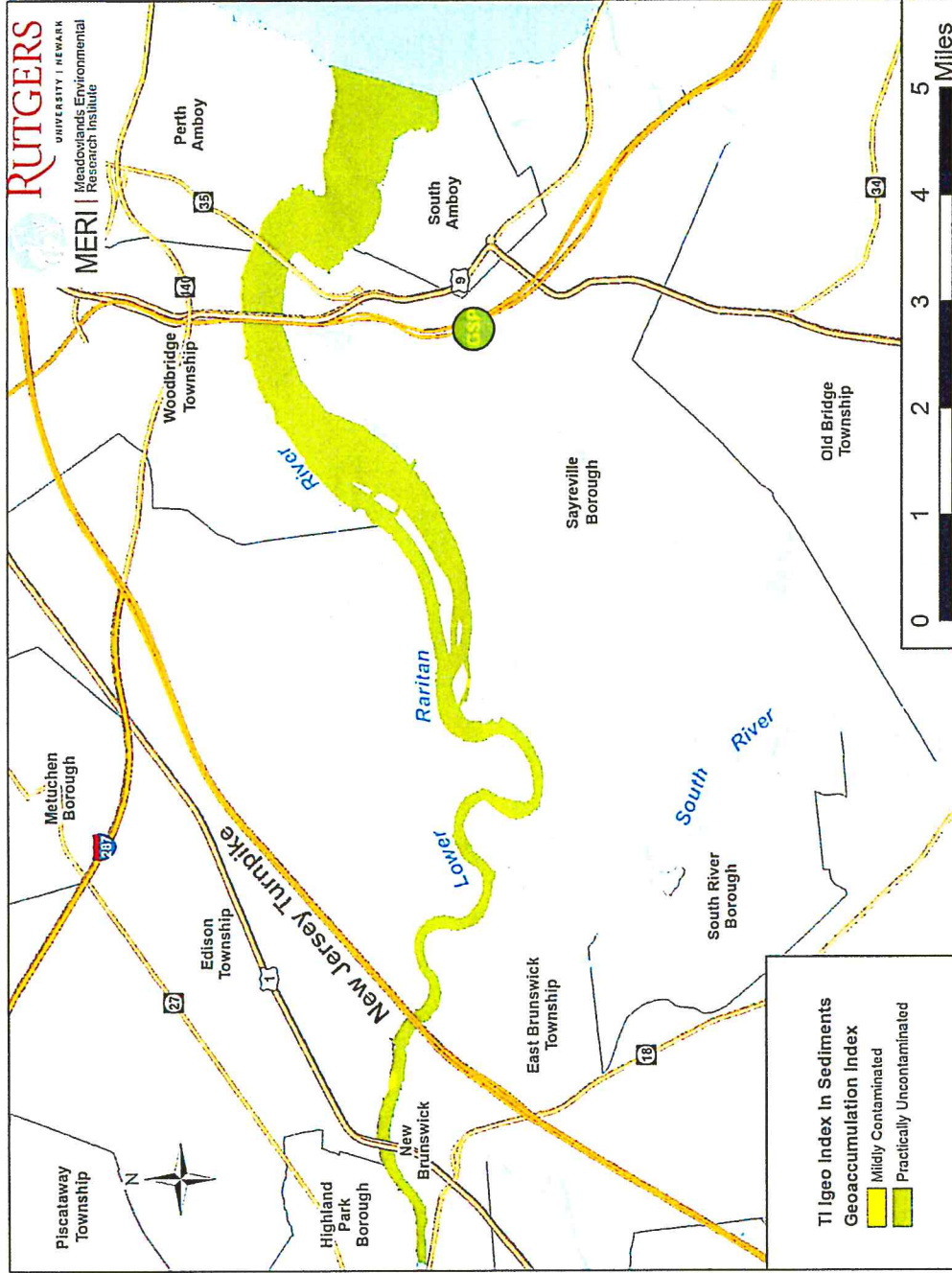
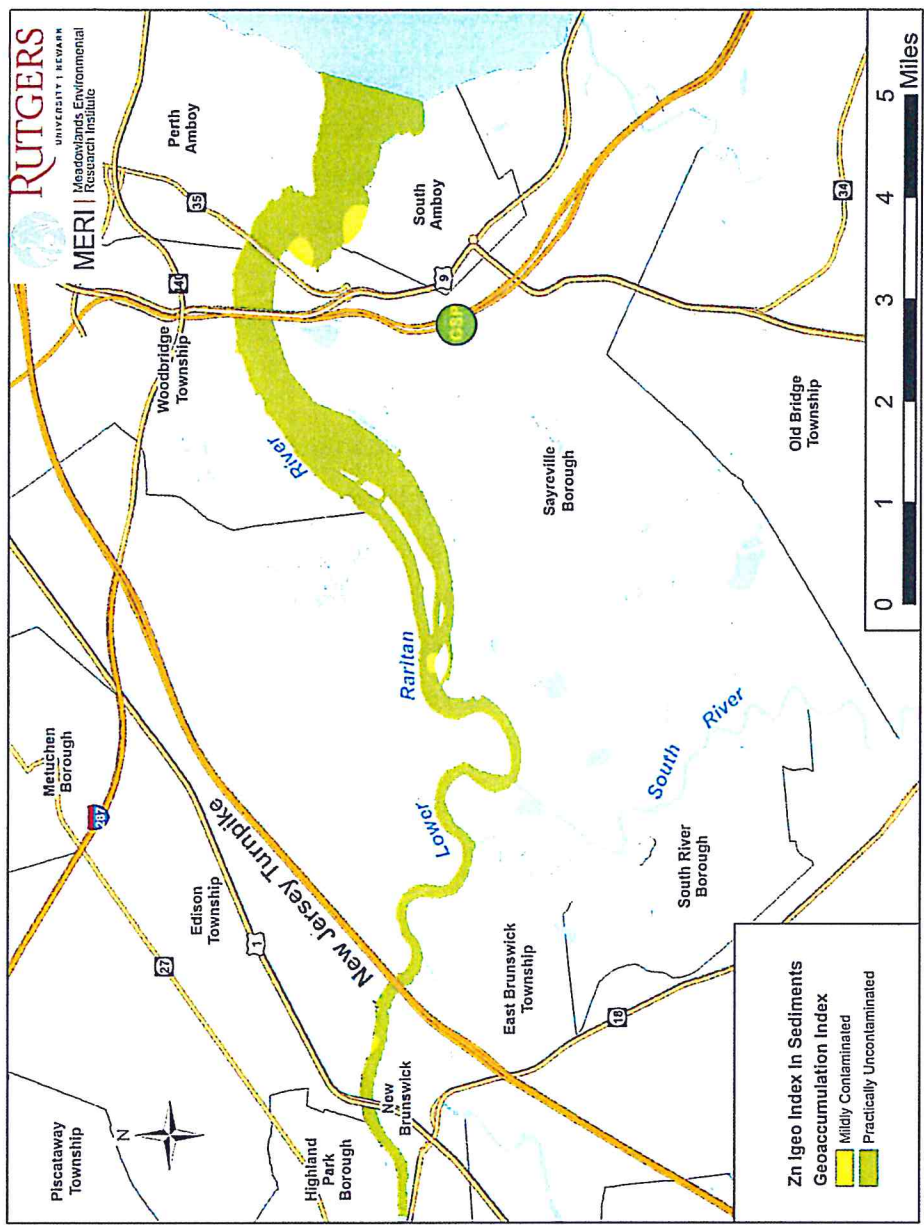


Figure 38. Spatial interpolation of the geoaccumulation index showing concentration of Zinc in the Lower Raritan River surficial sediment compared to natural background levels



Comparing current and historical sediment contamination records in the Lower Raritan River sediment

Five historic sampling locations (2000-2006) are available to compare with MERI's findings from 2017 (Figure 39). When comparing the EPA and MERI datasets at the 5 overlapping sampling locations (P1-P5) (Figure 40. A-K), we find that the concentration trends remained the same for every trace metal. MERI's data from 2017 show higher concentrations of cadmium, mercury, and selenium compared to EPA's data from 2000-2006. The EPA data showed higher amounts of nickel, antimony, and zinc in 2000-2006 compared to 2017, this could be explained by natural attenuation over time. It's interesting to note that between 2000-2006 and 2017, peak concentrations of silver, arsenic, copper, and lead moved slightly upriver (Figure 40 A, B, E, and H).

When comparing matching PCB congeners and OCP data from 2000-2006 to 2017 (Figure 41. A-J), we see that concentration levels remained about the same. Our data indicates that natural attenuation seems to be accruing with the majority of PCB congeners. PCB 128 was the only one that showed higher concentrations in 2017 compared to 2000-2006. Also worth mentioning is that MERI's metal analysis was performed on dry sediment samples and the organics were analyzed from wet sediment, while there is no information regarding studies that contributed to the EPA-STORET records. .

Figure 39. Map of the study area showing the original sampling locations from EPA's STORET database and MERI's current sampling locations

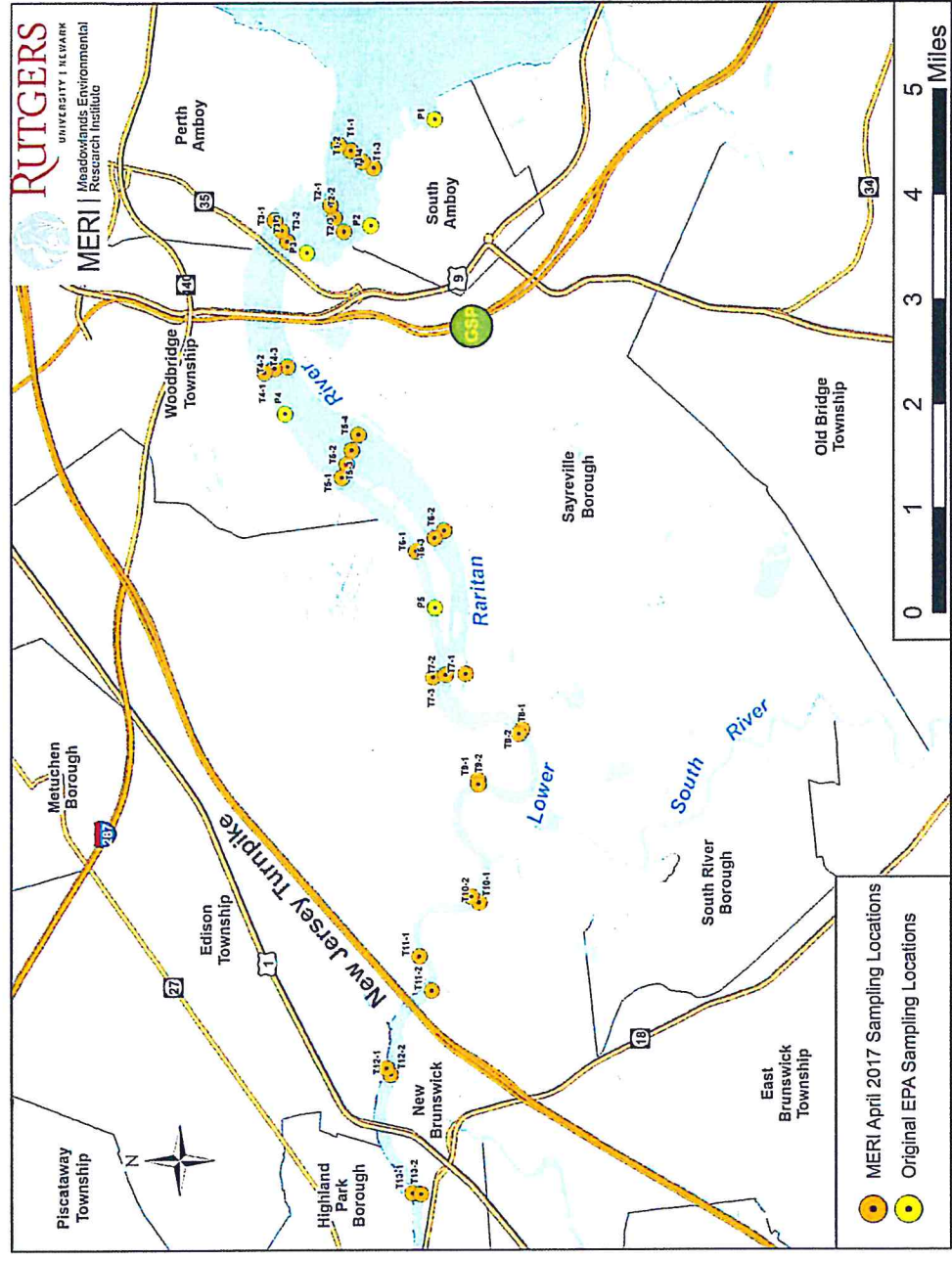


Figure 40. Summary of current (2017) and historical (2000-06) sediment metals concentration compared at five distinct sampling locations (P1-P5) from the bay up to New Brunswick

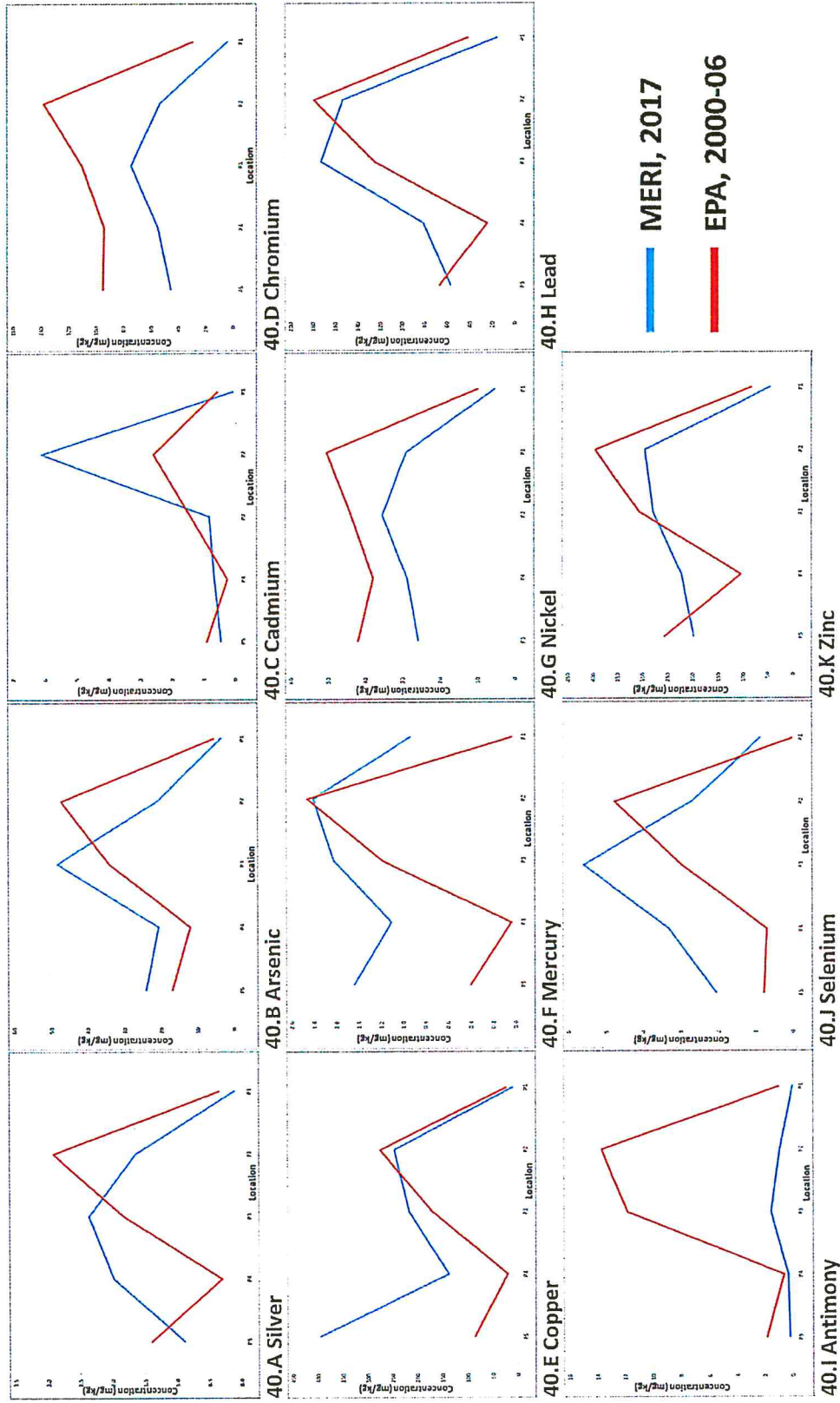
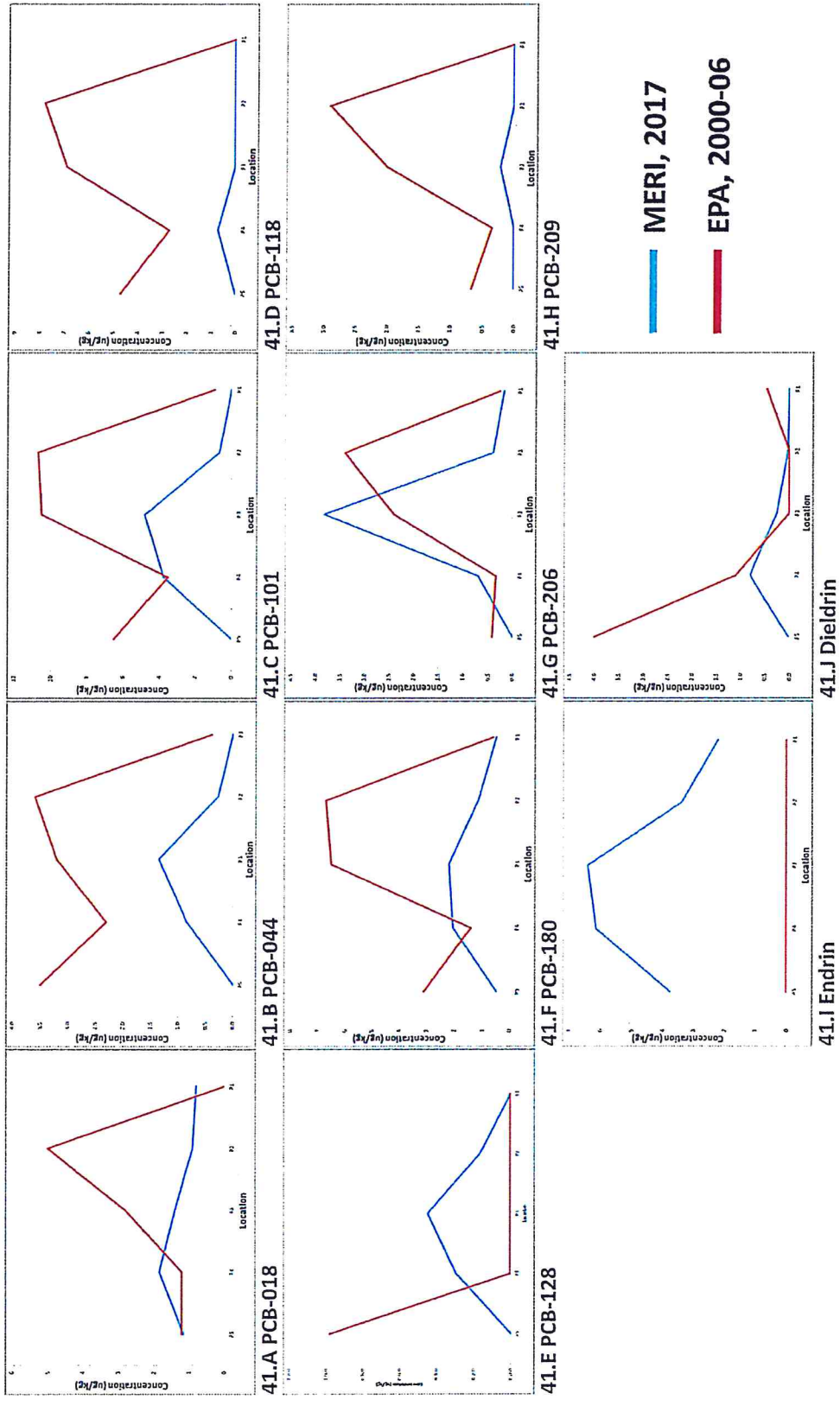


Figure 41. Summary of current (2017) and historical (2000-06) sediment PCB congener and OCP concentration compared at five distinct sampling locations (P1-P5) from the bay up to New Brunswick



1.4 Conclusions

Water quality measurements were made at the surface and a foot from the bottom during an ebbing of the tide. No measurements were made at very shallow stations (Table 1, N/R). Salinity measurements near the Raritan Bay resulted in values of 13 Practical Salinity Units (PSU). Upriver from transect 7 salinity drops to less than 1 PSU. Before crossing the turnpike overpass on the bay side, salinity on the higher reaches of the water column was slightly lower than salinities near the bottom however, these differences disappear upriver. For most of the locations sampled there were no significant differences in turbidity, oxygen reduction potential (ORP), dissolved oxygen and pH between the top and bottom of the water column indicating that overall the water column was well mixed.

Only contaminants associated with the grain size fraction of less than 63 μm are reported in this study. By selecting this grain size threshold we were able to remove grain size as a variable when comparing contaminant concentrations. Table 2 shows the summary statistics for metal concentration and the respective ERL and ERM criteria. On average, Mercury and Nickel were the only metals that exceeded the effects range medium (ERM) screening criteria (Table 3). In other words, 50% of case studies show that benthic organisms would be adversely impacted by existing Hg and Ni concentrations in the Raritan sediments. All metals but Cr and Cd exceeded the ERL criteria where 10% of case studies show an adverse impact to benthic organisms. Beryllium (Be), Antimony (Sb), Selenium (Se) and Titanium (Ti) do not have ERM or ERL criteria. Concentrations of PCB and OCP follow the same pattern across the different sampling stations (Figure 9). In terms of PCBs the ERL criteria is exceeded in all cases but for locations P1 and P5. The effects range medium criteria is only exceeded at T7-1 (Crab Island). When metal concentrations are compared to the natural background levels from the local geology, six elements: Hg, As, Cu, Cd, Se, and Ag were found to have concentrations greater than normal background levels.

Discreet hotspots have emerged from this study that may need more attention. These hotspots include the area on the bay side of the NJ Parkway that encompasses transects T1, T2, and T3. Another well-defined hotspot is along the P7 transect, at Crab Island in Sayreville. Smaller hotspots form along T12 mainly due to the high Cr, As, and Zn concentration and around T5 and T6 with high Zn, Tl, Pb, Ni, and Hg concentrations compared to the rest of the study area.

Chromium, Nickel and Antmony show some degree of attenuation when comparing the five overlapping locations (P1-P5) between 2000-2006 and 2017. Mercury on the other hand showed no indication of attenuation and 5 out of 4 locations showed increased concentrations in 2017. Organic contaminants on the other hand by the most part show decreased concentrations in the sediments today compared to 2000-06.

2. Component II – Historical Land Use Report in the Lower Raritan Basin

The impacts of anthropogenic activities following the industrial revolution are well known. Pollution histories for various metals are so well-studied that the timing of their impact can be used to date sediments (Kemp *et al.*, 2013). Researchers in various locations meticulously recorded the degradation on their waterways due to increased industrial activity and trash disposal (Marshall, 2004). We have records from various local and regional rivers of increasing industrial pollutants, increasing nutrients from farming and detergent use, and increased loads of sediment from runoff (Church, 2006; Cooper and Brush, 1993; others). In the Raritan River, recreational use and a strong fishery exist until the First World War, after which pollution reduced or destroyed these uses (Jeffries, 1962). Improvements in environmental legislation, such as the Clean Water Act, have greatly reduced the amount of pollution entering the Raritan River; however, because of storage of pollutants in sediments, many of the tidal marshes surrounding the river need extensive remediation as they will continue to contribute pollution to the river as sediment becomes resuspended (Christiansen, *et al.*, 2000).

Considerably less is known about the pre-industrial history of the Raritan River. Understanding pre-industrial pollution levels, and in particular, establishing base-line conditions prior to European settlement, is imperative if remediation is to take place. Knowledge of base-line conditions allows us to better understand how the health of the river has changed and how best to remediate it. We also establish reasonable standards for remediation.

Here, we present our findings on the pollution history of the Raritan River from pre-European settlement through the present. By collecting sediment cores along the sediment gradient and from areas with differing amounts of anthropogenic influence, we are able to see how humans have impacted the water quality of the Raritan River through time. We measured changes in pollutants such as metals and organics and analyzed the change in nutrient impacts by observing changes in diatom communities. These changes were placed into historic context by using a composite chronology to create an age-depth model. Changes were compared within each core in order to see how pollution changed through time. We also compared changes among sites so that we could better understand how areas with greater or smaller amounts of anthropogenic influence were impacted by industrialization and urbanization of the region.

Overall, we found that nutrients increased at the time of colonization. A second increase occurred around the time of industrialization. Metal and organic pollution generally increased around the time of industrialization. Among the study sites, the site with the greatest amount of anthropogenic impact was found to have the greatest increases in pollution loads. This is consistent with the surface water sampling, in that this region of the river had a much higher amount of most pollutants than anywhere else in the study area.

Overall, we were able to reconstruct the pollution history of the Raritan River from pre-European settlement through the present. These findings allow a comprehensive look at how anthropogenic activities have impacted the Raritan River, and allow us to make better-informed decisions regarding restoration.

2.2 Methods

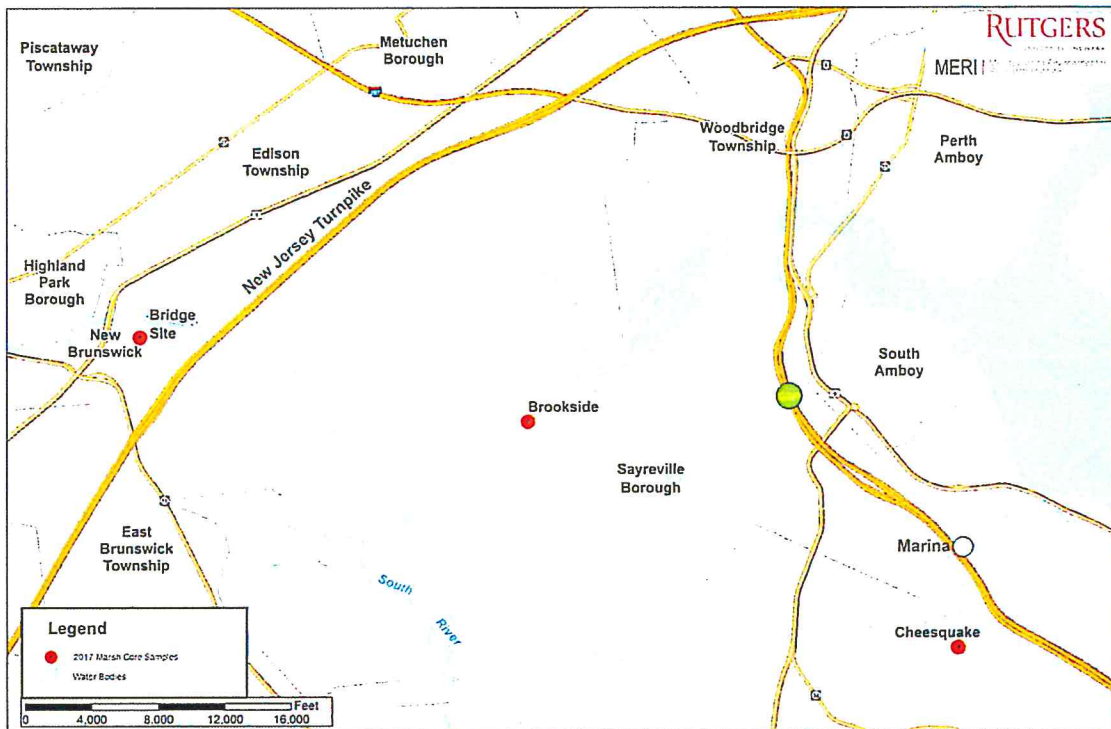
2.2.1 Coring and Sample Selection

Three sites were chosen along the Raritan River for coring (Figure 42). The sites were chosen with consideration to the following:

1. Sites should cover a range of salinities, and
2. Sites should cover a range of pollution levels.

We initially planned to include both high and low marshes, however, in early investigations, little difference was seen between them with regards for historical pollution levels. A much greater difference was seen when comparing among salinities and pollution levels, and so these characteristics were the focus of this study.

Figure 42: Location of the coring sites



The first site, located near New Brunswick between the New Jersey Turnpike Bridge and the Route 1 Bridge (40.49°, -74.41°), will hereafter be called “Bridge” site. This site is located in a

freshwater tidal marsh, with a salinity of 0.1 ppt. Very dense *Phragmites australis* (common reed) dominates the site in low-lying areas which are inundated twice daily. Some sparse trees live in areas at a slightly higher elevation, which are less frequently inundated. The Bridge site had a moderate amount of anthropogenic disturbance.

The second site is located near Sayresville close to Brookside Avenue (40.48°, -74.34°) and will hereafter be referred to as “Brookside” site. Here, the site is tidally inundated by brackish water and is dominated by a mix of *Spartina patens* and *P. australis*. The surface salinity measured at this site was approximately 1.7 ppt. A former factory is located near this site, and many nearby marshes have a layer of crushed bricks coating them. This site was selected to avoid this issue. Additionally, water chemistry monitoring revealed this site as a hotspot for high levels of pollutants (see *Component I*). Brookside site had the highest amount of anthropogenic disturbance.

A third site in the Raritan Bay completed our transects of sites along the salinity gradient of the tidal Raritan River. In the low marsh *Spartina alterniflora* (long form) dominates and the high marsh is vegetated by *Spartina patens* and *Distichlis spicata*. This site, located in Cheesequake State Park (40.44°, -74.27°), will be referred to as “Cheesequake”. This site has a salinity of 12 ppm. Cheesequake was the site with the least amount of anthropogenic disturbance.

At each site, a Russian-type peat sampler was used to extract four replicate sets of cores in order to ensure that we had enough sediment for all analyses and for an archived core. For each core, two bore holes were used to collect alternating 50 cm intervals of sediment, with 10 cm overlaps to ensure complete sections (De Vleeschouwer, *et al.*, 2010). We cored at each site to refusal to ensure enough sample was collected to include pre-industrial materials.

2.2.2 Geochemistry

We collected samples every 4 to 8 cm in the top 80 cm of core material in order to assess the amount of pollutants in the sediments. Samples were collected from Replicate A from the Bridge Site and Replicate C from the Brookside Site. We based our sampling interval on the local accumulation rate of 3.1 cm/yr (Kemp, *et al.*, 2013). Samples weighed at least 10 g of sediment

in order to perform both organic pollutant analysis and metal analysis.

In order to assess the amount of organic pollution through time PAH, PCBs, and OCPs were extracted from the samples. To extract organics, we first used an 1:1 mixture of hexane and acetone in an accelerated solvent extractor (ASE 100, Dionex, USA). We then cleaned the samples using gel permeation chromatography (GPC, Autoprep 2000, O I Analytical, USA) and concentrated the extracts at 30 °C using rotary evaporation.

We separated PCBs and OCPs by fractioning using a florisil column. We analyzed sample extracts for 16 PAHs using Agilent 6890N gas chromatography and a 5975 inert mass spectrometer and quantified them using the internal standard method. Samples were analyzed for 109 PCB congeners and 18 OCPs. We identified congeners based on relative retention time. We spiked PCB and OCP surrogates in order to complete a QC recovery check.

We determined metal concentrations using EPA Method 200.8 (microwave-assisted acid digestion of sediment). Quality control was maintained by digesting a standard reference material 1944 (New York/New Jersey Waterway Sediment, NIST) alongside the samples. We analyzed the samples using an Inductively Coupled Plasma Mass Spectrometry (ICP-MS).

Once pollutants were extracted, their concentrations were compared throughout the depth of the core. Metals in particular have well defined dates associated with their peaks, based on the timing of pollution regionally. The peaks and initial onsets of metal pollution were used to assign some of the dates included in the age-depth model. In this location, initial copper pollution occurred in 1875 ± 25 , initial lead pollution occurred in 1900 ± 5 , the cadmium peak occurred in 1963 ± 7 , the nickel peak occurred at 1969 ± 11 , and the lead peak occurred at 1974 ± 5 (Bricker-Urso et al., 1989; Donnelly et al., 2001; Metcalfe & Derwent, 2014; Kemp, et al., 2013; Hurst, 2002; Marcantonio, et al., 2002; Lima, et al., 2005).

We used ^{210}Pb ($t_{1/2} = 22.3$ years) and ^{137}Cs ($t_{1/2} = 30.2$ years) to establish a portion of the chronology. ^{137}Cs activity was analyzed by direct gamma counting on a low-background, high-efficiency Germanium detector coupled with a multi-channel analyzer. We packed samples into standardized vessels and placed them in the counters for approximately 24 hours. We calibrated the detectors using natural matrix standards (IAEA-300, 312, 314) at the energy of interest (661 keV) in the standard counting geometry for the associated detector.

We measured total ^{210}Pb using alpha spectroscopy following the methodology of Nittrouer *et al.* (1979). We spiked 1.5 g of sample with ^{209}Po , as a yield determinant, and then partially digested them with 8 N nitric acid (HNO_3) by microwave heating. Polonium-209 and ^{210}Po in solution was then electroplated onto nickel planchets in a dilute acid solution (modified from Flynn, 1968). We subtracted the ^{210}Pb activity supported by ^{226}Ra from the total ^{210}Pb activity in order to determine the amount of excess ^{210}Pb . This assumes that supported ^{210}Pb activity for a given core is equal to the uniform background activity found at depth (Nittrouer *et al.*, 1979). We calculated sediment accumulation rates using the constant flux–constant sedimentation (CF–CS) model (Appleby and Oldfield, 1992). Down-core ^{137}Cs activities were used to substantiate the ^{210}Pb -determined accumulation rates.

Finally, we selected three samples from each core in the bottom 50 cm to send for radiocarbon dating at NOSAMS. Samples were individual rhizomes from *Spartina alterniflora* and *Spartina patens* at Cheesequake and Brookside, and single roots or other plant material from Bridge as this site was freshwater rather than marine and *Spartina* species were not present. At NOSAMS, AMS dating was used to get the most precise date with the least amount of sediment used. Standard radiocarbon calibration (intcal13) was used to determine the age before present at the time of deposition.

2.2.3 Pollen Analysis

Pollen samples were collected every 4 cm in the region of the cores anticipated to include the start of settlement based on other dating methods. Samples were processed by Dr. Vaughn M. Bryant using the methods of Faegri and Iversen (1964), in which samples are exposed to a series of acid washes in order to remove extraneous materials, such as organics and silicates. Once the pollen grains were extracted and concentrated, we preserved them in glycerol. We placed preserved samples on slides and identified and identified and counted 100 pollen grains. Analyses were completed using a magnification of 400x.

We used pollen counts to identify changes in vegetation related to land-clearance, which occurred when the Europeans settled in New Jersey. For example, in this region shifts from an

abundance of Quercus to Ambrosia indicate deforestation in 1795 (Russell, 1980). An additional pollen horizon was observed in the Bridge Site: Chestnut Blight, a decrease in Castanea pollen due to the widespread death of chestnut trees in 1920 (Brugam, 1978; Clark and Patterson, 1984).

2.2.4 Constructing of an Age-Depth Model

Bchron is an extension for R which uses Bayesian models to analyze age-depth relationships (Haslett & Parnell, 2008). Bchron is able to take a composite chronology and associated methodological and depth errors and determine a best-fit age depth model with 95% confidence intervals. We used Bchron to create our age-depth model. To do so, we input the chronohorizons from metal pollution, radiocarbon dating, pollen, and ^{137}Cs and ^{210}Pb analysis. We also included the core extraction year. Bchron used these dated depths to construct a model of age vs. depth for each site, as well as a confidence interval associated with it.

2.2.5 Diatom Analysis

We collected diatom samples every 10 cm in the top 100 cm of core in order to encompass pre-colonial (background) nutrient load through the present. This allows us to see what nutrient levels in the river were like prior to European settlement, how it changed during the industrial revolution, and how it fares in the present. Samples were weighed and placed in 50 mL Falcon Tubes. Once in the Falcon Tubes, samples were exposed to 35% hydrogen peroxide overnight, until the amount of bubbling reduced. We then placed the tubes in a warm water bath for two to three days, depending on the organic content of the samples. We allowed the samples to cool before placing them in the centrifuge to spin at 3500 rpm for 3 minutes then decanted. Fresh DI water was added to the tubes and they were centrifuged again. We completed the centrifugation procedure three times, each time decanting and replacing the water in order to wash the hydrogen peroxide from the samples.

Once the samples were clean, we added DI water up to 10 mL. We then placed water on a coverslip and used a micropipette to add a known amount of sample slurry. Coverslips dried overnight and were adhered to slide using NAPHRAX. We kept extra sample in order to make additional slides if needed.

We identified to species level and counted at least 100 valves from each sample under 1000x. Relative abundances were determined for each species. Species were grouped based on their nutrient preferences and the percentage in each group was traced through time. This allowed us to determine how the nutrient load in the Raritan River has change from pre-European settlement through the present.

2.3 Results

2.3.1 Age-Depth Models

In order to construct a composite age-depth model, we used a suite of methods: radionuclides, pollen, and metal pollution history. Cadmium, copper, nickel, and lead were measured downcore (Figures 43-45). At Brookside, we found that copper pollution, which designates 1875 ± 25 years began at 70 cm (Bricker-Urso et al., 1989; Donnelly et al., 2001). Initial lead pollution (1900 ± 5 years) occurred at 60 cm, and the lead peak (1974 ± 5 years) occurs at 34 cm (Hurst, 2002). The cadmium peak (1963 ± 7 years) was present at 40 cm (Metcalf & Derwent, 2014; Kemp, et al., 2013). Finally, the nickel peak (1969 ± 11 years) occurred at 34 cm (Kemp, et al., 2013). At Bridge Site, the start of copper pollution was located at 55 cm. We found the start of lead pollution and the lead peak at 55 and 34 cm respectively. The cadmium and the nickel peaks both occurred at 36 cm. Finally, at Cheesequake, the initial copper pollution was found at 33 cm. The initial lead pollution occurred at 40 cm and the lead peak at 12 cm. We found the cadmium peak at 9 cm, and the nickel peak at 4 cm.

In addition to metals, we also looked at radionuclide, specifically ^{14}C , ^{137}Cs , and ^{210}Pb . ^{210}Pb was generally used to corroborate the sedimentation rate established using ^{137}Cs . We were able to identify a ^{137}Cs peak at all three sites. This peak corresponds with the peak in atmospheric nuclear weapons testing in 1963 (He and Walling, 1996). The ^{137}Cs peak was found in Brookside at 27 cm and at Cheesequake at 13 cm. At Bridge Site, we were unable to use ^{137}Cs due to large errors in measurement. We were able to calculate sedimentation rate based on the CSCF model for ^{210}Pb at both Bridge Site and Brookside. To include this information in the model, we determined the age of the deepest sample using the sedimentation rate. At Bridge Site, the sedimentation rate was 0.43 ± 0.03 cm/year, the deepest reliable age was 43 cm and the age determined for this sample was 1913 ± 2 years. We found a sedimentation rate of 0.42 ± 0.03 cm/year at Brookside, with a deepest reliable date at 37 cm, with an age of 1932 ± 5 years. We also used radiocarbon dating for older sediments. We were able to date three samples at Brookside. The shallowest site we dated was located at 55 cm and returned a date of 273 ± 15 years before present. We dated a second sample at 85 cm which returned a date of 453 ± 15 years before present. Our third sample at 110 cm returned a date of 173 ± 15 years before present, attesting to the high degree of mixing which occurred at these sites. We sent three dates from

Bridge Site as well, located at depths of 47 cm, 63 cm, and 83 cm. All three samples returned dates indicating that the samples were likely deposited post-1950, which is inconsistent with other chronometers and likely represents mixing. At Cheesequake, three samples were sent for radiocarbon dating within our study depth: 62 cm, 81 cm, and 93 cm. These samples returned dates of 155 ± 15 years, 380 ± 15 , and 605 ± 20 years, respectively.

Finally, we used pollen horizons to determine the age of sediments. We looked for a shift in the ratio of oak to ragweed pollen to less than 1, which indicates that deforestation has occurred and it is 1795 ± 55 years (Russell, 1980). We also looked for the decline or elimination of chestnut pollen, which corresponds to the Chestnut Blight which occurred at 1920 ± 10 years (Brugam, 1978; Clark and Patterson, 1984). The settlement peak was found at 58 cm at Brookside, 58 cm at Bridge Site, and 60 cm at Cheesequake. We found the Chestnut Blight horizon in Bridge site only, at 54 cm.

Figure 43. Brookside Metals, colors in figure represents pre-land clearance (green), post-land clearance, but pre-industrial (yellow), and post-industrial (red) land uses.

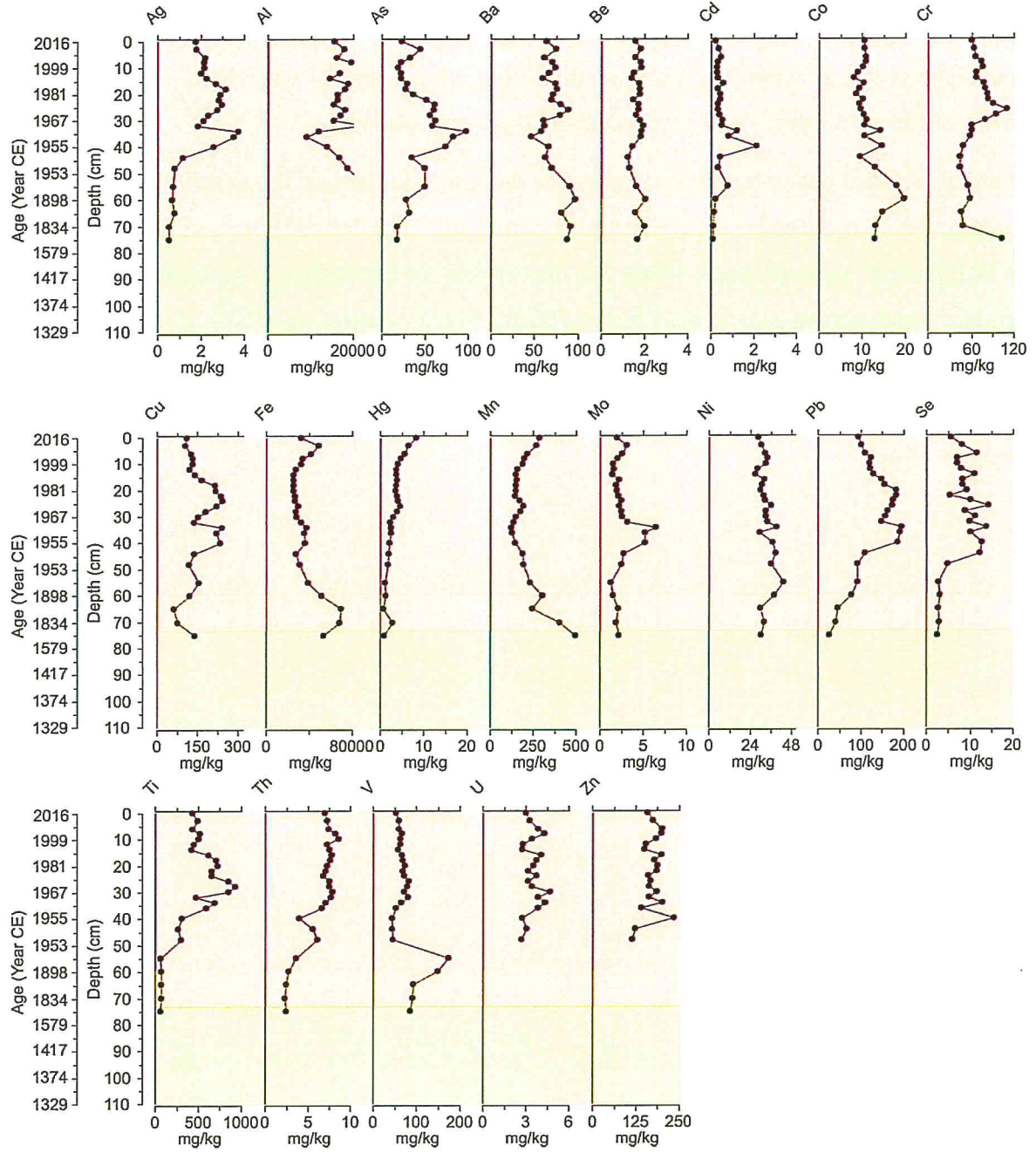


Figure 44. Bridge Site Metals, colors in figure represents pre-land clearance (green), post-land clearance, but pre-industrial (yellow), and post-industrial (red) land uses.

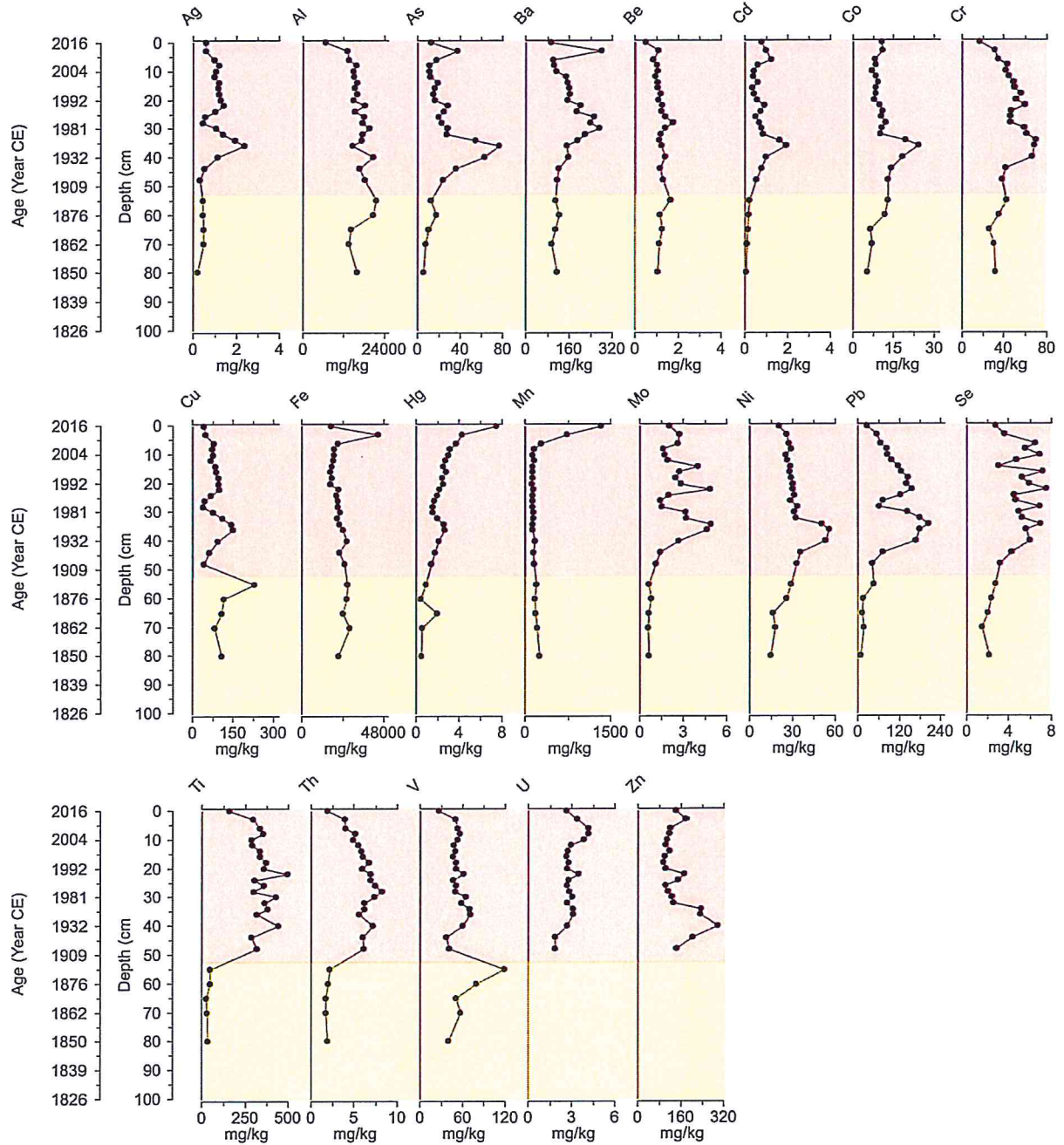
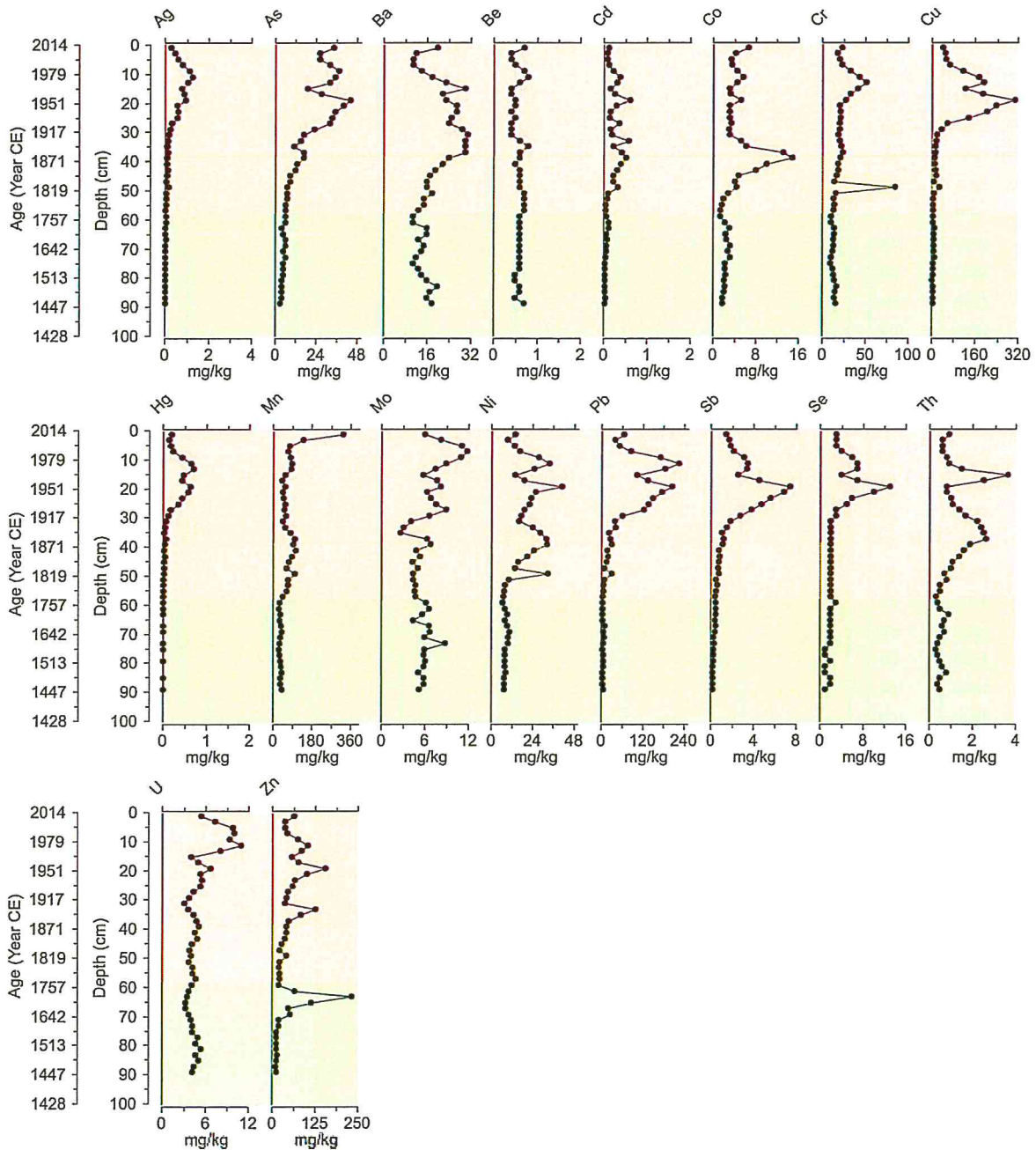


Figure 45. Cheesequake Site Metals, colors in figure represents pre-land clearance (green), post-land clearance, but pre-industrial (yellow), and post-industrial (red) land uses.



By combining these methods, we constructed a composite chronology in Bchron for each site. Based on these reconstructions, we were able to determine that the top 100 cm of Brookside dates from pre-European settlement to present, capturing major land use changes associated with the impacts of settlement, deforestation, and industry (Figure 48). At Bridge Site, the bottom of the 100 cm core pre-date the industrial revolution, thus enabling a comparison of pre-industrial conditions with pollution levels that occurred following the industrial revolution through the present (Figure 49). We found that the sediments at Cheesequake are deposited the most rapidly of the three sites, such that the bottom of the core greatly pre-dates settlement, allowing us to observe water quality far before European settlement, so that comparisons to post-settlement, and post-industrial conditions can be made (Figure 50). Cheesequake was also the least bioturbated site, resulting in the least amount of uncertainty in the age-depth model. Because sediments were very mixed at Bridge Site, the uncertainty is rather high; however, differentiation between pre- and post-industrial sediments can still be made. Brookside was intermediate, and a reliable age-depth model resulted from the sediment analysis there.

Figure 48. Brookside Site Age-Depth Model showing the various marker types that were used to determine the pre- and post-settlement as well as the post-industrial contamination levels

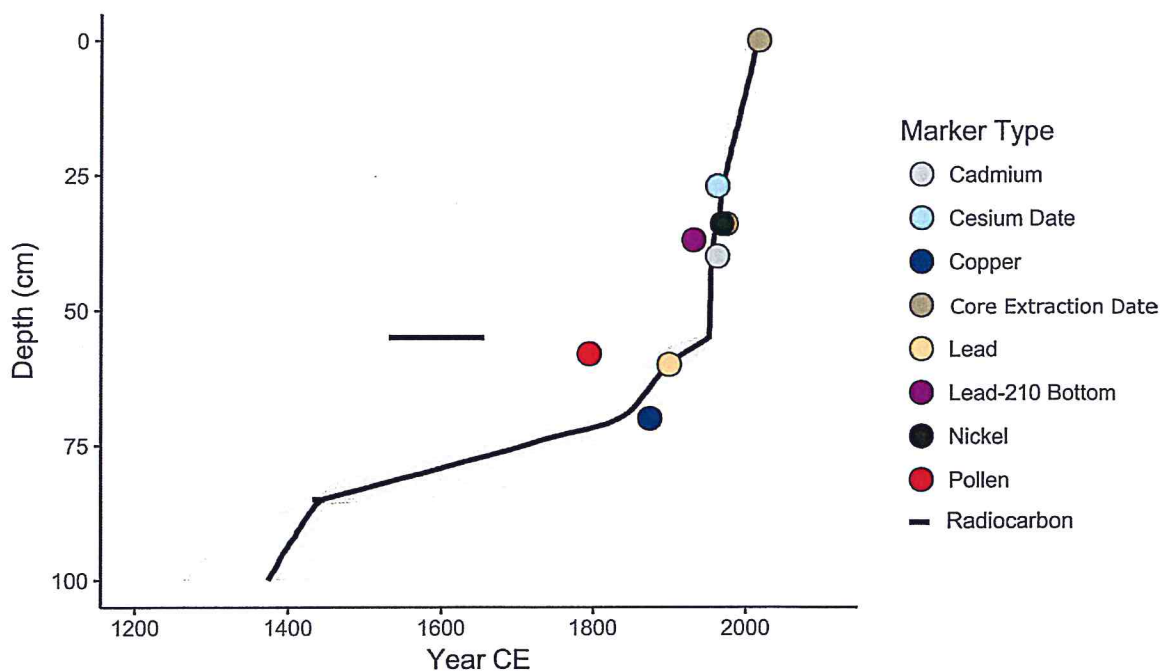


Figure 49. Bridge Site Age-Depth Model showing the various marker types that were used to determine the pre- and post-settlement as well as the post-industrial contamination levels

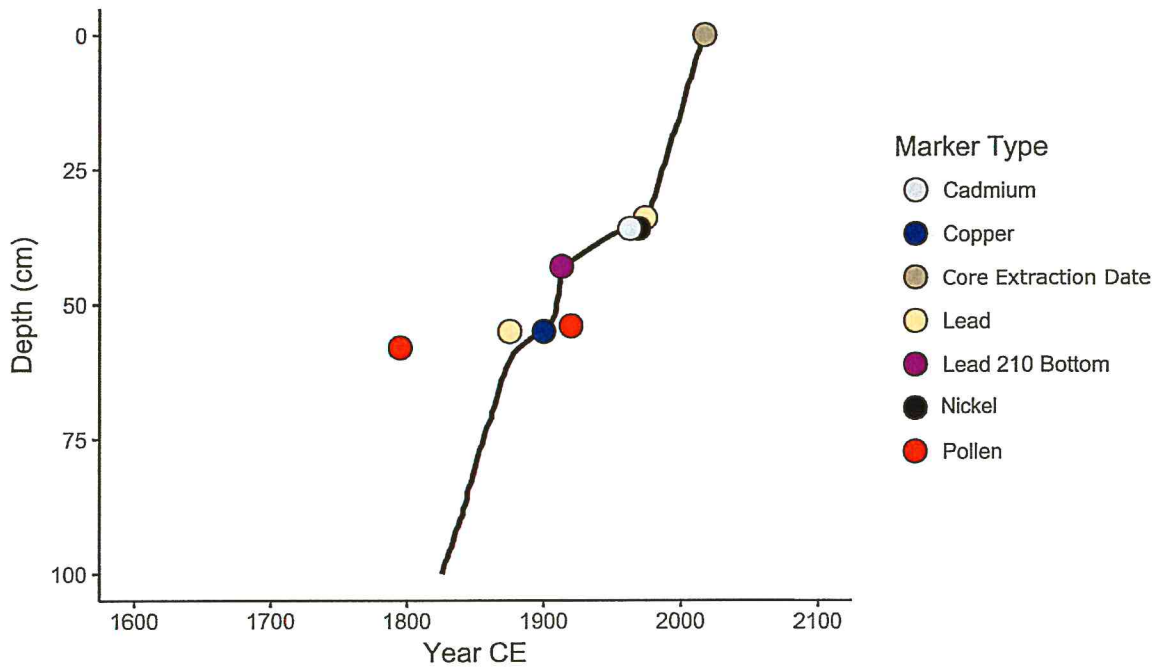
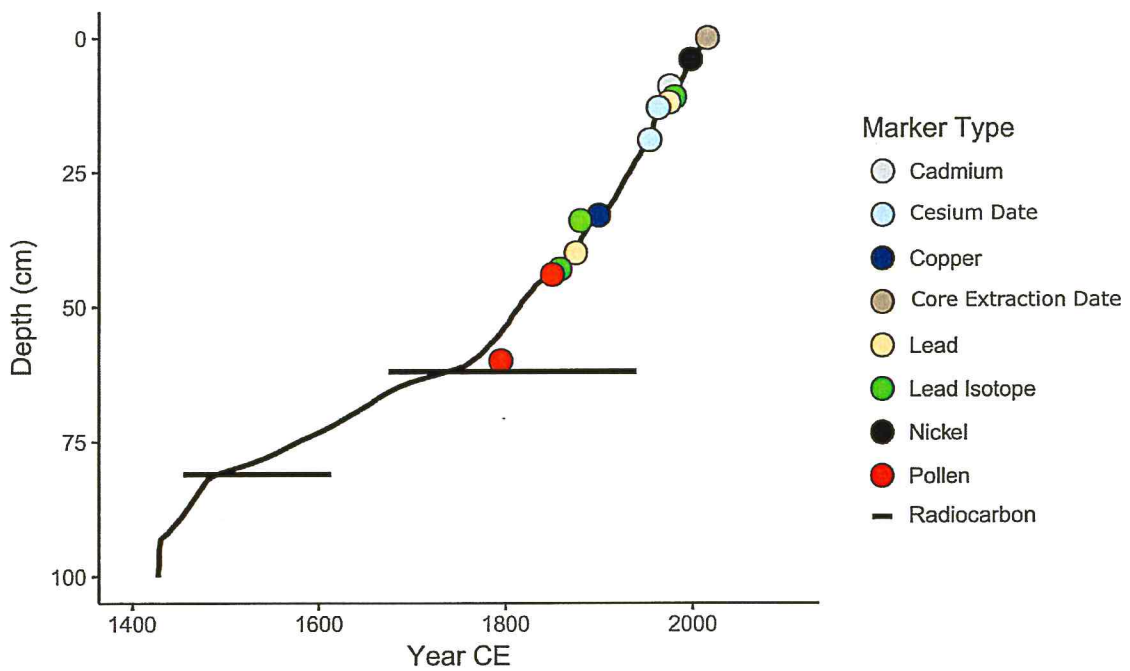


Figure 50. Bridge Site Age-Depth Model showing the various marker types that were used to determine the pre- and post-settlement as well as the post-industrial contamination levels



2.3.2 Pollution History

Metals, organic pollutants, and nutrient loads are all factors that influence water quality. We looked at these three aspects historically in our cores.

Brookside was the most disturbed site. In Brookside, metals were lowest prior to European settlement. Following settlement, metals generally increased very slightly (Figure 43). Around 1900, metal levels increased drastically. During the 1960s and 1970s, metal levels decreased slightly, possibly as a result of environmental legislation which was prevalent during this time. This can be seen in the changes in the average concentrations of select metals. In the four metals we used for chronology, there is an increase in concentration from pre-deforestation to post-deforestation in cadmium, nickel, and lead (Table 5).

Table 5 Summary of the metal and organics concentration values from the core samples

	Brookside	mg/kg																				ug/kg		%			
		Ag	Al	As	Ba	Be	Cd	Co	Cr	Cu	Fe	Hg	Mn	Mo	Ni	Pb	Sb	Se	Ti	Th	V	U	Zn	PCB	OPC	Low Nutrient Diatoms	High Nutrient Diatoms
All Samples	Mean	2.04	17970	42.7	72.2	1.70	0.47	11.5	68.5	160	35961	3.34	207	2.55	33.0	129	0.11	8.09	470	6.29	74.2	3.51	173	101	26.3	18.3	5.55
	Median	2.16	17493	35.4	70.8	1.74	0.33	10.6	65.1	143	32317	3.57	184	2.20	32.3	127	0.06	8.27	486	7.16	67.5	3.46	175	83.5	22.7	15.0	6.00
	std dev	0.94	3950	21.5	12.1	0.20	0.41	2.82	17.9	52.9	12517	1.76	87.2	1.25	3.80	48.1	0.11	3.50	261	2.00	29.1	0.57	27.9	50.6	15.6	11.4	3.91
Pre-deforestation	Mean	0.52	24000	17.8	89.4	1.86	0.12	13.1	75.7	110	60512	1.85	450	2.03	31.2	33.6	NA	2.74	66.7	2.39	88.1	NA	NA	NA	NA	28.8	3.75
	Median	0.52	24000	17.8	89.4	1.86	0.12	13.1	75.7	110	60512	1.85	450	2.03	31.2	33.6	NA	2.74	66.7	2.39	88.1	NA	NA	NA	NA	27.5	3.00
	std dev	0.01	1206	0.42	2.2	0.21	0.00	0.20	39.0	46.5	10463	1.38	64.6	0.24	1.11	9.23	NA	0.25	4.14	0.10	3.63	NA	NA	NA	NA	9.32	3.10
Post-deforestation Pre-Industrial	Mean	0.48	17326	14.1	117	1.21	0.15	9.21	31.3	111	25165	1.20	180	0.73	21.1	14.3	NA	2.25	37.7	1.87	65.4	NA	NA	NA	NA	12.0	18.0
	Median	0.72	24385	30.4	88.7	1.82	0.18	17.2	51.4	92.3	60545	0.99	276	1.83	33.7	62.4	NA	3.02	68.0	2.61	121.19	NA	NA	NA	NA	19.0	6.00
	std dev	0.09	2790	2.5	10.8	0.33	0.04	3.59	8.56	43.7	12793	0.46	40.0	0.47	5.39	22.8	NA	0.29	1.48	0.21	40.6	NA	NA	NA	NA	NA	NA
Post-Industrial	Mean	2.29	16838	46.1	69.1	1.67	0.53	10.9	69.4	171	31494	3.68	179	2.66	33.0	143	0.11	9.04	543	6.98	68.7	3.51	173	101	26.3	11.2	6.67
	Median	2.23	16679	46.7	69.0	1.74	0.40	10.4	65.8	155	30104	3.73	166	2.33	32.6	148	0.06	8.99	514	7.28	65.5	3.46	175	83.5	22.7	9.50	6.00
	std dev	0.78	3068	21.5	10.2	0.19	0.42	2.25	16.6	48.4	6135	1.65	43.0	1.33	3.92	34.9	0.11	2.91	211	1.23	25.9	0.57	27.9	50.6	15.6	7.57	4.55
Bridge Site																											
All Samples	Mean	0.95	16101	24.2	159	1.18	0.67	10.9	46.0	89.4	22243	2.32	227	2.27	30.4	93.6	0.03	4.70	282	5.16	55.6	2.95	148	82.6	15.6	13.7	22.3
	Median	1.02	15963	18.3	153	1.16	0.61	10.2	46.0	83.0	21335	2.12	144	2.01	29.2	84.1	0.01	4.85	318	5.95	51.1	2.81	129	77.2	14.7	13.0	21.0
	std dev	0.51	2974	17.2	56.1	0.24	0.45	4.23	13.1	40.6	5550	1.40	253	1.30	9.77	58.1	0.03	1.77	136	2.05	17.0	0.60	53.8	35.0	6.08	6.86	8.12
Pre-deforestation	Mean	NA	NA	NA	NA	NA	NA	NA	NA	NA	NA	NA	NA	NA	NA	NA	NA	NA	NA	NA	NA	NA	NA	NA	NA	NA	NA
	Median	NA	NA	NA	NA	NA	NA	NA	NA	NA	NA	NA	NA	NA	NA	NA	NA	NA	NA	NA	NA	NA	NA	NA	NA	NA	NA
	std dev	NA	NA	NA	NA	NA	NA	NA	NA	NA	NA	NA	NA	NA	NA	NA	NA	NA	NA	NA	NA	NA	NA	NA	NA	NA	NA
Post-deforestation Pre-Industrial	Mean	0.42	17091	10.9	111	1.25	0.14	8.73	34.0	128	25317	0.86	206	0.66	20.8	20.1	NA	2.20	37.8	1.92	69.6	NA	NA	NA	NA	20.0	13.3
	Median	0.47	15927	10.8	110	1.16	0.13	7.07	32.6	109	26252	0.53	193	0.63	17.9	16.1	NA	2.18	34.8	1.91	57.4	NA	NA	NA	NA	17.5	15.5
	std dev	0.12	3654	4.6	10.3	0.23	0.04	3.34	6.38	57.9	2514	0.64	32.8	0.08	6.26	14.3	NA	0.51	9.75	0.17	31.2	NA	NA	NA	NA	6.93	3.88
Post-Industrial	Mean	1.07	15865	27.4	170	1.17	0.79	11.4	48.9	80.1	21511	2.67	232	2.65	32.7	111	0.03	5.30	340	5.93	52.2	2.95	148	82.6	15.6	9.80	28.0
	Median	1.06	16000	22.7	158	1.16	0.74	10.3	47.2	76.4	20997	2.50	141	2.62	30.0	116	0.01	5.25	337	6.08	50.6	2.81	129	77.2	14.7	11.0	27.0
	std dev	0.49	2843	17.6	56.5	0.25	0.41	4.32	12.7	30.3	5858	1.31	283	1.14	9.10	50.0	0.03	1.39	68.2	1.42	10.3	0.60	53.8	35.0	6.08	4.09	5.83
Cheesequake																											
All Samples	Mean	0.29	NA	15.7	18.8	0.57	0.18	3.99	20.9	50.8	NA	0.17	65.2	6.34	16.1	50.7	1.63	3.11	NA	1.04	NA	5.06	52.0	42.1	13.9	6.67	9.41
	Median	0.09	NA	9.0	17.0	0.60	0.12	3.10	18.0	11.8	NA	0.05	55.0	5.97	13.7	17.8	0.81	2.00	NA	0.80	NA	4.50	41.0	38.9	9.87	2.00	8.50
	std dev	0.35	NA	12.5	6.2	0.11	0.15	2.80	13.1	75.3	NA	0.21	46.9	1.96	9.18	64.4	1.83	2.45	NA	0.75	NA	1.85	43.6	18.0	10.7	8.37	5.25
Pre-deforestation	Mean	0.05	NA	5.0	14.5	0.60	0.06	2.28	13.2	6.58	NA	0.02	38.1	5.91	8.25	5.91	0.35	1.78	NA	0.53	NA	4.27	40.4	42.3	8.01	18.0	3.57
	Median	0.05	NA	5.0	14.5	0.60	0.06	2.20	13.0	6.20	NA	0.02	37.0	5.92	7.90	5.45	0.33	2.00	NA	0.50	NA	4.23	19.0	42.3	8.01	14.8	4.00
	std dev	0.01	NA	0.97	2.5	0.06	0.03	0.55	1.8	1.94	NA	0.00	7.81	1.00	1.02	1.53	0.11	0.55	NA	0.16	NA	0.61	55.1	8	7.04	9.22	1.80
Post-deforestation Pre-Industrial	Mean	0.10	NA	10.5	20.2	0.64	0.26	6.55	24.0	12.5	NA	0.04	84.1	4.88	20.6	17.5	0.82	2.00	NA	1.33	NA	4.35	37.6	29.4	8.53	6.45	13.5
	Median	0.09	NA	9.0	18.0	0.60	0.22	4.80	19.0	11.6	NA	0.03	83.0	4.76	21.0	17.8	0.81	2.00	NA	1.10	NA	4.29	38.0	29.5	8.87	2.00	16.0
	std dev	0.04	NA	3.9	5.6	0.08	0.15	4.47	20.5	6.54	NA	0.02	16.2	1.08	9.99	9.31	0.23	0.00	NA	0.75	NA	0.43	18.6	7	1.51	8.35	6.16
Post-Industrial	Mean	0.67	NA	30.8	21.7	0.50	0.23	3.92	27.1	126	NA	0.37	83.0	7.92	21.0	122	3.57	5.38	NA	1.31	NA	6.50	68.5	47.8	17.5	3.30	9.96
	Median	0.60	NA	32.0	23.0	0.45	0.18	3.40	22.0	123	NA	0.40	58.0	7.66	19.0	128	3.27	4.50	NA	0.95	NA	5.43	62.5	45.7	14.4	1.67	9.33
	std dev	0.33	NA	7.3	6.8	0.13	0.14	1.10	10.2	84.7	NA	0.21	68.8	2.08	8.15	60.3	1.84	2.96	NA	0.83	NA	2.46	31.8	20.6	12.4	4.48	4.19

Copper decreased slightly, but this likely resulted from a low number of samples in pre-deforestation sediments, and mixing. The average concentration of all four metals increased following industrialization. PAHs we also observed at this site. We found that both PCBs and OPCs increased in the 1950s through the 1970s (Figure 51). We did not capture pre-industrial PAHs at this site. Nutrients were observed by categorizing diatoms by their preference for high nutrient concentrations or low concentrations (Potapova *et al.*, 2015). At Brookside, we found that diatoms preferring low nutrient concentrations decreased following deforestation in 1795 (Figure 52). Concurrently, the abundance of diatoms preferring high nutrient concentrations increased slightly during this time. Diatoms that prefer low nutrient conditions stay generally low in abundance following industrialization, while diatoms that prefer high nutrient concentrations continue to increase after industrialization.

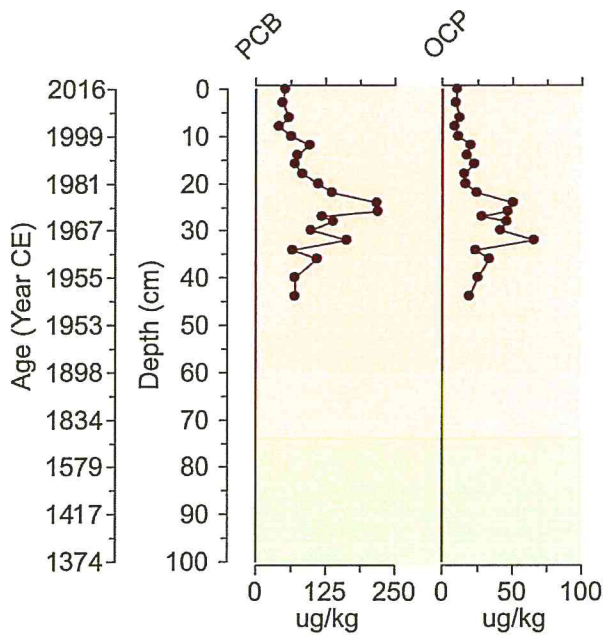


Figure 51. Brookside Organics, colors in figure represents pre-land clearance (green), post-land clearance, but pre-industrial (yellow), and post-industrial (red) land uses.

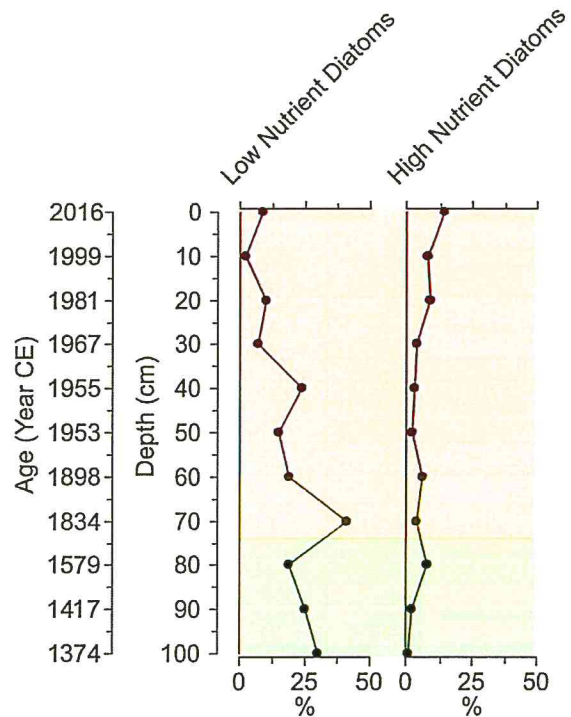


Figure 52. Results of Diatom Analysis at the Brookside Site, showing distribution of Low and High Nutrient Diatoms over time.

The Bridge Site was moderately disturbed. At Bridge Site, we were unable to sample pre-deforestation sediments. We did find, however, that metals increased in sediment concentration following industrialization (Figure 44). Copper decreased slightly in average concentration, again likely due to mixing and a smaller sample size prior to industrialization (Table 5). The other three metals, cadmium, nickel, and lead, all show a increase in concentration following industrialization. PCBs and OPCs were not sampled prior to industrialization. PCBs and OPCs were both found to be very variable at this site, however, and generally show an increase during the 1920s (Figure 53). The wide variations of PCBs and OPCs here may be related to mixing, which was found to be very problematic at this site. Diatom reconstructions of nutrient levels showed a near complete loss of diatoms preferring low nutrients after industrialization occurred (Figure 54) (Potapova and Charles, 2007). We found that diatoms with a preference for moderate nutrient levels became very variable after industrialization. Finally, we found that diatoms which are tolerant of or prefer high nutrient levels increased following industrialization.

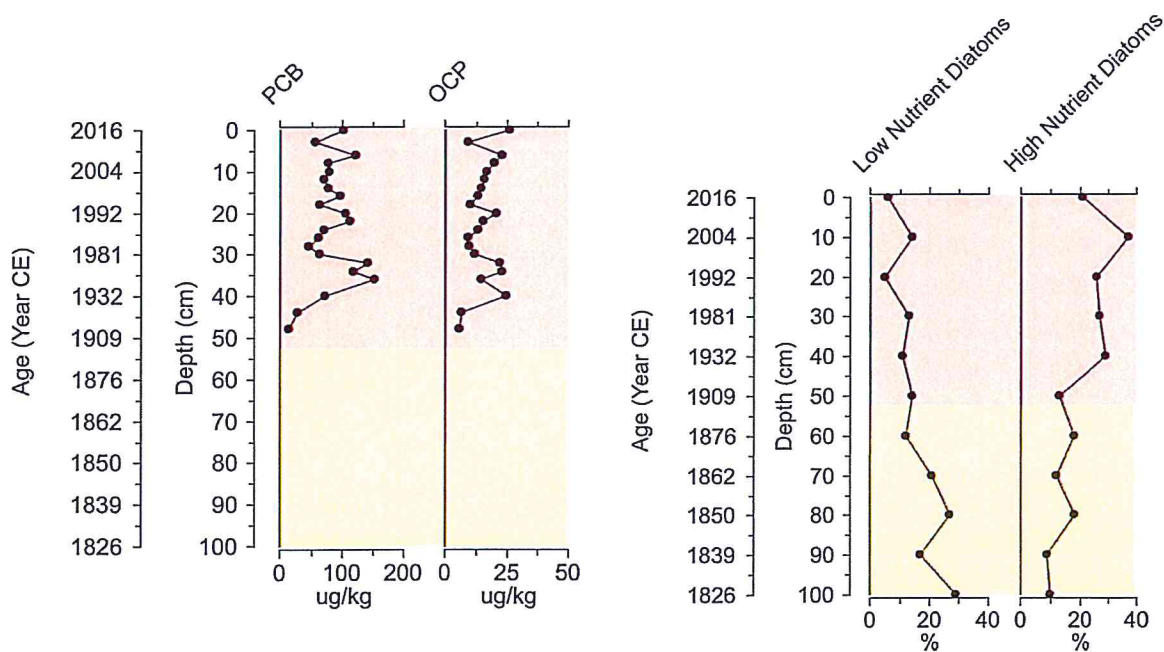


Figure 53. Bridge Site, colors in figure represents pre-land clearance (green), post-land clearance, but pre-industrial (yellow), and post-industrial (red) land uses.

Figure 54. Results of Diatom Analysis at the Bridge Site, showing distribution of Low and High Nutrient Diatoms over time.

At Cheesequake, our least disturbed site, we found that cadmium, copper, nickel, and lead increased slightly following deforestation (Figure 45). Following industrialization, all four metals increase greatly. The average of all four metals reflects this, with the post-industrial average being 3 to 17 times higher than the pre-deforestation average. PCBs and OPCs also increased following industrialization (Figure 55). PCBs increased only slightly, from 42.3 ug/kg prior to deforestation to 44.5 ug/kg following industrialization (Table 5). OPCs however doubled following industrialization (Table 5). Both were variable. Here, diatoms showed a similar pattern to the other two sites. Diatoms which prefer low nutrient concentrations decreased following settlement, and particularly following industrialization (Figure 56) (Potapova *et al.*, 2015). Concurrently, diatoms which prefer high nutrient concentration increased following settlement and industrialization.

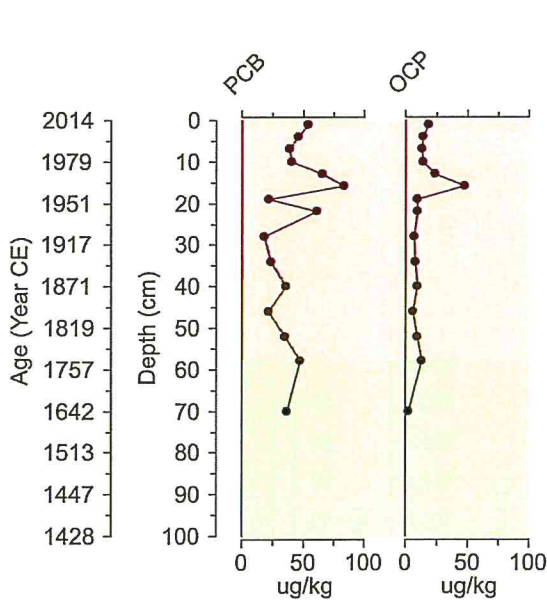


Figure 55. Cheesequake Site, colors in figure represents pre-land clearance (green), post-land clearance, but pre-industrial (yellow), and post-industrial (red) land uses.

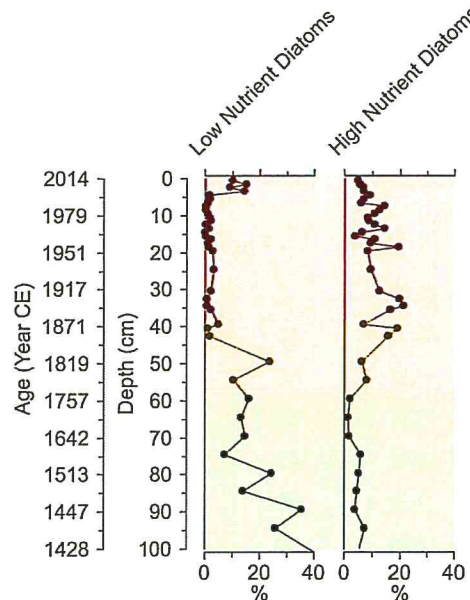


Figure 56. Results of Diatom Analysis at the Cheesequake Site, showing distribution of Low and High Nutrient Diatoms over time.

When the three sites are compared, Cheesequake, for the most part, has the lowest pollution levels, which Brookside has the highest (Table 5). Bridge Site is intermediate. Considering the post-industrial concentrations of metals, with the exception of copper, Cheesequake has the lowest concentrations. Brookside has the highest concentration of all metals. Similarly, Cheesequake has the lowest levels of PCBs and is similar to Bridge Site in OPCs concentrations. Brookside has nearly twice the concentration of PAHs as Cheesequake. This is consistent with surface water samples documented elsewhere in this report. Water samples taken near Brookside tend to be much higher in all pollutants than any other location in the river.

2.4 Conclusions

Overall, we were able to show that pollution levels including metals, organic pollutants, and nutrients all increased following industrialization throughout the Raritan River. In some cases, we were also able to show an increase following deforestation. We found that sites with a greater amount of anthropogenic impact showed the highest increases in pollution levels. These changes were consistent with finding that the site with the greatest anthropogenic impact, Brookside, also had the highest surface water contamination.

We found mixing to be an issue, particularly in Brookside and Bridge Site. Mixing results from the activities of burrowing animals such as worms or crabs, or the growth of plant roots, and is also referred to as bioturbation. Bioturbation can make establishing an age-depth model difficult because signals may be smeared over several centimeters. Bridge site was the most bioturbated, and thus age markers near the bottom were both noted as pre-deforestation (in the case of pollen), and modern/1950. Additionally, pollution such as PAHs and markers such as diatoms are similarly smeared. This resulted in larger errors on ages and less obvious pollution patterns. Despite this, we were able to interpret many of the expected environmental changes at these sites.

Previous studies in various locations have helped identify the behavior of organic and inorganic pollutants in wetland systems. Sanger *et al.* (1999) compared industrial and urban watersheds to suburban and forested watersheds in North Carolina. Like our results, the areas with greater anthropogenic impact, specifically the urban and industrialized areas had much higher concentrations of organic pollutants such as PCBs and PAHs than forested and suburban areas. Additionally, in our study, the increased amount of pollution in the river is near our most polluted site, Brookside. This may imply that historically deposited pollutants can be remobilized and redeposited onto the surface. In the study by Sanger *et al.* (1999) core samples contained both historical and contemporary sources, likely representing a remobilization of historical sediments and that because organic pollutants bind tightly to organics in wetland sediments, these environments can be historical sinks, but potential contemporary sources.

Metals also tend to adhere more closely to finer grains in sediments, resulting in the potential for greater contamination of wetlands and surface water (Gambrell, 1994). However, the marshes studied here are consistently wet, which reduced the potential for metal contamination to

contribute to decreased water quality through surface runoff. Because sediments that drain and dry out are frequently prone to oxidation, and thus they are at increased risk for metals to become less firmly adhered to grains, and more prone to contaminating runoff (Gambrell, 1994).

These findings can help us set realistic and achievable goals for restoration. Additionally, they help point to additional considerations, such as sediment resuspension. Because sediments are often resuspended as marshes are reworked, contaminants stored in sediments may re-enter the waterway, causing surface water pollution. Contaminant can also leach through groundwater. Because sediment can be stored for a very long time, this means that contaminant stored in marshes may be a problem for a long time, however, because metals bind tightly to wetland soils, causing them to be immobilized by capping them under additional sediment is possible (McKee *et al.*, 2005; Gambrell, 1994).

Several solutions are possible for this sort of problem. Because wetland sediments are frequently good sinks of contaminants, they could be capped to prevent the loss of contaminants from surface layers (Gambrell, 1994; Sanger *et al.* 1999). If the pollution levels are incompatible with bringing back vegetation, or there is concern that it might re-enter the system through vegetation or runoff, removal and disposal could also be considered (Zedler & Leach, 1998). Additionally, studies have shown that vegetation can effectively move contaminants farther below ground. In Weis and Weis (2003), *Phragmites* was shown to uptake more metals and store more of them below ground, where they are less accessible, than *Spartina*. Because *Spartina* stored the metals in its leaves, they were more frequently excreted via the salt gland and additionally, more likely to be present in leaf litter, which can be consumed by detritus feeder and enter the food chain (Weis & Weis 2003). Because of this, careful consideration would be needed in determining which plants could best serve the remediation efforts while still allowing the environment to be as close to natural as possible.

Overall, it is important to consider several additional studies when planning how to best proceed with remediating the Raritan River and the marshes surrounding them. There are several studies we recommend. First, additional historical sites should be identified and sampled, particularly in marshes adjacent to portions of the river with higher bed-sediment contamination. This would help establish the location of the most impacted sites and identify potential sources. We would also improve our knowledge of the timing of impacts by sampling back to pre-European

conditions. Secondly, additional bed sediment samples should be taken to monitor changes in the bedload contamination levels. Ideally, these samples would be taken annually for several years to monitor what changes are occurring in the river. Pairing them with surface water samples would assist in understanding how the contaminants in the sediments are impacting water quality. Collecting multiple sets of water quality samples throughout tidal cycles and throughout the year would allow us to observe how pollution from contaminated marshes might move through the river. Third, once a site is selected to be remediated, studies on its hydrology and the prevalence of erosion at the site are needed to establish which remediation method is appropriate. A groundwater hydrology study would help establish how much contamination is escaping from the marsh and entering the river. Because deeper sediments are from time with less environmental regulation, they may have increased contamination. If water flows through them and picks up contamination, they may still contribute to poor water quality. On the other hand, if they are not contributing to water quality in this way, removing overlying, cleaner sediments may re-expose them and allow them to leach contaminants into the system even more easily. During and after remediation, the site should be monitored to ensure remediation efforts are effective (Spencer & Harvey, 2012). Multiple aspects, including physical and biogeochemical processes as well as ecological and morphological indicators, should be considered to identify the effectiveness of any plan put into place (Spencer & Harvey, 2012). By monitoring multiple aspects of the remediation effort and its outcome, we can ensure that the water quality and environmental health of the site is improving as expected and that pollutants have been effectively sequestered or fully removed.

3. Discussion

To assess the river's environmental past and present we used a multidisciplinary approach where biology, chemistry, statistics and computer modelling were combined to gain a greater understanding into the spatial and temporal distribution of priority pollutants and contaminants in the Lower Raritan River.

Water quality analysis revealed that at the time of sampling there was considerable mixing of the water column as shown by measurements of salinity, temperature and dissolved oxygen. Figure 23 sums up the findings of the sediment chemistry analysis. Metal accumulation in the sediment tends to be higher at the first bend in the river, around the GSP bridge as well as further upriver around Crab Island and around the sand bar island on the southern bank. When compared to natural metal accumulation (Figures 26-38) only Arsenic, Copper, Mercury, Selenium, and Silver showed considerable enrichment in the sediment. Those metals along with Nickel, Lead and Zinc all exceeded the ERL thresholds. Mercury concentrations on the other hand were above the ERM levels in almost all sampling locations (Table 3). Overall organics and metals coincided on the same hotspots.

When comparing earlier sediment contamination records to our findings (Figure 40-41) the possibility of natural attenuation emerged for Chromium, Nickel and Antimony, while the rest of the metals showed no change in contamination levels between 2000 and 2006. In 2017 the metal concentration of Silver, Arsenic, Chromium and Selenium peak slightly upriver compared to measurements in 2000-2006. A similar slight attenuation pattern was found for most of the PCB congeners but they still exceeded the ERL criteria. Among the OCPs Endrin showed a marked increase from 2000 to 2017. Our results suggest active sources of Mercury and OCPs still exist and are having an impact in the Lower Raritan.

When looking at the surrounding wetlands of the river we found that industrialization led to increased pollution due to anthropogenic activity in the tidal Raritan River. These changes were most pronounced in the sites closer to anthropogenic influences and were least pronounced at the more undisturbed site. This is consistent with findings in surface water pollution, which showed that a greater amount of metals and organic pollutants were present in the water near Brookside, our most polluted site, than anywhere else in the study reach. This may imply that these pollutants are continuing to be put into the waterway by resuspension. These findings can help

to identify the timing of pollution in the tidal Raritan River. Additionally, they could also be used to establish reasonable standards for restoration and remediation efforts.

Overall, it is important to consider several additional studies when planning how to best proceed with remediating the Raritan River and the surrounding marshes. There are several studies we recommend. First, additional historical sites should be identified and sampled, particularly in marshes adjacent to portions of the river with higher bed-sediment contamination. This would help establish the location of the most impacted sites and identify potential sources. We would also improve our knowledge of the timing of impacts by sampling back to pre-European conditions. Secondly, additional bed sediment samples should be taken to monitor changes in the bedload contamination levels. Ideally, these samples would be taken annually for several years to monitor what changes are occurring in the river. Pairing these samples with surface water samples would assist in understanding how the contaminants in the sediments are impacting water quality. Collecting multiple sets of water quality samples throughout tidal cycles and throughout the year would allow us to observe how pollution from contaminated marshes might move through the river. Third, once a site is selected to be remediated, studies on its hydrology and the prevalence of erosion at the site are needed to establish which remediation method is appropriate. A groundwater hydrology study would help establish the amount of contaminants escaping from the marsh and entering the river. Since deeper sediments are from times with no environmental regulation, they may be an active source of contaminants. On the other hand if they are not contributing to water quality in this way, removing overlying, cleaner sediments may re-expose them and allow them to leach contaminants into the system even more easily. During and after remediation, the site should be monitored to ensure remediation efforts are effective (Spencer & Harvey, 2012). Multiple aspects, including physical and biogeochemical processes as well as ecological and morphological indicators, should be considered to identify the effectiveness of any plan put into place (Spencer & Harvey, 2012). By monitoring multiple aspects of the remediation effort and its outcome, we can ensure that the water quality and environmental health of the site is improving as expected and that pollutants have been effectively sequestered or fully removed.

4. References

- Appleby, P., & Oldfield, F. (1992). Application of 210-Pb to sedimentation studies. In M. Ivanovich, & R. Harmon (Eds.), *Uranium-Series Disequilibrium: Applications to Earth, Marine, & Environmental Studies* (pp. 731-778). Oxford, UK: Oxford University Press.
- Bricker-Urso, S., Nixon, S., Cochran, J., Hirschberg, D., & Hunt, C. (1989). Accretion rates and sediment accumulation in Rhode Island salt marshes. *Estuaries*, *12*, 300-317.
- Brugam, R. (1978). Pollen indicators of land-use change in southern Connecticut. *Quaternary Research*, *9*, 349-362.
- Christiansen, T., Wilberg, P., & Milligan, T. (2000). Flow and Sediment Transport on a Tidal Salt Marsh Surface. *Estuarine, Coastal and Shelf Science*, *50*, 315-331.
- Church, T., Sommerfield, C., Velinsky, D., Point, D., Benoit, C., Amouroux, D., Donard, O. (2006). Marsh sediments as records of sedimentation, eutrophication and metal pollution in the urban Delaware Estuary. *Marine Chemistry*, *102*, 72-95.
- Clark, J., & Patterson, W. (1984). Pollen, Pb-210, and opaque spherules; an integrated approach to dating and sedimentation in the intertidal environment. *Journal of Sedimentary Research*, *54*, 1251-1265.
- Cooper, S., & Brush, G. (1993). A 2,500-year history of anoxia and eutrophication in Chesapeake Bay. *Estuaries*, *16*, 617-626.
- De Vleescheuwer, F., Chambers, F., & Swindles, G. (2010). Coring and sub-sampling of peatlands for palaeoenvironmental research. *Mires and Peat*, *7*, 1-10.
- Donnelly, J., Bryant, S., Butler, J., Dowling, J., Fan, L., Hausmann, N., Webb III, T. (2001). A 700-year sedimentary record of intense hurricane landfalls in southern New England. *Geological Society of America Bulletin*, *113*, 714-727.
- Faegri, K., & Iverson, J. (1964). *Textbook on Pollen Analysis*. New York, New York: Hafner.
- Flynn, W. (1968). The determination of low levels of polonium-210 in environmental materials. *Analytical Chimica Acta*, *43*, 221-227.
- Forstner U., Muller G. (1981). Concentrations of Heavy Metals and Polycyclic Aromatic Hydrocarbons in River Sediments: Geochemical Background, Man's Influence and Environmental Impact. *GeoJournal*, Vol. 5, No. 5: *Water Pollution*, p. 417-432
- Gallagher, F.J., Pechmann, I., Grabosky, J., Bogden, J., Weis, P., 2008. Soil metal concentrations and vegetative assemblage structure in an urban brownfield. *Environmental Pollution* *153* (2), 257-496

- Gambrell, R. (1994). Trace and toxic metals in wetlands - A review. *Journal of Environmental Quality*, 23, 883-891.
- Haslett, J., & Parnell, A. (2008). A simple monotone process with application to radiocarbon-dated depth chronologies. *Journal of the Royal Statistical Society*, 3, 399-418.
- He, Q., & Walling, D. (1996). Rates of Overbank Sedimentation on the Floodplains of British Lowland Rivers Documented Using Fallout ¹³⁷Cs. *Geografiska Annaler. Series A, Physical Geography*, 78, 223-234.
- Hurst, R. (2002). Lead isotopes as age-sensitive genetic markers in hydrocarbons. 3. Leaded gasoline, 1923-1990 (ALAS model). *Environmental Geosciences*, 9, 43-50.
- Jeffries, H. (1962). Environmental characteristics of Raritan Bay, a polluted estuary. *Limnology and Oceanography*, 7, 21-31.
- Juang, K.W., Lee, D.Y., Ellsworth, T.R., 2001. Using rank-order geostatistics for spatial interpolation of highly skewed data in heavy-metal contaminated site. *Journal of Environmental Quality* 30, 894e903.
- Kemp, A., Horton, B., Vane, C., Bernhardt, C., Corbett, D., Engelhart, S., Cahill, N. (2013). Sea-level change during the last 2500 years in New Jersey, USA. *Quaternary Science Reviews*, 81, 90-104.
- Lima, A., Bergquist, B., Boyle, E., Reuer, M., Dudas, F., Reddy, C., & Eglinton, T. (2005). High-resolution historical records from Pettaquamscutt River basin sediments: 2. Pb isotopes reveal a potential new stratigraphic marker. *Geochimica et Cosmochimica Acta*, 69, 1813-1824.
- Long, E.R., MacDonald, D.D., Smith, S.L., and Calder, F.D. 1995. Incidence of adverse biological effects within ranges of chemical concentrations in marine and estuarine sediments. *Environmental Management* 19(1):81-97
- Marcantonio, F., Zimmerman, A., Xu, Y., & Canuel, E. (2002). A Pb isotope record of mid-Atlantic US atmospheric Pb emissions in Chesapeake Bay sediments. *Marine Chemistry*, 77, 123-132.
- Marshall, S. (2004). The Meadowlands Before the Commission: Three Centuries of Human Use and Alteration of the Newark and Hackensack Meadows. *Urban Habitats*, 4-27.
- McKee, L., Ganju, N., & Shoellhamer, D. (2006). Estimates of suspended sediment entering San Francisco Bay from Sacramento and San Joaquin Delta, San Francisco Bay, CA. *Journal of Hydrology*, 323, 335-352.
- Metcalf, S., & Derwent, D. (2014). *Atmospheric Pollution and Environmental Change*. Routledge.

- Nittrouer, C., Sternberg, R., Carpenter, R., & Bennett, J. (1979). The use of Pb-210 geochronology as a sedimentological tool: Application to the Washington coast shelf. *Marine Geology*, 31, 297-316.
- Potapova, M., & Charles, D. (2007). Diatom metrics for monitoring eutrophication in rivers of the United States. *Ecological Indicators*, 7, 48-70.
- Potapova, M., Desianti, N., & Velinsky, D. (2015). *Barnegat Bay Nutrient Inference Model*. Philadelphia, PA: Academy of Natural Sciences of Drexel University.
- Russell, E. (1980). Vegetational Change in Northern New Jersey from Precolonization to the Present: A Palynological Interpretation. *Bulletin of the Torrey Botanical Club*, 107, 432-446.
- Sanger, D., Holland, A., & Scott, G. (1999). Tidal creek and saltmarsh sediments in South Carolina Coastal estuaries: II. Distribution of Organic Contaminents. *Archives of Environmental Contamination and Toxicology*, 37, 458-471.
- Spencer, J., & Harvey, K. (2012). Understanding system disturbance and ecosystem services in restored saltmarshes: integrating physical and biogeochemical processes. *Estuarine, Coastal, and Shelf Science*, 106, 23-32.
- Weis, J., & Weis, P. (2004). Metal uptake, transport and release by wetland plants: implications for phytoremediation and restoration. *Environment International*, 30, 685-700.
- Zedler, J., & Leach, M. (1998). Managing urban wetlands for multiple use: research, restoration, and recreation. *Urban Ecosystems*, 2, 189-204.

5. Acknowledgements

This study was sponsored by the Mushett Family Foundation. We would like to thank Hank and Mark Daaleman and the Foundation for trusting MERI with this task and their continuous support throughout the study.

We would like to acknowledge Margaret Christie, Benjamin Horton, Jennifer Walker and Jennifer Clear from RU Marine & Coastal Sciences for their work in the assessment of wetland core samples and historical anthropogenic influence, as well as Margaret Christie as the author of Component II - Historical Land Use Report in the Lower Raritan Basin. We would like to thank the staff of the Marine & Coastal Sciences Department for their professionalism and continued support of the study.

We would like to thank Chip Haldeman, captain of the Rutgers Research Vehicle to make our field outing seamless and effective.

Great thanks goes to the MERI staff for the endless hours of mucky field work of Francisco Artigas, Joe Grzyb, Michael Stepowyj and Brian Wlodawski, for the infinite patience of Cheryl Yao, Yefim Lewinsky and Joe Grzyb while running the sample analysis, the countless screen time from Michael Stepowyj and Ildiko C. Pechmann spent on the computer modelling, and Sandy Speers for taking care of the business end of it and getting the group organized throughout the study.